Evaluation of Handheld Aerosol Extinguishers with Respect to Toxicity and Corrosivity

by

Alen Topic

A thesis

presented to the University of Waterloo

in fulfillment of the

thesis requirement for the degree of

Master of Applied Science

in

Mechanical Engineering

Waterloo, Ontario, Canada, 2015

AUTHOR'S DECLARATION

I hereby declare that I am the sole author of this thesis. This is a true copy of the thesis, including any required final revisions, as accepted by my examiner.

I understand that my thesis may be made electronically available to the public.

Abstract

Defense Research and Development Canada is undertaking a research project that will look for alternatives to replace their existing Halon 1301 fire suppression systems with a safer and more effective option. At the current moment, the study focuses on a relatively new and emerging alternative in fire suppression, aerosol extinguishment agents. Previous studies have been done on the effectiveness of aerosol suppression agents; however, there is very little data related to the potential impacts due to accidental exposure to the agents after discharge into a compartment without a fire, or similarly due to exposure in conjunction with fire suppression. Therefore, there is a need for more in depth experimental analysis to determine if the agents are safe enough to use for fire suppression applications where exposure of personnel, environment and equipment to the aerosols cannot be avoided. The research presented in this thesis will focus on comparison of the characteristics of two specific aerosol variants designed for use in a 20 m^3 occupied space.

To evaluate the potential for physiological impact, experiments were designed to assess the aerosol systems in fire scenarios similar to those that naval Rapid Response Team (RRT) would experience. Thus, the aerosols were tested in five different scenarios, including fires fuelled by diesel fuel and wood cribs, as well as under cold agent discharge situations. Temperatures in the compartment were monitored throughout each test using 80 Type K thermocouples. The compartment environment and, particularly, evidence of NO_x, CO, HCN and NH_3 production, were investigated for each situation using Novatech P-695 and Gastec STR-800 pre-calibrated tube testing systems. Finally various materials were exposed during the various test situations in order to better assess the potential for corrosion of selected materials due to agent deposition.

The thesis includes a detailed description of the experimental design, measurement apparatus and techniques used in the research, as well as key results from each of the tests performed. It was found that, NO_x, NH_3 and CO are produced during discharge of aerosol suppression agents. In addition, there is some evidence to suggest that deposition of aerosol particulates, combined with fire residues, could contribute to degradation of surfaces when left unattended for long periods of time.

Acknowledgments

I would like to thank my professor Dr. Elizabeth Weckman, for her patience, advice and guidance throughout the entire research study. Her attention to detail, coupled with years of experience and expertise, made this research study a complete success. Her dedication to her students and to the program is splendid and I know every student that graduates under her supervision, leaves the program with a whole new positive outlook on life.

I would also like to thank Mr. Gordon Hitchman for his help and support throughout the testing process. Your guidance and experience was irreplaceable and it certainly translated into the quality of the test results obtained. Had it not been for your help, this research would have taken a lot longer.

Tom Sheehan, my colleague who at the time of testing was under supervision of Dr. Weckman, needs to be thanked. Had it not been for you, I would have had a much harder time procuring all the resources for testing. You made it easy for me to focus on toxicology while you handled the physical testing. Your research results, coupled with mine, are able to explain the aerosol extinguishers much better than when we began. Hopefully the information will be of great help to the Royal Canadian Navy.

Finally I would love to thank my family for their ever loving support throughout the entire research study. First to my parents Nedeljko i Milanka Topić, who have sacrificed everything to make sure I had all the resources needed to graduate; your undying love made everything possible. Secondly, I want to thank my wife Dragana Nedić, who has been nothing but supportive throughout the entire thesis. Thank you again, without all of you, this would not mean anything.

Table of Contents

List of Figures

List of Tables

1   Introduction

Engineers strive to design present day fire suppression systems in as ecologically friendly a manner as possible, while still providing effective suppression and control of a broad range of fire situations. By these measures, encapsulated micron aerosol agents (EMAA) have been shown to offer numerous key advantages. First, aerosol agents are thought to be environmentally friendly, especially as compared to halogen based agents which are excellent fire suppressants but contain compounds which have been directly linked to climate change. Further, unlike gaseous systems which need high pressures to operate, aerosol agents are dispersed into the fire compartment using a pyrotechnically triggered generator, which is small in both size and weight. In addition, the majority of aerosol suppression systems are relatively inexpensive to install and maintain, since they do not require piping, pumps or compressed gas systems for their operation and most have a guaranteed shelf life of 10 years [1]. Finally, aerosol suppression agents have been demonstrated to provide the highest effectiveness in terms of agent weight to extinguishing power ratio. A study performed by National Institute of Standards and Technology (NIST) showed that in order to control a fire, aerosol agents have to be applied, on average, at the lowest concentration relative competing suppression agents such as Halon 1301 or conventional CO_2 suppression agents [2]. The necessary concentration of aerosol was shown to be 50 g/m^3, compared to 300 g/m^3 of Halon and 700 g/m^3 of CO_2 to provide similar control of fires [2]. This allows great flexibility in the use of aerosol systems, and allows design of smaller and more versatile systems tailored to different fire suppression scenarios. All of the above factors point to the significant advantages which might be accrued in use of aerosol suppression agents as compared to the more conventional gaseous suppression agents.

Unfortunately, however, there are also some potential disadvantages to the use of aerosol agents for the suppression and control of fires. These relate to potential thermal impacts during generation of the aerosol agent itself, evolution of toxic gases during generation and discharge of aerosol agents and other effects, such as corrosion or fouling of materials, due to deposition of aerosols on surfaces within a compartment during suppression of the fire. To understand these further, the mechanisms of generation and dispersion of aerosol agents is briefly discussed below.

The particulate aerosol, which is the main suppression agent generated from an aerosol suppression system, is produced via thermal decomposition of a solid, aerosol forming compound or compounds in the presence of a hydrocarbon binding agent. While the exact composition of aerosol generation materials in most units is proprietary, pyrotechnic aerosol extinguishing systems such as those used in this research involve base compounds such as

potassium nitrate (KNO_3) mixed with an organic oxidizer and binding agent. Upon activation, the base materials react to generate fluid aerosols in the proximity of the units. These can be comprised of compounds such as potassium carbonate (K_2CO_3) and potassium bicarbonate ($KHCO_3$), as well as ammonium bicarbonate (NH_4HCO_3). This process is known to generate significant heat and flames, with rapidly expanding hot gases and dispersion of liquid aerosol material over a short period of time after triggering the unit [3]. The combustion temperature of a KNO_3 based solid tablet is between 1200-2100°C [4]. While an effective fire suppression agent is being produced in conjunction with the generation of any heat and flames, suppression systems based on pyrotechnically generated aerosols can eject flames and hot gases up to 1 m from the canisters and render the metal surfaces of those canisters red hot [5], thus potentially posing significant thermal hazards if not carefully designed.

There is also potential cause for concern over toxic gas evolution arising from the use of aerosol agents for fire suppression even though they are often described as environmentally friendly fire extinguishing agents [1, 2, 6]. During aerosol activation and particulate discharge, gases such as CO_2, N_2, and H_2O are generated via a series of reactions and mix with ambient air; however, due to the combination of reactions taking place and the temperatures involved, there is also the potential for the production of other species such as oxides of nitrogen (NO_x or NO and NO_2), hydrogen cyanide (HCN), ammonia (NH_3) and carbon monoxide, CO [3] depending on the nature of the base compounds and details of the reaction and decomposition processes involved. For example, Kidde International Research found that certain KNO_3 based pyrotechnic aerosols can produce relatively localized NO concentrations between 300-600 ppm [5] and CO between 350-3000 ppm [6]. Pyro-aerosols have also been shown to produce trace amounts of hydrogen cyanide (HCN), between 10-15 ppm [6], possibly due to the formation of NO in the presence of unburned hydrocarbons and combustion radicals which in turn may lead to the formation of HCN. In the presence of even low concentrations of CO and NO_x, penetration of the ultra-fine potassium salt aerosols could also lead to further irritation and possible interference with pulmonary function of human mucus membranes [6]. As such, emission of gases from aerosol suppression units may be particularly important, especially in the context of the relatively confined spaces encountered in marine, naval and many other fire situations. Even if such extinguishing agents are only utilized in normally unoccupied spaces, similar to the case for Halon suppression systems at present, there is still the potential for human exposure either due to improper confinement of a compartment following suppression or through accidental release of the unit.

Aerosol based fire suppression agents, then, produce a buoyant mixture of micron-sized liquid and particulate aerosols carried in a gaseous medium that consists of a broad range of decomposition and oxidation products. For effective suppression, this mixture should be well

dispersed throughout the fire compartment and therefore, the liquid and particulate aerosols and gases will come into contact with surfaces and equipment. In a fully developed fire scenario, exposure of equipment to heat, flames and hot toxic gases produced from the burning fuels has the potential to cause damage. Suppressing the fire by the quickest means will minimize the damage due to the fire, but when the fire is suppressed using aerosol agents, there may be the added potential for corrosion or deposition of residue from the aerosol agent itself. Further, in the case of accidental discharge of an aerosol suppression system, or activation of such a system for very small fires in large compartments, the resultant residue may be of considerable concern.

Deposition of the residue from aerosol suppression agents onto electronics and samples of various metal and polymer materials commonly used in electronics has been evaluated to some degree, but not in sufficient depth to fully appreciate any possible long term effects [5, 7]. Technical white papers outlining tests on some pyrotechnic aerosol extinguishers note that after a fire is suppressed most of the suppression agent can be exhausted in the same manner as smoke, but results do indicate that a slight film may be left on surfaces [8, 9]. Manufacturers recommend removing the aerosol residue using a damp cloth, vacuum or compressed air. In the case of large compartments with thousands of sensitive electronic devices, this process could prove expensive and time consuming and it would be extremely difficult to ensure that all surfaces had been cleaned.

Additional studies conducted in the early 1990s [10] indicate that aerosol agents are non-corrosive to electrical and structural materials, although the cited references could not be found and therefore were not reviewed as part of this work. More recently, Jacobson et al. conducted a corrosion study on the GreenSol aerosol material and found that the agent was non-corrosive against 12 common metal and polymer materials [7]. In the study, the exact composition of the agent tested was not published and unfortunately, the composition of the aerosol has been demonstrated to make a significant difference in its interaction with materials. For example, pyrotechnically generated aerosols based on perchlorates of nitrogen produce potassium chloride, which is known to be corrosive to aluminium and certain grades of steel [5]. In other units, the major active agent is KNO_3. In KNO_3 units which operate on the principle of thermal decomposition of the potassium nitrate, the resultant powder residue is likely comprised mainly of potassium carbonate which alone has been shown to be non-corrosive to most metals and alloys [11], but when dissolved in water results a medium to strong basic solution [12]. For systems operating on other principles, the nature of the discharged gases and particulates is often not known. In these situations or when other acidic compounds are present, the potential for corrosion would seem to exist.

Despite the potential advantages to the development and use of aerosol agents for fire suppression, on preliminary review of the topic, it was determined that there is a dearth of

understanding of the temperatures, as well as the nature and concentrations of gases and particulates, involved with aerosol suppression, therefore making it difficult to weigh the advantages versus potential disadvantages of their use. As such, the current research is focussed on characterization of the gases and particulate matter formed during discharge of, and suppression with, handheld aerosol suppression units. In particular, the objectives of this research are:

1) to investigate the nature and concentrations of prime gases evolved during aerosol generation and discharge into non-fire compartments, as well as during aerosol generation, discharge and control/suppression of four different diesel and wood fire scenarios

2) to gain a better understanding of impacts of use of aerosol suppression systems through
   a. A preliminary study into aerosol deposition on surfaces and electronic devices, including personal protective equipment, and
   b. An investigation into the potential for short or long term corrosion of a selection of materials due to deposition and interaction with particulates and gases generated from aerosol suppression units, both into an empty compartment and into a compartment when the diesel and wood fires are present.

To meet the above objectives, as series of full-scale tests were conducted at the University of Waterloo (UW) Fire Research Laboratory, while collaborating with Royal Canadian Navy (RCN) personnel from the Director of Maritime Ship Support and the Canadian Forces Naval Engineering School. Two different versions of commercial handheld aerosol units were used in a total of 8 diesel and wood crib fuelled compartment fire suppression tests. In addition, 6 cold discharge (agent only) tests were conducted in the same compartment to further characterize the properties of aerosol agent discharge into a compartment when no fire was burning. The tests were designed to aid the RCN in assessing the relative merits and potential drawbacks with use of handheld aerosol extinguishers as potential fire knockdown devices onboard naval vessels. Concentrations of various gases were measured during aerosol discharge and suppression to explore the potential creation of harmful by-products due to thermal decomposition and subsequent aerosol powder generation from the solid state agent contained in the handheld units. Aerosol powder deposition was observed after each test, and post suppression corrosion or other damage was monitored on a range of materials and electronic components. In particular, the set of experiments included in this thesis was aimed towards identification and preliminary investigation of possible impacts, such as toxic gas generation, aerosol deposition or corrosion of equipment, which could occur due to deployment of handheld aerosol extinguishers in a naval application. More generally, the data can be used to better understand the potential hazards that

pyrotechnically generated aerosol agent suppression devices may present when used or accidentally discharged within any compartment, whether or not there is a fire present.

In the thesis, Chapter 2 covers aerosol agent suppression theory, while experimental apparatus and methods are contained in Chapter 3. Following this, results of gas analysis are presented in Chapter 4, followed by XRD analysis in Chapter 5 and corrosion analysis in Chapter 6. Based on the results and discussion, conclusions and recommendations are summarized in Chapters 7 and 8 respectively as well.

2   Aerosol Agent Suppression Background and Theory

Development of a method of fire suppression that addresses different fire classifications and has no negative effects on the surrounding environment is a desired concept for many applications across the fire safety industry. In assessing different suppression methods, fire can be conceptualized as a fire triangle where heat, fuel and oxygen all need to co-exist for fire development. If any of these three sides of the triangle are removed, the fire will be extinguished [13]. Fire extinguishment can also be achieved via chemical routes, most notably through inhibition of the key chain reactions that drive hydrocarbon combustion [13]. To date, no other suppression system has done this more efficiently than Halon 1301.

In the 1940's, Halon was developed and quickly came into use as a cheap and efficient fire suppression agent. Due to its low cost and effectiveness, it quickly gained popularity and was widely implemented in many environments with fire hazards [14]. Halon 1301 is a good chemical inhibitor due to bromotrifluoromethane ($CBrF_3$) which splits into trifluoromethyl (CF_3) and bromine (Br) molecules under pyrolysis [15]. Trifluoromethyl (CF_3) and bromine (Br) scavenge free radicals (H, O^- and OH) that form at flame temperatures (1700° C) and catalytically recombine with the radical species to create new stable chemical compounds in the form of hydrogen bromide (HBr) and hydrogen fluoride (HF), a combined process which then halts further fire propagation [16]. While Halon 1301 has proven to be an excellent fire suppressant, hydrogen bromide (HBr) and hydrogen fluoride (HF) and related by-products have been linked to ozone depletion which has raised concerns with environmental protection agencies around the world and has resulted in virtually international consensus to phase out Halon agents from further use as fire suppressants as per Montreal Protocol in 1987 [14]. For that reason, member countries in the North Atlantic Treaty Organization (NATO) initiated a large effort by which to look at better, cleaner substitutes - substitutes like Encapsulated Micron Aerosol Agents (EMAA).

EMMA refers to a system of either liquid or solid particles ranging from 0.1 to 1 µm in diameter and which stay suspended in a gaseous medium. Examples of such aerosols range from smoke, fog and mist, through to fumes and haze [17]. Solid and gaseous aerosol mixtures, i.e. dispersion aerosols, will be the main focus of this thesis [17]. In these, the suppression agent is obtained via thermal decomposition and oxidation of a solid tablet in an enclosed generator that is designed to deliver an alkali salt particulate suppression agent suspended in the decomposition gases [17]. The particulate and gas mixture is dispersed within the fire compartment and fire control and suppression takes place through a combination of chemical, surface and thermal mechanisms as will be discussed in detail in the following section.

2.1 Pyrotechnically Generated Aerosol Systems

The first idea of an aerosol suppression agent came from a smoke pot, which delivered a dry chemical agent by means of solid propellant combustion (SPC) [18]. Modern pyrotechnically generated aerosols are produced through combustion or thermal decomposition of inorganic oxidizers and salts which are contained in an inorganic or organic epoxy fuel binder. These are encapsulated in a hermetically sealed container within which the aerosol is generated and discharged. The active chemical agent is usually an inorganic potassium salt, since after the halogens, potassium ions are most effective for chemical inhibition of hydrocarbon combustion processes [18]. Therefore, potassium nitrate (KNO_3) is often chosen as the key ingredient, although other strong oxidizers in use today include potassium perchlorate ($KClO_4$) and potassium chloride (KCl) [19]. The agent is thermally ignited using a pyrotechnic fuse or a resistive element [19]. Once the thermal decomposition process is initiated, the agent and the fuel binder interact; setting in motion a chain of highly exothermic chemical reactions which lead to the breakdown of the potassium compounds and produce the alkali metal salts [19]. The alkali metal salts form as liquids which solidify and are carried in the decomposition gases to the fuel source [18]. As they expand and rise due to buoyancy, the hot gases serve to disperse the solid particulate throughout the compartment while heat absorption by the aerosol particulate and some dilution by the hot gases, combined with further chemical interactions between the solid particles and the reacting zones in the fire, lead to suppression of the combustion and cooling of the fire compartment.

2.2 NO$_x$ Formation in Aerosol Environment

To better understand how aerosols hinder combustion the various stages in thermal decomposition, oxidation and other reactions involved in aerosol formation, as well as interactions of aerosols with their environment were examined. The findings are summarized in this section.

A series of reactions is involved in the four stage thermal decomposition and oxidation processes involved in aerosol formation from solid potassium nitrate (KNO_3) and an organic binder as contained in common aerosol suppression units. After initiation, the KNO_3 decomposes, setting off reactions with the organic binder as the first in a chain of reactions that drive aerosol fire extinguishment. The products of these initial reactions contain of mix of potassium bicarbonate ($KHCO_3$), potassium carbonate (K_2CO_3), carbon dioxide, nitrogen and water depending on the composition of the binder and other details of the aerosol unit design.

An aerosol compound's accelerant potassium nitrate (KNO_3) produces an exothermic reaction upon thermal decomposition generating a temperature of between 1200-2100℃ [4] For example, at temperatures of around 450℃ [20], the potassium bicarbonate ($KHCO_3$) may further decompose to potassium carbonate (K_2CO_3), carbon dioxide and water per reaction (R2).

$$2KHCO_3 + heat\ (450^0C) \rightarrow K_2CO_3 + CO_2 + H_2O \qquad (R1)\ [20]$$
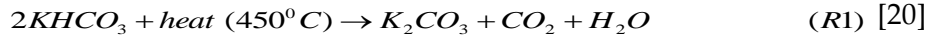
K_2CO_3 may also breakdown at higher temperatures, 700℃ [21], to potassium oxide (K_2O) and, again, carbon dioxide (R3).

$$K_2CO_3 + heat\ (700^0C) \rightarrow K_2O + CO_2 \qquad (R2)\ [21]$$
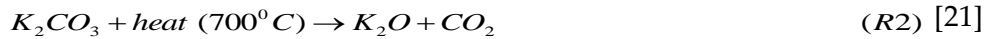
Finally, potassium oxide (K_2O) may undergo further thermal decomposition producing a K^+ ion via (R4)

$$2K_2O + heat\ (825^0C) \rightarrow 4K^+ + O_2 \qquad (R3)\ [22]$$
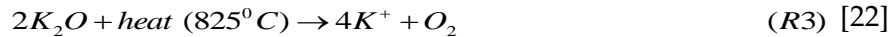
It is this newly formed K^+ ion that is thought to react with the hydroxyl (OH^-) radical from the burning fuel (in this research either a diesel pool fire or wood crib fire) through (R4) and (R5), and thereby partake in chemical inhibition of the combustion processes driving the fire through interruption of the H, OH, O radical pool necessary to sustain hydrocarbon combustion processes. Stable potassium hydroxide (KOH), an inorganic compound is a terminating product of this reaction as well.

$$K^+ + OH^- \rightarrow KOH \qquad (R4)\ [23]$$

$$K^+ + H_2O \rightarrow KOH + H^+ \qquad (R5)\ [23]$$
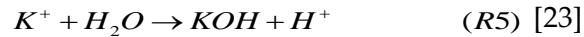
Of course, many other intermediate steps are involved in these processes depending on the fuel and ventilation conditions of the fire as well. One series of these may also lead to the formation of nitrogen oxides (N_xO_y) during decomposition of potassium nitrites as they interact with the combustion process. In the first instance, NO and NO_2 can be formed directly during thermal decomposition of potassium nitrate (KNO_3) following a route involving direct decomposition to potassium nitrite (KNO_2) with subsequent production of potassium oxide (K_2O), nitrogen dioxide and nitric oxide per,

$$2KNO_3 \rightarrow 2KNO_2 + O_2 + heat\ (1200^0C) \qquad (R6)$$

$$2KNO_2 + heat\ (410^0C) \rightarrow K_2O + NO_2 + NO \qquad (R7)\ [24]$$
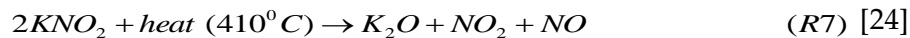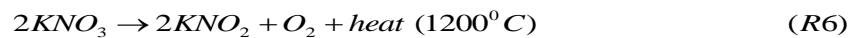
Additional NO₂ and NO formation can occur through side decomposition reactions as well, such as that of ammonium bicarbonate (NH₄HCO₃), which is sometimes found in the propellant mixtures and can impact OH⁻ consumption as well [18].

Formation of NO and NO₂ through the thermal decomposition of ammonium bicarbonate (NH₄HCO₃) again involves a large number of reaction paths, per a combination of (R9) through (R13), which will likely occur in combination with nitrogen oxide formation mechanisms commonly encountered during combustion reactions and discussed in the next section [25].

$$(NH_4)HCO_3 + heat\ (35^0C) \rightarrow NH_3 + CO_2 + H_2O \qquad (R8)\ [26]$$

$$NH_3 + OH \rightarrow NH_2 + H_2O \qquad (R9)$$

$$NH_2 + OH \rightarrow NH + H_2O \qquad (R10)$$

$$NH + OH \rightarrow NO + H_2 \qquad (R11)$$

$$NO + OH \rightarrow NO_2 + H_2 \qquad (R12)$$
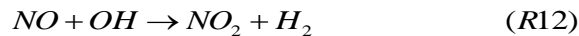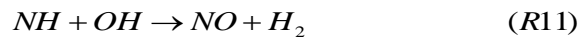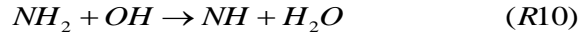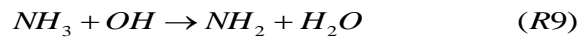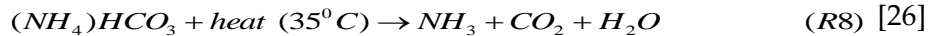
2.3 NOₓ Formation in the Combustion Environment

There are three generally accepted ways in which nitrogen oxides can be formed during aerosol production and the combustion processes taking place in the fires of interest in this research. These are the thermal NOₓ or Zeldov'ich mechanism, the prompt NOₓ mechanism and mechanisms related to fuel bound nitrogen [27]. The former two mechanisms may occur in differing levels in both diesel and wood fires, while the latter may be important due to the fuel bound nitrogen generally present in diesel fuels.

Thermal NOₓ is associated with hydrocarbon-air combustion in environments where temperatures range between 1125 to 1725⁰C [28]. In this situation, NO is primarily formed through O-attack on N₂ in the combustion air via reaction (S1) equation [23]:

$$O_2 + N_2 \rightarrow NO + N \qquad (S1)\ [29]$$

As such, formation of NOₓ via thermal mechanisms can occur both in the flames and in the post flame zones [29]; however, in fuel rich, and thus cooler, combustion environments it might be expected to predominate mainly in the hotter and active flaming regions of the fire.

In contrast to thermal mechanisms for formation of NOₓ, the prompt NOₓ formation entails a large number of relatively fast intermediate reactions involving nitrogen and oxygen

9

free radicals. Prompt NO forms in lower temperature regions and under fuel rich conditions, often near the flame zone since it requires the presence of CH_x radicals. In this case, NO is produced via the following route, [28] [29].

$$CH + N_2 \rightarrow HCN + N \qquad (S2)$$
$$N + O_2 \rightarrow NO + O \qquad (S3)$$
$$HCN + OH \rightarrow CN + H_2O \qquad (S4)$$
$$CN + O_2 \rightarrow NO + CO \qquad (S5)$$

[30]
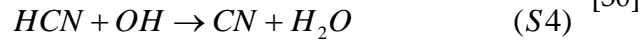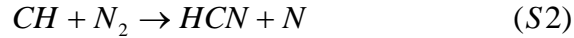
Finally, in fuel bound nitrogen, NO_x is primarily formed through direct oxidation of nitrogen or nitrogen containing compounds in the fuel [28]via a series of reactions similar to those for prompt NO_x and that lead to the formation of nitric oxide (NO) and nitrogen (N_2) [28, 31]. A secondary formation pathway can involve oxidation of nitrogen contained in any char but for the fuels used in this research (diesel and wood), and the generally very limited extent of such reactions even for heavily char forming fuels, this path is not expected to play a role in the present study.

Trends in NO_x formation with equivalence ratio are further explained by Baukal et. al [28]. As the O_2 concentration in the reaction zones increases from fuel rich towards stoichiometric levels, the flame temperature increases which leads to an increase in the formation of NO_x because the thermal mechanism of NO_x formation is exponentially dependent on temperature. As the O_2 concentration continues to increase towards fuel lean conditions, the flame temperature again decreases such that peak values of NO_x would be expected to form, via the thermal mechanism at least, under near stoichiometric conditions [28]. In reality, the highest flame temperatures may be found slightly to the rich side of stoichiometric which may also shift the predicted peak in NO_x formation slightly as well. For the case of a fire, it is hard to postulate what concentrations of NO_x might be formed in a given situation since the formation of NO_x is also impacted by the level of turbulence and turbulent mixing that might occur inside a real fire compartment. Turbulent mixing and air entrainment will tend to produce both temporal and spatial fluctuations in temperature and equivalence ratio, which will significantly influence the NO_x formation rates [29].

Experimental testing carried out by Shihadeh et al. [32] using a diffusion burner and fuel oil no. 6 as a fuel provides some insight into the relative levels of NO_x production across a range of equivalence ratios. For an equivalence ratio (ϕ) of 1.13, on order of 58 ppm NO_x was produced at 2% controlled oxygen (O_2) at the burner exit [32]. In contrast, for a lower equivalence ratio of ϕ = 0.9, the NO_x emissions were measured to be in the range of 90 ppm, while at ratios higher than 1.13, ϕ = 1.4, they dropped to around 55 ppm [32]. For ratios above ϕ = 1.13, the temperature and oxygen concentration are reduced enough that formation of NO_x is lower than for leaner ϕ = 0.9

or near-stoichiometric mixtures [27]. In addition, at higher equivalence ratios there are more unburned hydrocarbons, promoting reactions that further lower the NO_x emissions such as those shown in (N1) through (N3) [27]:

$$CH + NO \rightarrow HCN + O \qquad\qquad (N1)\ [27]$$

$$CH_3 + NO \rightarrow HCN + H_2O \qquad\qquad (N2)\ [27]$$

$$HCCO + NO \rightarrow HCN + CO \qquad\qquad (N3)\ [27]$$
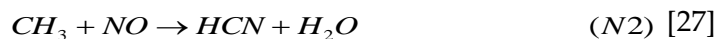
For equivalence ratios higher than $\phi = 1.4$, these reactions can lead to the formation of other nitrogen-containing, and potentially very toxic species such as hydrogen cyanide (HCN), a number of cyano species (CN) and amine species (NH_i) as previously mentioned [27].

If formed during aerosol suppression in fuel rich conditions, HCN might further interact with potassium hydroxide (KOH) to form potassium cyanide or it might react to form cyanite salt or liquid cyanide. One sample reaction of liquid cyanide formation can be seen below.

$$HCN + (H, OH) \rightarrow CN + (H_2, H_2O) \qquad\qquad (N4)$$
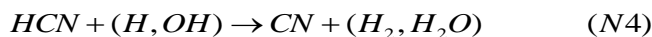
Since the above reactions are clearly dependent on temperature, in attempts to minimize uncertainty inside the test environment, the aerosol canisters were deployed, in so far as possible, into an environment with the same average compartment temperature in every test. The chosen value of 900K was determined by examining temperature traces from the four thermocouples positioned on vertical rakes at locations 200 cm above the compartment floor.

Based on the above discussion, it is clear that it would be an extremely complex task to attempt to determine the equilibrium that would be achieved amongst all the aforementioned competing reaction pathways during aerosol suppression of any fire. As a result, these reactions are presented here to outline some of the many possible pathways that might be involved in the formation of aerosol suppression agents, as well as in their interactions with a fire environment. Aspects of these are also used later to support some of the discussion on chemical compounds that are experimentally observed during the present tests.

2.4 Toxicity and Exposure Thresholds

Based on the above discussion, a series of gases can be identified as important to characterization of the potential toxicity of gases produced during aerosol suppression of fires. By way of setting benchmark concentration values for later comparison with experimental measurements during suppression tests, existing exposure thresholds and guidelines for NO_x, HCN, NH_3 and CO exposure as outlined in occupational health and safety literature are discussed in this section.

Toxicological concentration thresholds for nitrogen oxides (NO_x) are generally specified with respect to measured values of NO_2, since better data exists with respect to toxicology of NO_2 than for NO, and NO_2 is most often used as an indicator for the presence of nitrogen oxides (NO_x). In addition, NO_2 is five times more acutely toxic than NO [33]. That said, it should be noted that there is little consistent evidence of long term health effects with exposure to NO_2 and there is still significant uncertainty in human exposure-response data for both acute (< 3 hour) and long term exposure [34]. According to the World Health Organization (WHO), sub-chronic or acute exposures to concentrations of NO_2 of as little as 2 ppm can have some physiological impacts particularly in the case of children between the ages of 5 and 12, and asthmatic adults [34]. As such, the levels of exposure proposed in the WHO guidelines are 0.1 ppm for continuous 1-hour exposures and 0.02 ppm for long term exposures [34]. In contrast in the USA, the Occupational Safety and Health Administration (OSHA) has set a higher 15-minute exposure limit of 5 ppm for NO_2 in workplace air, with an IDHL of 20 ppm [35]. They also indicate a permissible exposure limit of 25 ppm NO averaged over an 8-hour work shift, with an IDHL of 100 ppm [35]. Other published levels suggest ten minute exposure levels for NO_2 of 5 ppm; while exposure to several hundred ppm over the course of minutes is purported to cause deep lung irritation potentially leading to pulmonary edema or fluid buildup in lungs, which can also lead to death [33]. Although not as pertinent to this work, the EPA has established that the average concentration of NO_2 in ambient air in a calendar year should not exceed 0.053 ppm for outdoor exposures [36]. The above values can be used as benchmark levels against which to compare the NO and NO_x concentrations presented in this thesis, provided that note is taken of the overall lack of sound toxicological data for nitrogen oxides and consequent uncertainty in potential threshold and exposure values [35].

Compounds such as hydrogen cyanide, HCN, are thought to arise during aerosol generation possibly through the secondary reactions of NO in the presence of unburned hydrocarbons and various combustion radicals that were noted above. HCN is particularly worrisome since it is generally considered to be around 30 times more toxic than CO and can lead to serious health complications in humans if inhaled even at the relatively low concentrations and short exposure durations listed in Table 1-1 [37]. Concentration thresholds for HCN exposure are generally specified with respect to a time and type of exposure. Current OSHA guidelines stipulate that an 8 hour time weighted average level of 10 ppm of HCN (including skin exposure) is permissible [37]. In contrast, NIOSH indicates a lower threshold of 4.7 ppm as the 15 minute time weighted average exposure threshold for similar types of exposure. After ten minutes of exposure to concentrations of only 181 ppm, HCN gas will induce pulmonary edema with subsequent failure of the respiratory organs [37]. At the OSHA IDHL limit of 270 ppm, death is almost instantaneous after a few inhalations of HCN [37]. While the literature reviewed does not report measured HCN concentrations due to pyrotechnically generated aerosols that exceed

acute toxicity levels, the danger associated with HCN should dictate a high standard of care and vigilance in understanding the potential for HCN generation. As such, measurements of HCN concentration were attempted during several of the fire and agent only test scenarios conducted in this work.

In addition to the generation of NO_x and HCN during aerosol production, there is also some potential for formation of other nitrogen containing compounds such as ammonia (NH_3) due possibly to the decomposition of ammonium bicarbonate (NH_4HCO_3) to ammonia (NH_3), water (H_2O) and carbon dioxide (CO_2) when it reaches temperatures higher than 36^0C. Concentration thresholds listed for human exposure to NH_3 again differ depending on organization.

Table 2-1: Time to death following hydrogen cyanide inhalation in humans [37]

Dosage		Time to Death
mg/m³	ppm	
122	110	60 minutes
150	135	30 minutes
200	181	10 minutes
300	270	Immediate

Current OSHA guidelines indicate permissible levels of 35 ppm for 15-minute exposure times with 50 ppm threshold levels indicated for 8-hour time weighted average exposure to NH_3 [38]. In contrast, NIOSH indicates a similar permissible threshold of 35 ppm for 15-minute exposure but a lower value of 25 ppm as the 8-hour time weighted average exposure limit [38]. Similarly, ACGIH also indicates a STEL of 35 ppm and 25 ppm over an 8-hour time weighted average [38]. Other sources also suggest IDHL limits of 300 ppm [39]. Although no direct references to concentrations of NH_3 formed during aerosol generation were found in the literature, due to the potential, NH_3 concentration measurements were attempted during several of the fire and agent only test scenarios conducted in this work.

Carbon dioxide (CO_2) and other common exhaust gases are produced from the aerosol units during the combustion process involved in the primary stages of aerosol generation. Depending on conditions in which the oxidation reactions take place, both CO_2 and carbon monoxide (CO) can be produced. CO is a clear, colourless and poisonous gas for which toxicological concentration thresholds are again generally specified with respect to time weighted exposure values, but do vary considerably depending on organization. For example, the levels of exposure proposed in the WHO guidelines are approximately 90 ppm for 15 minute average exposures and less than 10 ppm for 8 hour time weighted average exposures [40]. In contrast in

the USA, the Occupational Safety and Health Administration (OSHA) has set a higher 8-hour weighted average exposure limit of 50 ppm for CO in workplace air, with a ceiling level of 100 ppm [41]. Other published levels suggest 8-hour exposure levels for CO of 35 ppm with ceiling levels of 200 ppm [41]; while exposure to 2000-5000 ppm is purported to cause death in minutes. The National Research Council (NRC) set Emergency Exposure Guidance Levels (EEGLs) for CO based on exposure time as: 10-minute EEGL: 1,500 ppm, 30-minute EEGL: 800 ppm, 60-minute EEGL: 400 ppm, and 24-hour EEGL: 50 ppm with a lethal concentration threshold for humans of 5000 ppm for 5 min [42]. CO levels produced from pyrotechnically generated aerosol units will vary widely based on the solid tablet composition. Kopylov et al. [6] studied the CO production from five different pyrotechnic aerosol combinations, all about 1 kg in initial mass. The study revealed that the concentrations of CO varied between 572 and 4000 mg/m^3 which, based on the molecular weight for CO of 28 g/mol, equates to a concentration range of approximately 464 to 3243 ppm [6]. The range of CO concentrations observed in the experiments in ref [6] highlights how dependent the production of CO is on the initial pyrotechnic tablet composition and reaction conditions, but also that the potential for CO production during aerosol activation should not be overlooked.

Based on review of the public literature [5, 6], it is clear that there is sufficient variability in the stated toxicity of pyrotechnically generated aerosol systems to warrant a more stringent, thorough, and independent toxicology study. Due to such uncertainty, the RN Institute of Naval Medicine approved pyrotechnic aerosols for use in unmanned compartments only, stating that personnel must be able to vacate within two minutes before CO levels become prohibitive [43]. To further investigate this issue, CO concentrations, as well as concentrations of NO$_x$, HCN and NH$_3$ were assessed during agent only and fire suppression scenarios in the present study.

This literature review shows that even though there is some understanding of the aerosol generation and fire suppression, further research and testing is needed to understand certain concerns raised by the proposed use of aerosols as an alternative method for fire suppression. The focus of the present research is to do a more detailed scientific evaluation into the potential impacts caused by aerosol dispersion. The research will look at a subset of gases produced during generation of aerosol powder and fire suppression by two different variants of handheld pyrotechnic aerosols when they are discharged in a repeatable fashion into an environment that closely resembles the conditions of the ISO 9705 fire test method. By controlling key parameters inside the testing environment, such as thermal layer, time of suppression and suppression technique, a better understanding will be gained of the gases produced during aerosol generation and fire suppression. In addition to examination of the gases produced, preliminary experiments were also made to gain further insight into the potential for corrosion of various materials and/or

sensitive electronic hardware by the aerosols generated during cold discharge and fire suppression scenarios conducted in this research.

3   Experimental Apparatus and Techniques

The overall experimental approach adopted in this work follows sections of the IMO MSC Circular 1007 Machinery Space Test Protocol [44]. The Circular provides guidelines for testing aerosol extinguishing systems against machinery space fires as defined by the International Convention for Safety of Life at Sea (SOLAS). The protocol as written, however, is more applicable to testing of larger scale fitted aerosol extinguishing systems than to handheld aerosol extinguishers appropriate for use in the smaller spaces of interest in this work. Hence, for the present research this protocol was reviewed and those portions deemed most applicable to handheld aerosol extinguisher evaluation were incorporated into the experimental plan. Further, the experimental plan was held consistent with that used for related research into other aspects of the aerosol extinguishing units [45, 46].

3.1   Burn Compartment

The burn compartment used in the aerosol testing was the University of Waterloo modified 6.1m (20ft) shipping container. It was configured for tests as shown in Figure 3-1 and Figure 3-2 below and described in detail in [46]. This burn compartment closely mimics the specifications set by the ISO 9705 room fire test environment [47].

As shown in Figure 3-1, the UW shipping container facility is comprised of two sections, the burn room and the control room. The control room holds all of the electrical equipment to support testing, including the field point data logger used for data acquisition and electrical cabling used for powering the instrumentation. The burn room measures 2.4 m wide x 3.6 m long x 2.4 m tall, for a total volume of 20.74 m^3. At one end is a door measuring 0.91 m wide x 1.75 m tall which provides ventilation to the compartment. The compartment walls and ceiling are made of 2 mm thick Corten steel, insulated with a 25.4 mm layer of Fibrefrax Durablanket insulation and clad with 1.25 mm (18 gauge) aluminum sheeting. The floor is finished with fire brick [48]. Temperatures in the compartment were monitored throughout each test using 80 Type K thermocouples. These were positioned to measure gas temperatures across six vertical and four horizontal rakes at specific co-ordinate system positions [19].
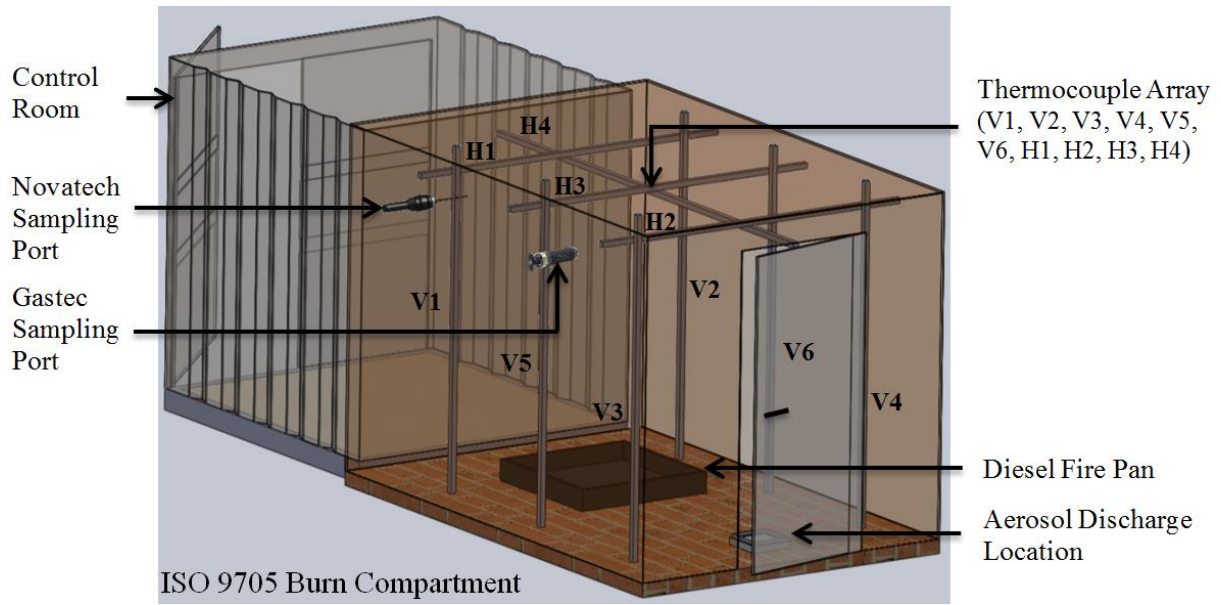
Figure 3-1: Shipping container burn room configured to mimic machinery space onboard navy vessels
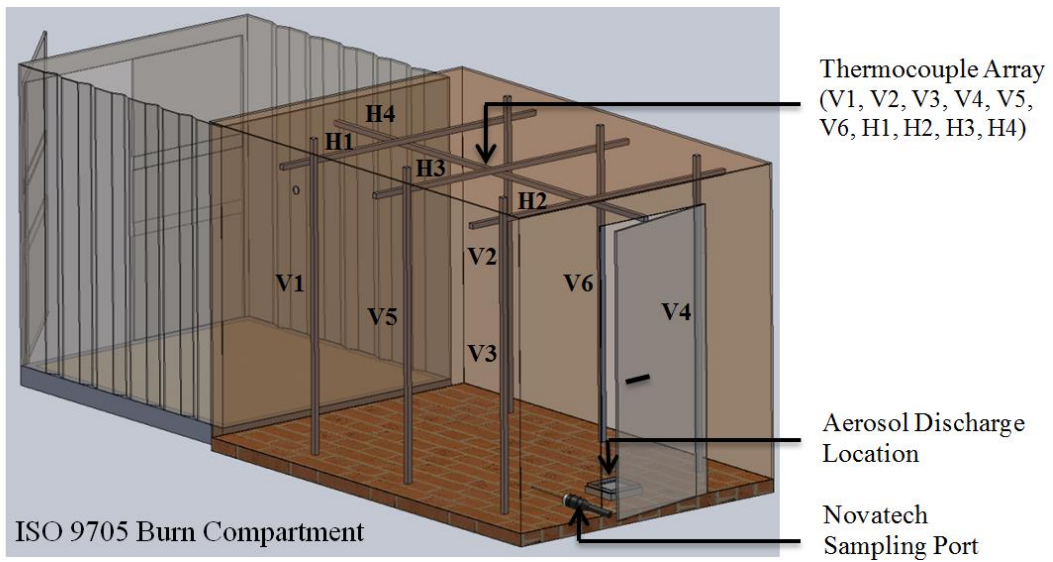
Figure 3-2: UW shipping container burn room configured for agent only test

Gas samples were withdrawn from two gas sampling ports positioned approximately 2 m above the floor and 1 m apart on the same side of the burn compartment as shown in Figure 3-1. The

Novatech P-695 samples were withdrawn from the location closest to the back of the compartment via a 6 m long heated PTFE coated line with an internal graphite filter that prevented particulates from entering the sampling cell. Samples for the Gastec STR-800 unit were withdrawn via a hand pump from a port approximately 1 m away and closer to the door of the compartment Figure 3-2. Both gas sampling ports were positioned high in the compartment for all of the fire characterization and aerosol fire suppression tests.

During the first set of agent only tests, gas samples were withdrawn at a location near the floor of the compartment to measure gas concentrations generated very close to the discharge ports of each aerosol unit, as shown in Figure 3-1. In later agent only tests, samples were withdrawn from high in the compartment Figure 3-2 in order to directly compare data to measurements obtained during fire characterization and suppression tests.

As per the locations above, gases in this study were sampled in regions where the highest concentrations were expected to occur rather than attempting to capture gas samples that might provide either averaged or integrated values of concentration in the compartment. This is because gas concentration measurements are highly dependent on details of the compartment and the fire geometry, location of sampling probe and ventilation conditions in a given experiment. Thus, gas samples withdrawn at the highest ports in the compartment during both suppression and agent only tests provide concentration data representative of those gas concentrations that would be found in the upper layer of a compartment during accidental aerosol discharge or during fire development and subsequent suppression using an aerosol agent. On the other hand, in the aerosol only tests for which the data were sampled close to the discharge of the aerosol unit, measured gas concentrations are indicative of 'worst case', localized gas concentrations that would be seen in gases issuing directly from the unit during activation and discharge. In either case, it must be cautioned that gas concentrations at other locations within the compartment are expected to be significantly different than those reported in the present work. Instead, results presented here are anticipated to represent values close to the maximum concentrations of gases that could accumulate in a compartment and migrate to other areas on a vessel, albeit they would dilute quickly due to significant mixing as they travelled downstream from the present sampling locations, through the compartment and out of a compartment opening.

3.2   Aerosol Units

The two commercial aerosol fire suppression units that were tested in this research were the StatX First Responder® with a single unit rated for use in fire compartments of no more than 20 m^3 and the DSPA Manual Firefighter® with a single unit rated for use in fire compartments of no more than 18 m^3. These are shown in Figure 3-3 a) and b) respectively.

a) StatX First Responder®   b) DSPA Manual Firefighter ®

Figure 3-3: Two different aerosol suppression agents

The aerosol units were supplied by each manufacturer together with design criteria, operating instructions, drawings and technical data. The respective company representatives delivered the aerosol units to UW and provided training and technical support in their use to ensure proper and repeatable activation per manufacturers' instructions. UW maintained a collaborative relationship with both industrial partners throughout the testing [46].

3.3   Test Fires and Programme

Key details of all of the fire loads and scenarios investigated are outlined in this section. The test programme involved the fire loads described in and the scenarios outlined in Table 3-1. Each test listed in Table 3-2, was conducted several times for both aerosol units. The initial fire suppression tests are also described in further detail in [45] and [46].

Table 3-1: Fire loads used in aerosol testing

Fire	Type	Fuel	Fire Size, MW
A	0.82 m² with 10 ℓ of diesel over a 105 ℓ water base	Diesel	0.9
B	Softwood crib	Spruce	0.12
C	0.1 m² tray with 0.2 ℓ methanol	Methanol	0.03
D	Butane lighter	Butane	0.0005

Table 3-2: Aerosol suppression test programme

Test No.	Fire Suppression Test Scenarios
	Characterization Fire: 0.82 m² tray unobstructed diesel pool fire with no suppression Gas concentration measurements and exposure of material coupons (mild and high tensile steel, copper beryllium, computer disc, Nomex and computer boards)
1	Fire A: 0.82 m² tray as unobstructed diesel pool fire Gas concentration measurements and exposure of material coupons (mild and high tensile steel, copper beryllium, computer disc, Nomex and computer boards), copper beryllium, high tensile and medium tensile steel, circuit board and CD disc.
2	Fire A: 0.82 m² tray as an obstructed diesel pool fire under engine enclosure mock-up Gas concentration measurements
3	Fire A: 0.82 m² tray as obstructed diesel pool fire under engine enclosure mock-up; activate extinguisher, slide into fuel pan to simulate units falling into a watery bilge Gas concentration measurements
	Characterization Fire: Four softwood cribs near back wall of test room as unobstructed Class B fire with Fire C: as an ignition source – 1 methanol ignition fire Gas concentration measurements taken
4	Fire B: Four softwood cribs near back wall of test room as unobstructed Class B fire with Fire C: as an ignition source – 1 methanol ignition fire Gas concentration measurements and aerosol suppression performed
5	Fire D: Activate unit in burn room with no fire Gas concentration measurements and exposure of material coupons (copper beryllium, high tensile and medium tensile steel, Nomex, open computer tower, circuit board and computer disc).

3.3.1 Characterization Tests

Reference conditions for the tests were set via characterization tests which used an unobstructed diesel fire, Fire A, with no suppression. The door of the compartment was set to three different conditions: fully open, open to 0.3 m gap and fully closed. In a second set of characterization tests, an unobstructed wood crib fire, Fire B was used with the compartment door open to 0.3 m. This fire scenario was designed to simulate a general 'Class A' fire in a shipboard compartment.

3.3.2 Suppression and Agent Only Tests

The two handheld aerosol units were employed against the four different instrumented fire scenarios (unobstructed diesel, obstructed engine enclosure fire, obstructed bilge fire and softwood crib fire) and also deployed in an aerosol agent only scenario. The first fire scenario was the same open diesel pool fire as used during the compartment characterization tests, Fire A, where the fire was allowed to reach a steady state burn before the unit was deployed. The second fire scenario consisted of an obstructed diesel fire, again based on Fire A, where a 1.4 m x 1.3 m x 0.46 m steel structure was suspended 0.4 m over the floor to simulate an engine enclosure. The third scenario, again involving Fire A as the base fire, involved activation of the extinguishers and then placing them into a pan of water 0.3 m deep to simulate the units falling into a watery bilge. The final fire scenario was a wood crib fire, using Fire B and designed to simulate a general 'Class A' fire in a shipboard compartment. As a reference case, the units were also discharged into the test compartment when no fire was present (agent only). Once the agent was activated in the agent only tests, the compartment door was sealed for the duration of the experiment.

In the final diesel characterization, and the initial series of unobstructed diesel, obstructed engine enclosure and softwood crib fires, the door was held open (with a set 0.3 m opening) after discharge of the aerosol agent, while the door was closed immediately after discharge during the obstructed bilge fire and agent only tests. A second round of testing was conducted for comparison and enhancement of these initial results. In the second round tests, the compartment door was closed after discharge of the agent and was held shut for the 10-15 minute duration of the test for all four fire and the agent only scenarios.

3.4 Gas Analysis Instrumentation and Test Methods

In all tests, gas concentration data were gathered using a Novatech P-695 measurement system, capable of detecting unburned hydrocarbons (UHC), nitric oxide (NO), nitrous oxides (NO_x), oxygen (O_2), carbon monoxide (CO) and carbon dioxide (CO_2). In addition, a Gastec STR-800 hand pump system with pre-calibrated gas absorption tubes was employed during some tests to measure NO and NO_2, as well as additional compounds such as hydrogen cyanide (HCN) and ammonia (NH_3). Since there is not a well-defined standard test procedure for gas analysis during full scale fire experiments, a variant of the ASTM E-800-5 standard test method was adopted for

gas concentration sampling and measurement in the present work [49]. Details of the instrumentation and methods are contained in the sections below.

3.4.1   Novatech Gas Sampling System

A Novatech P-695 system was directly connected to the heated gas sampling line shown in Figure 3-1 and was used to measure concentrations of NO, NO_x, CO, CO_2, O_2 and UHC with built-in analyzers [50]. These included a TML 41H system for measuring NO and NO_x and thus deducing concentrations of NO_2, Servomex 4900C gas analysers for measuring O_2, CO_2 and CO and a Baseline 8800H unit for measuring total un-burnt hydrocarbons (UHC). Each analyzer was calibrated before every test to ensure consistent 'zero' and 'span' values. During each experiment, the sampling train continuously collected gases at a flow rate of 1.8 ℓ/min and data was output at either 1125 or 2000 millisecond intervals, providing pseudo-time-resolved measurements of concentration in the upper regions of the compartment.

For nitrogen-based compounds, gas samples entered the detection cell where the amount of NO was determined by exposing the sample to ozone and measuring the resulting chemiluminescence signal. The NO_2 in the sample was also converted to NO and the combined concentration was reported as total NO_x [50]. Concentrations of NO_2 were then estimated as the difference between the measured concentrations of NO and NO_x. Oxygen concentrations were determined using paramagnetic sensor technology, while CO and CO_2 concentrations were measured, respectively, via single wavelength IR photometric methods. Finally, total UHC were determined via flame ionization detection. In all cases, voltage outputs from the detectors, linearly related to concentration, were sent to a National Instruments Compact Field Point distributed data logging system that allowed remote placement of the analogue to digital (A/D) signal conversion hardware. A conventional Ethernet protocol was used to communicate with multiple A/D units and to transfer the digitized signals back to a central computer located in the burn facility control room. The sampling frequency was either 1125 or 2000 millisecond as previously mentioned and all gas concentration channels were recorded simultaneously [46].

3.4.2   Novatech Sample Lag Time

There is an inherent time lag in the response of the Novatech P-695 system to a change in concentration due to the length of sample lines used in the experiments and the inherent time response of each sensor. Since it is important to account for this delay during analysis and interpretation of measured gas concentrations, the raw data file from each test was analyzed and an appropriate value of the characteristic detection lag time was used in generating the plots shown in Chapter 4.

3.4.3 Operational Principles for Chemiluminescence NOx Sampling

Stringent NO_x limits have pushed industries to re-evaluate safety of the human personnel when being potentially exposed to NO_x gases. Based on the low NO_x emissions and the ever evolving physiological awareness to NO_x, measurement devices are required to be more accurate and precise.

Historically, use of chemiluminescence to detect NO_x/NO has shown to be an accurate and reliable method for effluent gases. The basis for this technique involves NO reacting with ozone (O_3) molecules to create electrically excited NO_2 molecules [51]. Consequently, the newly formed NO_2 molecules produce energy in a light form, at a wavelength between 600 and 3000 nm. From there, the chemiluminescence analyzer utilizes a bandpass filter which truncates the observed wavelengths of light to the analyzer operating range of 600 to 900 nm [51]. The light emission is detected by a photomultiplier tube which is configured to output a voltage signal that is linearly proportional to the NO concentration [51]. The voltage output is converted into parts per million (ppm) using the curve fit derived based on the zero to span voltage pre-calibration curves.

The chemiluminescence analyzer operates in two stages by cycling every 6-10 seconds to facilitate measurement of the concentration of NO_2 as well. In the first stage (discussed above), the sample gas goes directly into the chamber where the NO concentration is measured. In the second stage, a valve cycles and the sample gas is sent to a catalytic convertor where it reacts with the molybdenum chips which are at a temperature of around 315^0C or 588 K. This chemical reaction converts the NO_2 in the sample gas to NO. The newly formed NO is then passed through the original NO cell where the combined quantity of NO is measured and the signal is output to the readout as concentration of NO_x. Finally, in the analysis software, the NO is subtracted from the mesured amount of NO_x to determine the concentration of NO_2. Once the second stage is over, the analyzer cycles again and closes the valve redirecting the sample gas and taking a new measurement of NO and the cycle repeats [52].

During calibration the microporcessor stores the sensor output signal in memory when gases of known NO concentration are passed through the sample train. In addition the microprocessor will use these calibration values along with the signal from the sample gas, temperature and pressure to calculate the final NO_x concentration [52].

While chemiluminescence detectors have proved to be an excellent means of measuring NO_x/NO concentrations inside a pre-defined compartment, they can suffer from some interference caused by CO_2 and O_2 in the effluents being analyzed [51]. A properly calibrated chemiluminescence analyzer should have minimized interferences such that errors would be held within a certain range [51]. For the purposes of this thesis, the equipment being used was a

Teledyne TML 41H analyzer which has a stated error range between 50 to 150mV on NO and NO_x outputs [52], respectively. This is approximately 3% of the span concentration, (i.e. if the span concentration is 1900 ppm the allowable error is ≈ 55 ppm).

3.4.4 Paramagnetic O_2 Analyzer

Using oxygen (O_2) concentration in an exhaust gas stream is one way by which to predict combustion efficiency, often in concurrence with oxygen consumption calorimetry. Currently in the industry, there are many methods available for O_2 sampling, ranging from alkaline pyrogallate chemical absorption to paramagnetic analysis [53]. For the purposes of this thesis, the method for O_2 determination is the Servomex paramagnetic analyzer, solely based on the fact that it is the primary means for detection available at the University of Waterloo Fire Research Laboratory. Oxygen (O_2) possesses strong magnetic properties which can be used to determine oxygen (O_2) concentration in a gas mixture [53]. During a measurement, oxygen (O_2) is attracted into a strong magnetic field inside the analyzer, whereas the other effluents bypass the magnetic field due to their diamagnetic characteristics.

Before start of each experiment analyzer was always re-calibrated using ambient air to read 20.95%, minimizing drift error to negligible amounts [54]. Furthermore, with respect to analyzers precision, Servomex paramagnetic analyzer produces an error of 0.1% for every 10^0C above ambient or 1% of the reading, whichever is greater [54]. Considering the operating temperature range of 900^0K and the fact that gas takes approximately 45 seconds to reach the analyzer, we can take a conservative estimate and assume that the gas would cool off to half of the sampling temperature, or 450^0K [48]. Therefore, the total precision error (assuming 20^0C or 293^0K is ambient) is 1.6 %.

3.4.5 Non-Dispersive Infrared CO and CO_2 Analyzers

Carbon dioxide (CO_2) and carbon monoxide (CO) form due to oxidation reactions taking place during thermal decomposition in aerosol generation, as well as in the fire. The Novatech P-695 system includes Non-Dispersive Infrared Sensors (NDIR), for determination of both CO and CO_2 concentrations. NDIR works on the principle of wavelength absorption, where the sample gas passes through two parallel infrared beams of equal energy that are directed at two corresponding optical cells [55]. A portion of the infrared radiation from each beam is absorbed by the gas (CO or CO_2) and the quantity of radiation absorbed is detected. A current is then outputted which is proportional to the concentration of gas in the sample, based on calibration with known reference gas mixtures prior to each field test [55].

Novatech's P-695 NDIR system has a full-scale measurement range of 3000 ppm for CO and 25% (250 000 ppm) for CO_2. With respect to CO, the errors due to accuracy and repeatability are ± 0.5 ppm [48]. The span drift error for the carbon monoxide is negligible since the analyzer

was re-calibrated at the beginning of each test day and the error from temperature increase is 3% of the reading or ± 1 ppm, whichever is greater [48]. Therefore, the maximum precision error that the analyzer can be off is ± 90 ppm (3%) at 3000 ppm sampled. With respect to CO_2, the errors due to accuracy and repeatability are <1% of the full scale [54]. The total precision error of the CO_2 analyzer is 1.04% of the reading [48].

3.4.6 Gastec STR-800 Sampling System

The sampling probe from a Gastec STR-800 hand pump system was directly inserted into the test container and used to pump known volumes of gases into pre-calibrated gas absorption tubes. Tubes were chosen to measure various concentrations of NO and NO_2, as well as additional compounds such as hydrogen cyanide (HCN) and ammonia (NH_3) during both agent only and fire suppression tests.

With respect to nitrogen oxides tube #10, precision error for NO_2 is 10 % (for the 2.5 to 20 ppm) and 5% (for 20 to 250 ppm), likewise precision error for NO is 10 (for 5 to 20 ppm) and 5% (for 20 to 200 ppm) [56]. With respect to hydrogen cyanide (HCN) sampling, two variations of tubes were used 12M and 12L. Precision error for 12M tube is 10 % (for 50 to 200 ppm) and 5% (for 200 to 800 ppm) [57]. Likewise, the precision error for 12L tube is 10% (for 2.5 ppm to 20 ppm) and 5% (for 20 to 60 ppm) [57]. Similarly to NO_x and HCN, 3M tube for ammonia (NH_3) was used in Gastec STR-800 Sampling and tube's precision error is 5% (for 50 to 500 ppm).

3.5 XRD Powder Analysis

X-ray diffraction (XRD) analysis was conducted on the raw solid aerosol tablets, as the well as on the powder aerosol generated during discharge of each handheld unit using MPD Powder X-ray diffraction system housed in Department of Chemical Engineering, University of Waterloo. For this, raw aerosol agent was collected into electro static bags and samples prepared for analysis. The X-rays are produced by a cobalt source and detection is accomplished using a scintillation counter X-ray point detector that converts the X-Rays into visible light, detected by a photomultiplier system.

The basic principle behind XRD analysis, then, is to determine the diffraction pattern generated through interaction of an X-ray beam with an unknown crystalline material and try to match that pattern to a database of known diffraction patterns from poly-crystalline compounds in order to identify the composition of the unknown powder. Since each crystalline material has a characteristic lattice structure comprised of an atom that is surrounded by electrons, when a crystal is hit by the X-Ray beam, it starts to oscillate with the same frequency to that of the incoming beam. Dependent on the crystal structure, the X-ray beam diffracts in a characteristic way on exit from the crystalline lattice. The angle of the incident and diffracted electromagnetic

waves, theta (θ), are added and the total change in electromagnetic wave angle, 2θ, is recorded. The XRD software then automatically matches the theta diffraction pattern against all the possibilities from a precompiled empirical database of patterns and determines the compound based on the highest percentage match between sample and library spectra [58].

A user can either perform a qualitative or quantitative XRD analysis. Both qualitative and quantitative analysis relies on accurate sample preparation, for which a random sample of 1-2 μm powder will usually produce an accurate set of peak intensities representative of the compound under test [59]. Qualitative analysis further involves identification of various phases as well as the determination of the quantitate proportions of the different phases in a multiphase compound. This is done by matching peak intensities, as well as overlaying an area under each peak in the diffractogram and comparing the measured information to known signature patterns in the databank [59].

3.6   Corrosion Analysis Test Methods

Aerosol residue and its potential corrosive effects were investigated by exposing coupons of various materials and electronic components during agent only tests, as well as unobstructed diesel pool fires with and without aerosol suppression as listed in Table 3-1. Functioning electronic circuit boards were placed within the compartment and subjected to the aerosol during selected tests. After testing, they were inserted into a working computer on a regular basis to determine any effects of aerosol powder residue on longer term operation of a device. An open computer tower was exposed and tested in a similar fashion. The material coupons exposed to aerosol agent included high tensile and medium tensile steels, a copper beryllium alloy, CD discs and Nomex fabric. Coupons were photographed and examined using optical microscopy before exposure to the agent and, immediately after exposure were stored in electrostatic bags in order to preserve any residue that had deposited on the surfaces during the fire suppression. Both the control and the exposed samples were examined visually and under an optical microscope on an approximately weekly basis over several months to monitor the potential for post-suppression damage due to long term exposure to the aerosol particulate.

An Olympus FV optical microscope with six objective lenses (50, 100, 200, 500 and 1000 times normal magnification) was used for the analysis. Images were recorded using a Photometrics Coolsnap camera and image processing done through Image-Pro Premium, version 6.3.0.512. In addition, Nikon D7000 high resolution digital camera was used in conjunction with Nikkor AF 85mm f/1.8 D portrait lens for image capture of pre-exposed coupons.

4 Formation of NO_x, HCN and NH_3 during Aerosol Discharge and Suppression

Measured concentrations of nitrogen oxides (NOx), O_2, HCN and NH_3 for the diesel characterization fires, for each of the four fire scenarios outlined in Table 3-1, and for the agent only tests are outlined and discussed in conjunction with representative compartment temperature profiles in this Chapter. While significant data has been compiled throughout the course of this research, only relevant graphs are contained here to convey the results as they pertain to particular discussion points.

4.1 Diesel Fire Characterization Test Results

To establish baseline concentration levels due to the diesel fires used in the aerosol suppression tests, gas concentration measurements were made during three diesel characterization fires with 1) the door fully open throughout, with 2) the door open to 0.3 m throughout and with 3) the door initially fully open and then closed at approximately three minutes after ignition. Representative values of measured concentrations of NO, NO_2 and NO_x are plotted in Figure 4-1 for the test with the door held open throughout the experiment and in Figure 4-3 for the test in which the door was closed after a hot layer had been established within the compartment. Time temperature profiles measured at various locations within the compartment and at height of 2m above the compartment floor are shown for the same tests in Figure 4-2 and Figure 4-4 respectively. Figure 4-1 and Figure 4-2 are formatted to indicate concentrations of NO and NO_2, with the sum of the two values providing the level of NO_x shown on the plot.

It can be seen from Figure 4-1 and Figure 4-2 that after ignition (0 seconds) for the test in which the door is held fully open, the concentration of O_2 measured in the hot fire exhaust gases near the ceiling of the compartment decreased and the temperatures in the compartment increased as the diesel begins to burn. The concentration of NO simultaneously increased to levels of approximately 25 ppm as the fire reaches steady state burning. Small concentrations of NO_2 are also measured (less than 5 ppm). At 160 seconds into the test, temperatures inside the compartment decline and concentrations of O_2 correspondingly increased, indicating that the fire is dying down. This was further ascertained from the raw video footage of the test.

It can be seen from the figure that combined concentrations of NO and NO_2 from the diesel fire alone remain below 40 ppm throughout the test. Gastec STR-800 samples withdrawn from the upper layer at 178 seconds into this test indicate concentrations of NO of approximately 22.5 ppm and of NO_2 of below 5 ppm respectively, confirming the order of magnitude of the Novatech P-695 measurements. In contrast, no measurable concentrations of NH_3 are detected in the Gastec STR-800 samples withdrawn at 280 seconds into the test.
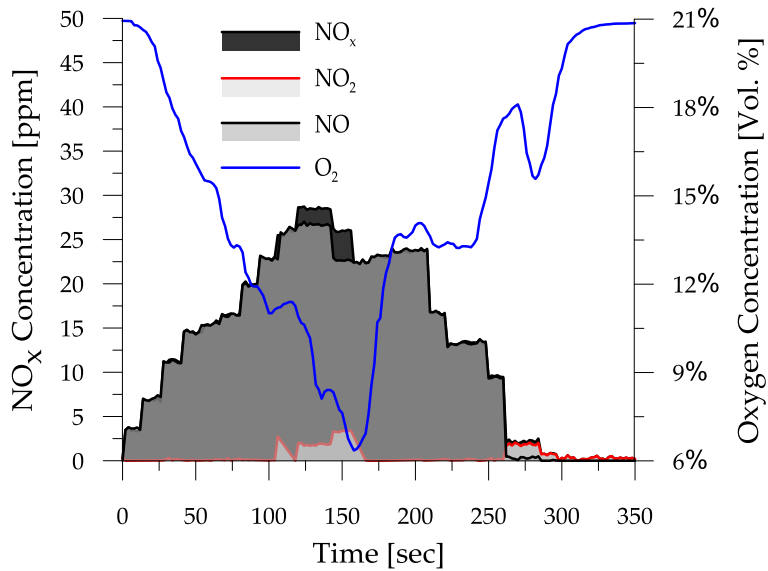
Figure 4-1: Measured NOₓ concentrations during a diesel fire characterization burn with a door fully open
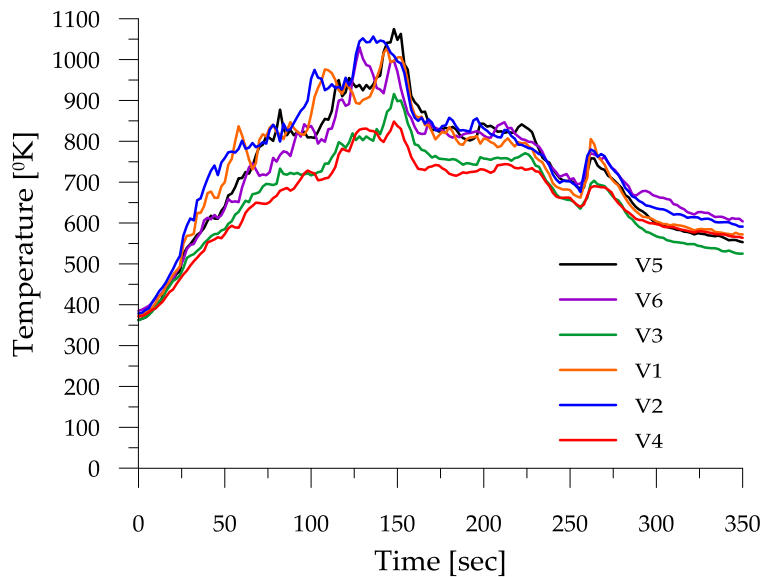
Figure 4-2: Measured temperature profiles during a diesel fire characterization burn with door fully open

For the two diesel characterization fires in which the door was held open at 0.3 m through the test (not plotted here) and for those in which the door was initially held open and then fully

closed at 3 minutes into the test (Figure 4-3 and Figure 4-4), concentrations of O_2 in the hot fire exhaust gases decrease and temperatures in the compartment increase in a similar fashion to those plotted above for the case with the door fully open. Concentrations of NO also grow after ignition, reaching slightly higher peak values than those seen for the test with a fully open door, between 20 and 25 ppm. This is most probably due to the containment of hot combustion gases within the test compartment. Once the door is closed, temperatures first decrease quickly and then decrease more slowly for the duration of the test. O_2 concentrations decrease slowly and NO levels gradually decay throughout the remaining duration of the test likely due to leakage from, and mixing within the compartment coupled to confinement and gradual extinguishment of the fire. In both of these latter tests, concentrations of NO_2 remain below 5 ppm throughout the test, as they did for the case with the door fully open, but the NO_2 concentrations appear to increase just after the fire is confined and then persist to the end of the test suggesting perhaps that some NO is being converted to NO_2 in the fuel rich gases of the confined fire. Combined levels of NO and NO_2 (i.e. total NO_x) again remain below 25 ppm for the full duration of the fire scenario.

Again, Gastec STR-800 samples confirm the order of magnitude of NO and NO_2 concentration measured by the Novatech P-695 system, and indicate that there is no measurable concentration of NH_3 in the upper layer gases.
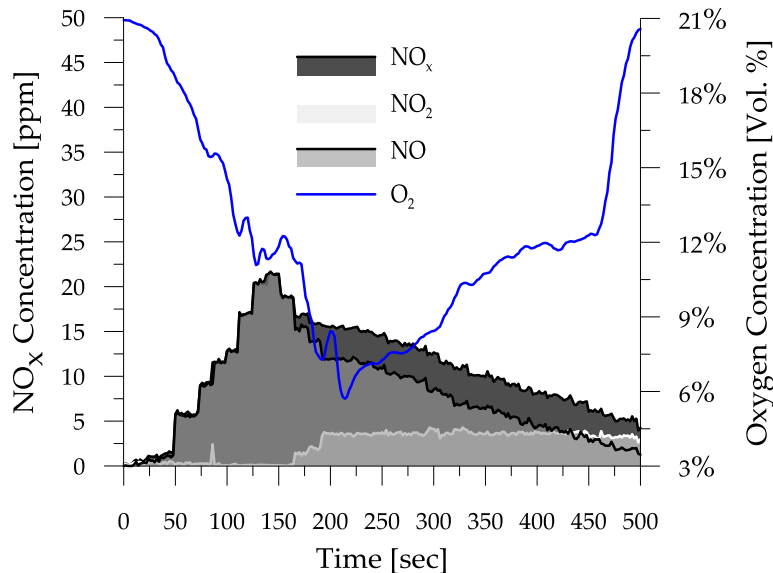
Figure 4-3: Measured NO_x concentrations during a diesel fire characterization burn with a door fully open and then closed after development of hot layer (900°K)
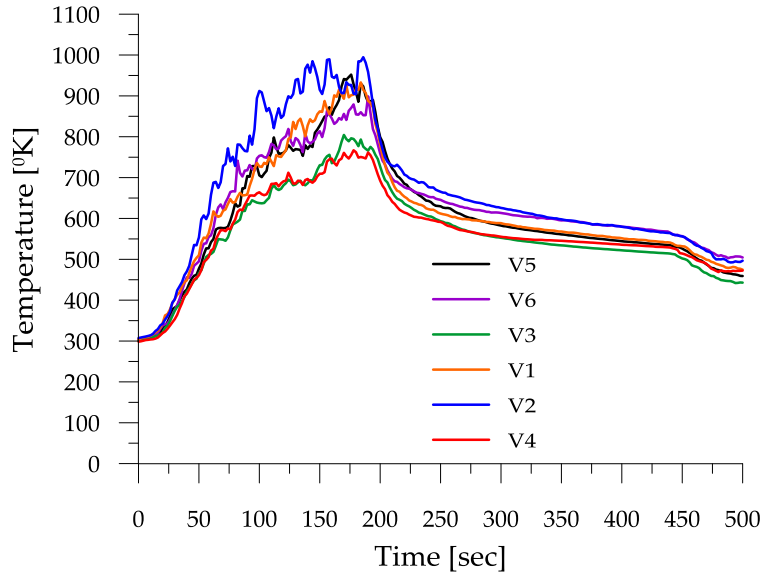
Figure 4-4: Measured temperature profiles during a diesel fire characterization burn with door fully closed.

4.2 Discussion of Diesel Fire Characterization Test Results

As discussed previously, both NO and NO_2 contribute to the total NO_x produced during the characterization fires. As expected based on literature relating to the combustion of diesel fuel, measured concentrations of NO are 3-10 times higher than those for NO_2 [60]. Measured concentrations of NO are in the range of experimental values obtained by Shihadeh et al. [32], when a similar test was performed using Oil No. 6. The average NO_2 concentrations in the hot gases from the diesel fire, when averaged across the 3 minute period of the open diesel burn, are well below threshold levels established by OSHA [35] and barely exceed one hour average exposure levels proposed by WHO [34]. Additional NO or NO_2 generated as a result of the aerosol activation, however, might exacerbate this situation during aerosol suppression of compartment fires. Therefore, NO_x concentration data measured during the various aerosol suppression scenarios are presented and discussed in the following sections.

4.3 Results for Unobstructed Diesel Burn with StatX Suppression

Concentrations of NO, NO_2 and NO_x were measured during four different unobstructed diesel burns with StatX aerosol agent suppression. Measured concentrations of nitrogen oxides are plotted (left hand axis) against time for the case with a 0.3m open door in Figure 4-5 and in Figure 4-7 for a representative case where the door was closed immediately after agent was discharged into the compartment. In both plots, measured O_2 concentrations are also plotted (right hand axis)

to indicate the state of the fire in the compartment at any time. Corresponding compartment temperature profiles for the case with the door held 0.3 m open are in Figure 4-6. In the latter test (Figure 4-7), after a fully developed fire was established within the compartment (hot layer temperatures of 900K), an aerosol unit was discharged and the compartment door was immediately closed and kept sealed for 10-15 minutes with the intent to compare results against 10 and 15 minute short term limits for exposure to NO_x [33, 34, 35]. To supplement the information on NO_x evolution, additional measurements of NH_3 and HCN concentration were made using the Gastec STR-800 sampling system in some of the tests.

For the StatX diesel fire suppression test shown in Figure 4-5 and Figure 4-6 with the door held open at 0.3m, NO levels increase after ignition of the diesel pool (0 seconds), reaching values typical of those measured during the diesel characterization fire discussed in Section 4.1. Upon activation of the StatX aerosol unit (129 seconds after ignition), measured concentrations of NO increase sharply to values exceeding 250 ppm, and then decrease back to ambient levels with time. This steep increase in NO concentration corresponds to the sharp decrease in temperature seen in Figure 4-6, confirming the potential relationship between the activation of the aerosol unit, the slight delay seen before onset of suppression (as evidenced by the delay in increase in measured concentrations of O_2 in Figure 4-5) and increased levels of NO measured in the compartment upper layer. Following this point, as concentrations of NO decrease, measured concentrations of NO_2 (175 seconds) increase to peak values of approximately 50 ppm, and subsequently decrease back to ambient levels (260 seconds). High values of NO_x are sustained for only a very short period of time (Figure 4-5) and hot layer temperatures quickly decrease because the compartment door is kept open during the test, allowing the hot upper layer gases to easily mix with ambient air and to escape from the compartment after suppression of the fire.
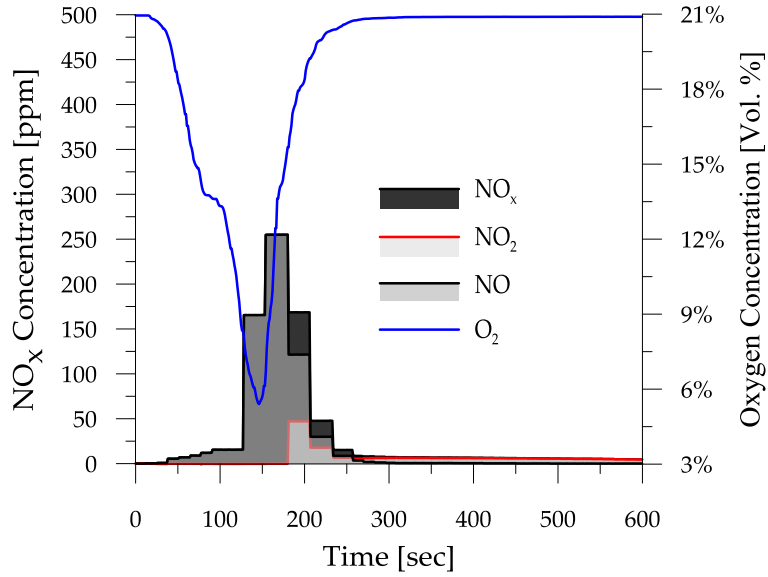
Figure 4-5: Measured NOₓ concentrations during unobstructed diesel burn, StatX suppression, door open
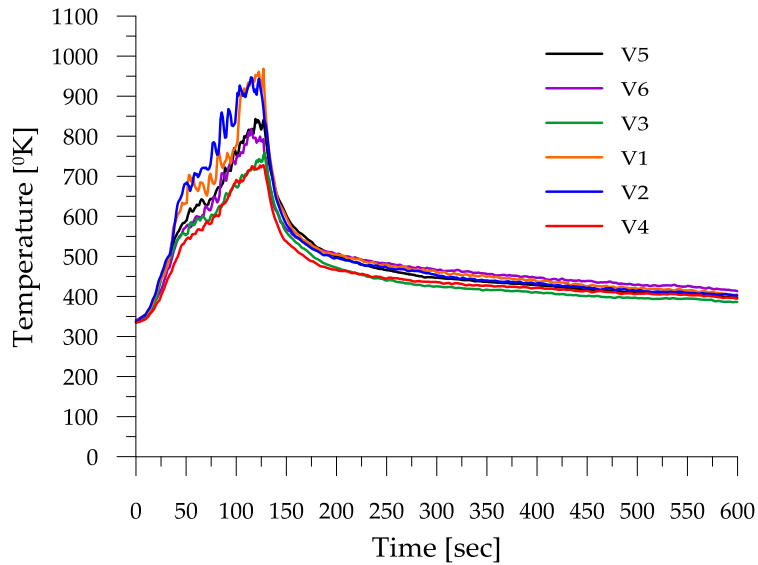
Figure 4-6: Measured temperature profiles during unobstructed diesel burn, StatX suppression, door open.

Results from a StatX suppression test conducted with the door closed immediately after activation of the aerosol unit are plotted against time in Figure 4-7. As with all other tests, measured concentrations of NO and NO_2 before activation of the unit are consistent with those measured during diesel characterization fires discussed in Section 4.2. After discharge of the

aerosol unit at 138 seconds after ignition of the fire, concentrations of NO increase to peak values of around 300 ppm and since the compartment door is closed, they decay fairly slowly over the remaining 10-15 minute duration of the test. Temperature profiles (not shown here) again confirm the correspondence between activation of the aerosol unit, suppression of the fire and notable variations in the levels of NO_x measured in the upper layer of the compartment. At the same time as NO concentrations increase, NO_2 concentrations increase to sustained values that are lower than NO concentrations, ranging between 65 and 75 ppm throughout the measurement period in this test and 65 to 100 ppm across all StatX diesel fire suppression tests that were conducted. The high concentrations of NOx in the upper gas layer, above 300 ppm, were confirmed through data from two more recent tests, which suggested that even higher concentrations of NO might be seen for short periods under some circumstances.
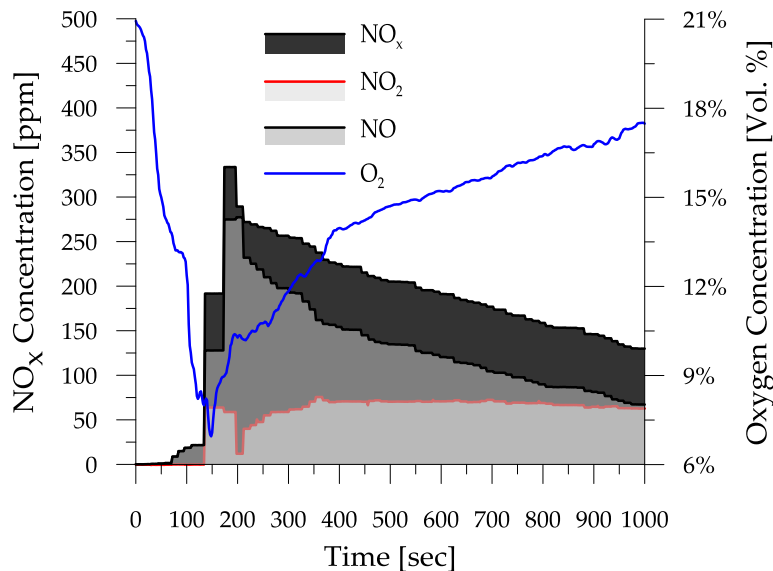
Figure 4-7: Measured NOx concentrations during diesel burn, StatX suppression, and door closed

Concentrations of NO and NO_2 measured using the Novatech P-695 system and plotted in Figure 4-7 were further compared to concentrations measured via Gastec STR-800 taken at 192 seconds into the test. In contrast to results presented in Figure 4-7, the Gastec STR-800 tubes indicated concentrations of NO and NO_2 of around 200 ppm as demarcated by the left edge of the thick black tape on the upper (NO_2) and lower (NO) sampling tubes shown in Figure 4-8. While these confirm combined NO_x concentrations of between 350 and 400 ppm, the NO_2 concentrations determined using the Novatech P-695 and Gastec STR-800 sampling systems do differ

significantly. Possible explanations include sensitivity of the Gastec STR-800 tubes and sampling system to interference from secondary species and soot in the gas stream [56], differences in gas sampling location and thus residence times and temperatures in the hot gas layer, differences in sampling methodology between the two systems, error in reading and marking the gas sampling tubes, and errors inherent in the methods by which the Novatech P-695 system deduces the concentration of NO_2 [50]. Nonetheless, the order of magnitude of the combined results suggests consistency across the measured concentration of total NO_x.

Figure 4-8: NO and NO2 concentrations measured using Gastec STR-800 tubes during suppression of diesel fire using StatX aerosol unit inside the UW burn room (192 seconds)

In addition to the NO_x measurements presented above, additional Gastec STR-800 samples were withdrawn at times of 520 seconds and 640 seconds into the test shown in Figure 4-7 to determine respectively whether any HCN or NH_3 was present in the hot layer gases after discharge of the aerosol unit. It can be seen, based on the left hand side of the black tape in Figure 4-9 that no measurable concentrations of HCN was observed in this test, or in any of the diesel fire suppression tests to date. In contrast, NH_3 concentrations of approximately 105 ppm were recorded in the present test as indicated by the left edge of the yellow tape on the sampling tube in Figure 4-10. Gastec STR-800 sampling at different times during several other tests confirmed the potential for NH_3 concentrations in the upper hot gases to reach values between 60 and 90 ppm during agent discharge into a closed compartment.

Figure 4-9: HCN concentration measured using a Gastec STR-800 tube during suppression of a diesel fire using StatX aerosol unit inside the UW Burn room (520 seconds)

Figure 4-10: NH3 concentration measured using a Gastec STR-800 tube during suppression of a diesel fire using a StatX aerosol unit inside the UW burn room (640 seconds)

4.4 Results for Unobstructed Diesel Burn with DSPA Suppression

Concentrations of NO, NO_2 and NO_x were measured during four different unobstructed diesel burns with DSPA aerosol agent suppression. Measured concentrations of nitrogen oxides are plotted (left axis) against time for one case with a 0.3m open door in Figure 4-11, while Figure 4-12 shows concentrations for the scenario in which the door was closed and sealed immediately after agent was discharged into the compartment. In both plots, measured O_2 concentrations are plotted against the right hand axis to indicate the state of the fire in the compartment. Additional measurements of NH_3 and HCN concentration were made using the Gastec STR-800 sampling system.

For the burn shown in Figure 4-11 in which the door is held 0.3 m open, NO and NO_2 levels first increase to values typical of those observed during the diesel characterization fire discussed in Section 4.2. Upon activation of the aerosol unit at 130 seconds after ignition, concentrations of NO and NO_x seen in the upper hot gases increase sharply to very high values, reaching levels near 400 – 500 ppm but unfortunately cap out at the saturation limit of the detection system (i.e. peak concentrations exceeded the detection limit of 500 ppm). Levels of NO_2 rise slightly after discharge of the agent and appear to reach values of between 50 and 100 ppm as the concentration of NO decreases at around 200 seconds into the test; however, measured NO_2 values are suspect in this test since they are determined as the difference between the NO and the NO_x values and therefore cannot be accurately determined when the detector is saturated. Once the NO and NO_x values decrease well below saturation, more representative values of NO_2 are again measured. Increasing O_2 concentrations in the compartment immediately after activation of the aerosol Figure 4-11, coupled with decreasing compartment temperatures (not shown here) indicate that the fire is partially suppressed shortly after aerosol activation. Following this, however, the fire again establishes itself until it is fully suppressed by oxygen starvation at 255 seconds after ignition. After this time, the levels of NO_x also decrease back to ambient concentrations due to mixing with air and ventilation through the 0.3 m door opening used for the tests. Accounting for the detection limits of the system, it is fair to say that relatively high concentrations of both NO and NO_2 were present in the upper layers of the burn compartment at the present measurement location for a period of time after discharge of the agent, even with a 0.3 m door opening.
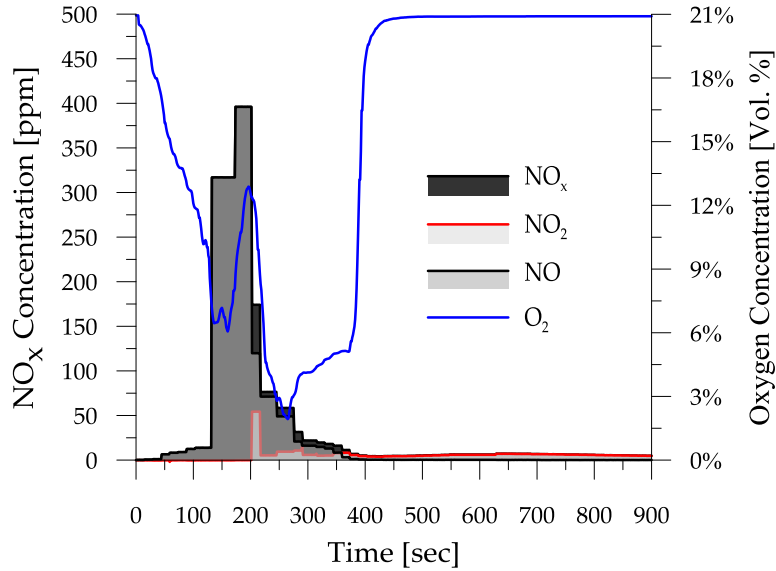
Figure 4-11: Measured NOₓ concentrations during diesel burn, DSPA suppression, door open

Subsequent to the test above, the same test was repeated except the compartment door was closed immediately after discharge of the agent. This scenario was intended to generate a 'worst' case scenario in which any gases generated due to interactions of the agent with the pre-existing hot fire gases would be trapped in the upper hot gas layers. In the identical earlier tests (not shown here), the detectors again saturated at concentrations of over 500 ppm almost immediately upon activation of the unit and remained saturated until the end of the test 10 minutes later since there was minimal ventilation and mixing in the closed compartment.

To better determine peak concentrations of gases which the accrue from discharge of the extinguishing agent into a compartment in which a fully developed diesel fire is burning, the Novatech P-695 NO and NOₓ detectors were modified and recalibrated to allow detection of concentrations as high as 1800 ppm. Results from one of several repeat tests conducted with the door closed immediately after activation of the aerosol unit are plotted against time in Figure 4-12. As with all previous tests, measured concentrations of NO and NO_2 before activation of the unit are consistent with those measured during diesel characterization fires discussed in Section 4.2. Between 60 and 120 seconds into the test, there appears to be a significant build-up of nitrous oxides locally at the position of the sampling probe just before the door is opened and the unit activated. After activation of the aerosol unit (136 seconds), the compartment door is closed and concentrations of both NO and NOₓ increase sharply to very high values. Suppression of the fire is further confirmed through the corresponding decrease in measured temperatures in the compartment. Right after the activation of the aerosol unit levels of NO appear to peak at values of around 775 to 800 ppm before decreasing again, though during repeat tests it has been

36

observed that actual peak values can vary substantially as a result of other factors which affect the interactions between the agent, fire and compartment hot layer, for example, ventilation and temperatures within the fire compartment during and after agent discharge. In the test scenario shown, even despite the increased detector range, NO_x concentrations climb to levels near the new saturation limit of the detection system. Although NO_2 concentrations during this period are again quantitatively suspect, it appears that they do increase to high levels - possibly due to a shift in equilibrium between production of NO and NO_2 as the compartment cooled with the suppression of the fire. Similar shifts in NO/NO_2 balance are seen in other tests as well. Finally, because the door remains closed, the concentrations of all species remain high through the duration of the 10 min test.
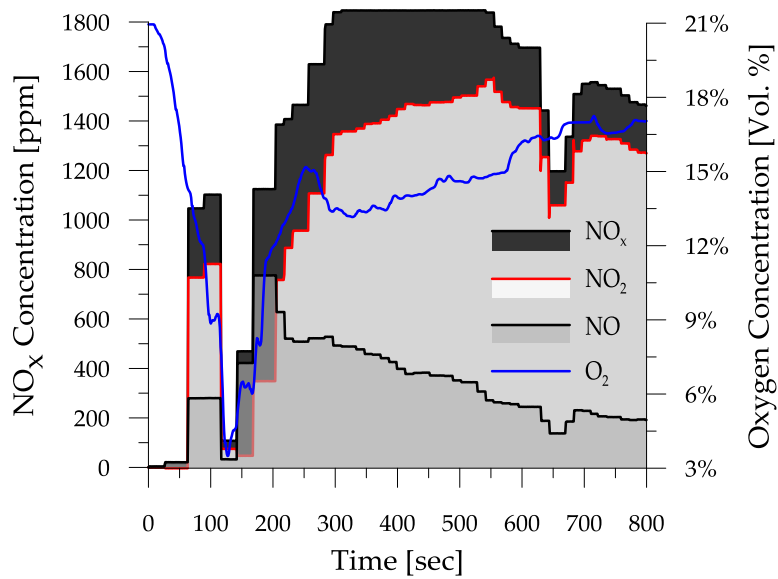
Figure 4-12: Measured NO_x concentrations during diesel burn, DSPA suppression, and door closed

The high concentrations of NO and NO_2 measured using the Novatech system were confirmed via Gastec STR-800 samples taken at around 340 seconds into the test shown in Figure 4-13. The absorbent in the sampling tubes saturated almost immediately during withdrawal of the hot gases indicating concentrations of both NO and NO_2 well over the 200 ppm threshold of the tubes and consistent with high levels such as those illustrated in Figure 4-12 .
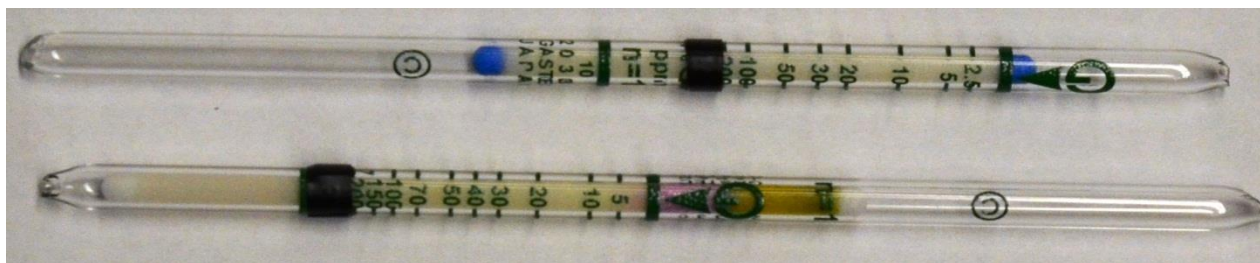
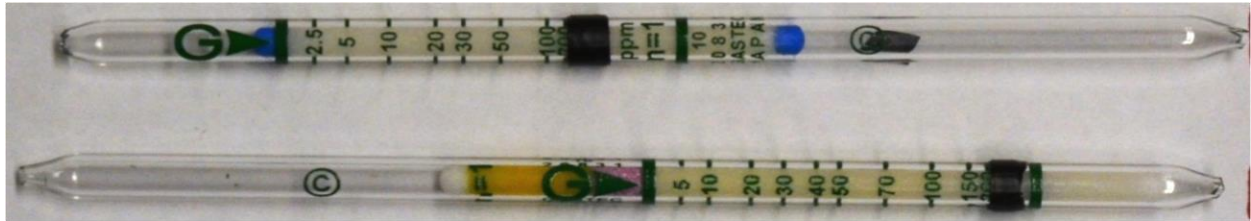**Figure 4-13: NO and NO₂ concentration measured using Gastec STR-800 tubes during suppression of a diesel fire using a DSPA aerosol (340 seconds)**

In addition to the NO_x measurements presented above, additional Gastec STR-800 samples were withdrawn at times of 490 seconds and 630 seconds into the test shown in Figure 4-12 to determine respectively whether any HCN or NH_3 was present in the hot layer gases after discharge of the aerosol unit. While no measurable concentrations of HCN were observed, NH_3 concentrations of approximately 500 ppm were recorded as marked by the left hand edge of the yellow tape on the sampling tube in Figure 4-14. The potential for NH_3 concentrations in the upper hot gases to exceed 500 ppm was also confirmed via Gastec STR-800 samples obtained at approximately the same time in a previous test.
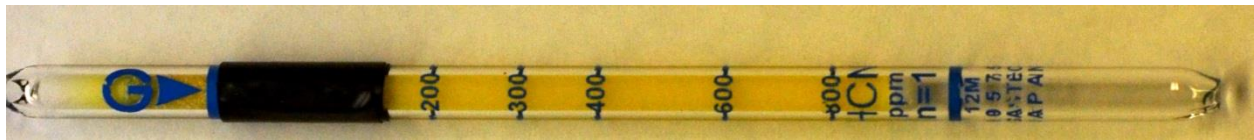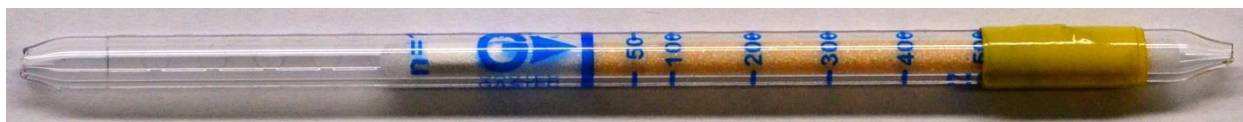

Figure 4-14: NH3 concentration measured using a Gastec STR-800 tube during suppression of a diesel fire using a DSPA aerosol unit inside the UW burn room (630 seconds)

4.5 Summary and Discussion of Open Diesel Fire Agent Suppression Results

Comparison of gas concentrations measured during StatX and DSPA activation and aerosol suppression of open diesel fires in the present compartment, Figure 4-5, and Figure 4-7 through Figure 4-12 respectively, suggest that, during and immediately after activation for both variants of aerosol extinguisher, both NO and NO_2 are produced at levels exceeding those expected due to the fire itself. The DSPA unit appears to contribute to the generation of considerably higher levels of and NO, NO_2 and NH_3 in comparison to the StatX unit, at least during the present tests.

Independent of suppression agent employed, peak measured concentrations of NO in the hot gases of the upper layer of the compartment surpass the IDHL limit for occupational exposure of 100 ppm set by OSHA [35]. During the DSPA suppression tests discussed here, the reported values of NO_2 concentration are not quantitatively reliable due to saturation of the Novatech P-

695 NO_x detector; no similar problems were identified for the StatX results although uncharacteristically high concentrations of NO_x were seen in one test. Nonetheless, for both aerosol units tested, measured NO_2 concentrations quickly rose to values that far exceed the 1-hour continuous exposure limit proposed by WHO [34], as well as both the OSHA IDHL and OSHA 15-minute exposure thresholds [35]. In addition, measured concentrations of NH_3 are well above the published exposure threshold values for both types of aerosol unit.

Caution is required in interpreting all of these results in terms of the global concentration of any of the above gases that might accrue during or after suppression of a fire. First, it must be emphasized that the fire scenarios tested represent aerosol suppression of diesel fires in small compartments under a 'worst' case situation, when the door is closed and the compartment confined immediately after the suppression unit is deployed. Thus any gases produced are essentially trapped within the upper layers of the compartment. In other situations the gases would likely be quickly diluted through mixing and ventilation throughout the space. Indeed, in other scenarios, when high concentrations are observed, they are often sustained for short periods of time. Secondly, the high reported concentrations are measured only locally by a sampling probe that withdraws gas from a single point which is immersed deep within the hot upper layer gas layer. As such, the probe will pick up changes in concentration due to variations in the combustion processes within the fire as it is suppressed, as well as those directly resulting from discharge of the aerosol agent and its interactions with other gases in the compartment. Therefore, concentrations in other locations within the compartment may be considerably different than those presented. Nonetheless, the preliminary single-point data presented here indicate the potential for formation of high concentrations of NO_x which points to a need for additional investigation into the emissions from both units and certainly underlines the importance of developing appropriate safety and operational procedures for use of handheld aerosol extinguishing units to minimize the likelihood that personnel could be exposed to levels above an OSHA threshold during conduct of normal fire response activities.

4.6 Results for Obstructed Diesel Burn with StatX Suppression

Following tests with the open diesel fire discussed above, two additional tests were conducted to measure concentrations of NO, NO_2 and NO_x during obstructed diesel fire tests in which a 1.4m x 1.3m x 0.46m steel structure was suspended above the diesel pool fire to simulate a fuel spill fire under an engine enclosure. After agent discharge, the compartment door was held 0.3m open so hot layer gases were not fully trapped within the compartment. The aerosol agent did not fully suppress the fire due to re-radiation from the hot engine enclosure, so the obstructed diesel pool fire continued to burn until the compartment door was closed, after which the fire was put out by confinement. Following this, the door was fully opened to vent the compartment of aerosol and fire gases.

Measured concentrations of NO, NO₂ and NOₓ (left axis) for one of the obstructed diesel burns with StatX aerosol agent suppression are plotted against time in Figure 4-15. In this test, the door is held 0.3 m open throughout. Measured O_2 concentrations are plotted against the right axis in Figure 4-15 and representative compartment temperature-time plots are included in Figure 4-16 to confirm the aerosol activation time and to indicate the state of the fire in the compartment during the test. Results from repeat tests followed similar trends; however, variations of 5 to 8% of the total range were observed in measured peak values of the NO₂ and NO concentrations respectively, as well as in the duration of high levels of all three gases.
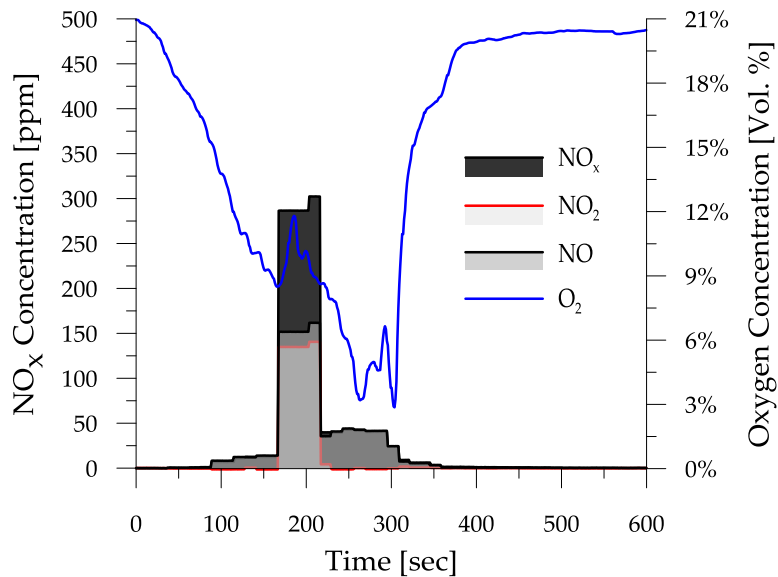
Figure 4-15: Measured NOₓ concentrations during diesel obstructed burn, StatX suppression, door open

As can be seen in Figure 4-15, after ignition of the diesel pool (0 seconds), NO levels gradually increase to values lower than those measured during the diesel characterization fire and discussed in Section 4.2. A potential explanation is the obstruction of fire gases which is changing the local fire characteristics, as well as re-directing the smoke and fire plume and prolonging the time taken for them to reach the sampling location. Upon activation of the StatX aerosol unit (170 seconds) and partial suppression of the fire, measured concentrations of NO increase sharply to values around 150 ppm in this test (118 ppm in the other test). As the fire re-ignites due to radiation from the hot engine enclosure and builds again, they decrease back to levels around 50 ppm until the fire is extinguished (310 seconds). As concentrations of NO increase after activation of the aerosol unit, measured concentrations of NO₂ simultaneously increase to values around 140 ppm (90 ppm in a repeat test) but decrease back to ambient levels more quickly than for NO. High values of NO, NO₂ and NOₓ appear to be sustained throughout

a 50 second period immediately after the agent is discharged. During this time, both the increasing O_2 concentrations shown in Figure 4-15 and the slight, sustained dip in temperatures observed in Figure 4-16 at around 165 seconds support the fact that the aerosol successfully acts to decrease the overall intensity of the fire and consequently, reduces the temperatures within the compartment. As the fire re-establishes itself with the door remaining open at 0.3m, compartment temperatures increase again while concentrations of O_2 decrease and concentrations of NO_2 decrease quickly to ambient while NO and NO_x concentrations fall to values more consistent with, albeit slightly higher than, levels seen during the diesel characterization fires. These latter values appear consistent with anticipated changes in the diesel fire environment due to presence of the engine enclosure obstruction as well as the overall higher compartment temperatures. After the fire is fully suppressed and the compartment door is fully opened (310 seconds), all measured concentrations drop back to ambient levels.
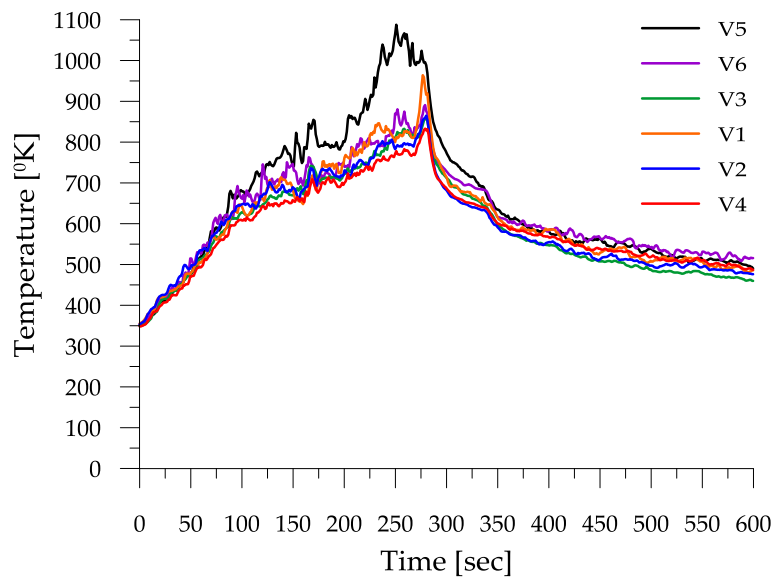
Figure 4-16: Measured temperature profiles during an obstructed diesel burn, StatX suppression, door open

In these tests, no data was obtained using the Gastec STR-800 STR measurement system.

4.7 Results for Obstructed Diesel Burn with DSPA Suppression

Concentrations of NO, NO_2 and NO_x were measured during two obstructed diesel burns with DSPA aerosol agent suppression, using the same compartment configuration as that described for the StatX obstructed diesel burns in Section 4.6 above. As was the case for the StatX tests, the aerosol did not immediately suppress the fire in either of these tests.

Measured concentrations of NO, NO_2 and NO_x (left axis) for one of the burns with DSPA aerosol agent suppression are plotted against time in Figure 4-17 with O_2 concentrations plotted on the right hand axis as well. Since the aerosol agent initially impacted the fire in much the same fashion for both tests, results from the two experiments are very similar in terms of peak concentrations, temperature profiles and the durations of high levels of all the measured gases.
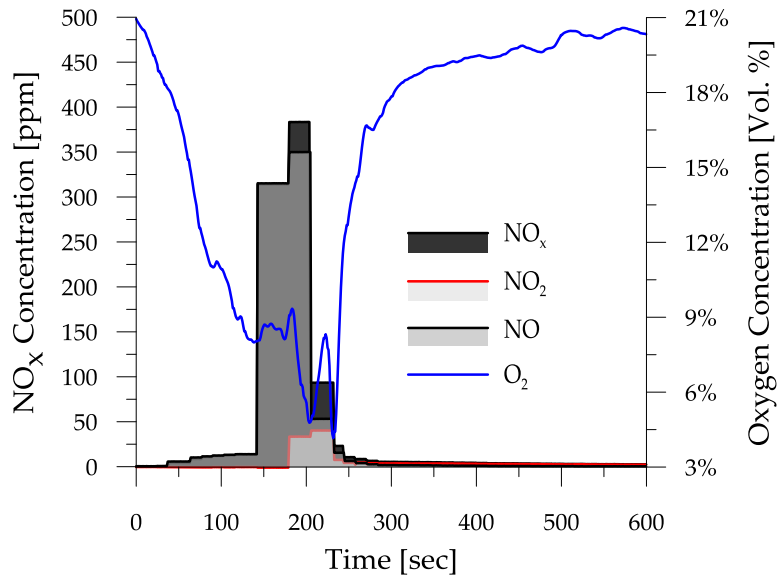
Figure 4-17: Measured NO_x concentrations during diesel obstructed burn, DSPA suppression, door open

After ignition of the diesel pool (0 seconds), NO levels gradually increase to values typical of, but slightly lower than, those measured during the diesel characterization fire (Section 4.2) but almost identical to those reported above in Section 4.6 confirming the consistency of the fire between these Stat-X and DSPA tests. Upon activation of the DSPA aerosol unit (144 seconds), the concentration of NO increases sharply to values approaching 375 ppm and stays at this level for a brief period. During this time, the aerosol appears to decrease the intensity of the fire slightly, as supported by the increase in O_2 concentration shown in Figure 4-17 between 140 seconds and 180 seconds and the corresponding dip in temperature seen in Figure 4-18 during that same time. The fire then appears to cycle in intensity several times before it is eventually suppressed. Following suppression, the door is opened and the compartment ventilated. In contrast to the previous tests using StatX suppression, concentrations of NO_2 do not appear to increase until the NO concentrations reach their peak values (178 seconds) and begin to decay. Peak values of at least 50 ppm NO_2 are measured before the aerosol suppresses the fire. After the

compartment door is fully opened (248 seconds), all measured concentrations drop back to ambient levels in much the same fashion as observed in other tests.
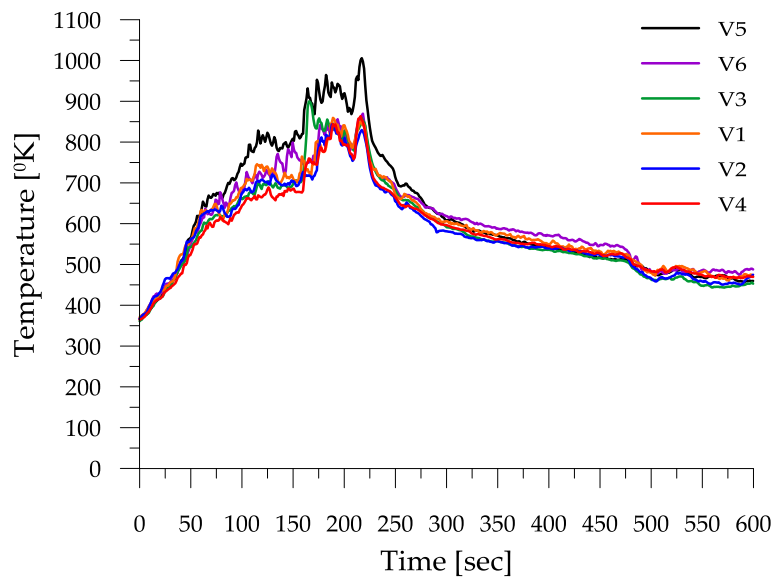
Figure 4-18: Measured temperature profiles during an obstructed diesel burn, DSPA suppression, door open

As in the Stat-X suppression test above, no data was obtained using the Gastec STR measurement system during this experiment.

4.8 Summary and Discussion of Obstructed Diesel Fire Results

Comparison of NO_x concentrations measured during StatX and DSPA activation and aerosol suppression of the obstructed diesel fires, Figure 4-15 and Figure 4-17, respectively, suggest that higher levels of nitrogen oxides are produced via interaction of the agent with the fire and hot fire gases in the burn compartment both during and immediately after activation of both variants of aerosol extinguisher. NO concentrations measured during tests with the DSPA unit appear to again be almost twice as high as those seen during tests with the StatX unit. Independent of unit, peak concentrations of NO measured in the present location surpass the IDHL limit for occupational exposure of 100 ppm set by OSHA [35]; however, it would again be expected that high concentrations would persist for only a fairly short period of time, being quickly diluted through mixing and ventilation.

Trends in the time evolution of NO_2 for the StatX and DSPA aerosol units in the obstructed diesel fire tests with the door held open at 0.3m are difficult to compare since in the DSPA test it is thought that the NO_x detector may have been saturated. For the StatX unit, NO_2 concentrations

are observed to increase to extremely high levels of 150 ppm immediately upon activation of the unit and simultaneously with measured increase in NO concentration in the hot gas layer. As in previous tests, concentrations of both NO and NO_2 decay relatively quickly back to ambient levels once the fire is fully suppressed and the compartment ventilated. In contrast, for the DSPA unit, NO_2 concentrations increase to levels above 50 ppm and similarly decrease after suppression of the fire. In both cases, NO_2 concentrations exceed the 1-hour continuous exposure limit proposed by WHO [34], as well as both the OSHA IDHL and OSHA 15-minute exposure thresholds [35]; again with note that these high concentrations are measured at only a single point deep within the hot upper layer gases and are sustained for only a very short periods of time. Overall, the results further support the importance of appropriate operational procedures to minimize the likelihood that any personnel could be exposed to such levels of NO or NO_2 during conduct of normal fire response activities.

4.9 Results for Obstructed Bilge Fire with StatX Agent Suppression

Concentrations of NO, NO_2 and NO_x were measured during two different obstructed bilge diesel burns, with StatX aerosol agent suppression. As outlined in Chapter 1, this test scenario entails a 1.4m x 1.3m x 0.46m steel structure suspended above the diesel pool fire to simulate a fuel spill fire under an engine enclosure. Once the fire reaches "steady state" conditions, the StatX aerosol unit is deployed inside the fiery bilge. Measured concentrations of NO, NO_2 and NO_x are plotted against time in Figure 4-19 for this scenario with the door closed on suppression, then opened to a 0.3 m opening at 230 seconds into the test. Figure 4-20 contains data taken during the same scenario in which the door was closed and sealed immediately after agent was discharged into the compartment and then held closed until the end of test. Measured O_2 concentrations for each case are plotted against the right hand axis to indicate the state of the fire in the compartment. These scenarios were intended to generate 'worst' case situations in which any gases generated due to the combined action of the agent and pre-existing hot fire gases would remain trapped in the compartment. Measurements of NH_3 and HCN concentration were made using the Gastec STR-800 sampling system for the scenario shown in Figure 4-20 as well.

In Figure 4-19, NO and NO_2 levels first increase to values similar to those measured during the obstructed diesel fires discussed in Sections 4.64.7, Obstructed Diesel Fire. Upon activation of the aerosol unit at 128 seconds after ignition, concentrations of NO and NO_x seen in the upper hot gases increase sharply to very high values, reaching levels near 260–275 ppm as the fire is suppressed. The gradually increasing O_2 concentrations seen in Figure 5-2, coupled to closer examination of temperature time traces from within the burn compartment (not shown here) confirmed that the fire went out fairly quickly after discharge of the aerosol agent. Levels of NO_2 rise slightly after discharge of the agent and appear to reach values of between 50 and 75 ppm as compartment temperatures decrease, O_2 concentration levels increase and the concentration of

NO decreases. These variations may well relate to a shift in equilibrium between production of NO and NO_2 as the compartment cools with suppression of the fire. Similar evolution of NO_2 concentrations is evident in the previous test results, but it appears to be more marked in this test. When the door is opened at 230 seconds into the test, the concentrations of all species return to ambient values as the hot gases exit the compartment and mix with fresh air.

As in some of the previous tests, measured concentrations of NO, NO_2 and NO_x may not be quantitatively correct during the time periods over which very high values of NO_x are observed because it cannot be accurately determined when the detector is saturated. It is evident, however, that high concentrations of both NO and NO_2 are present in the upper layers of the burn compartment after agent discharge and until the door to the compartment is opened.
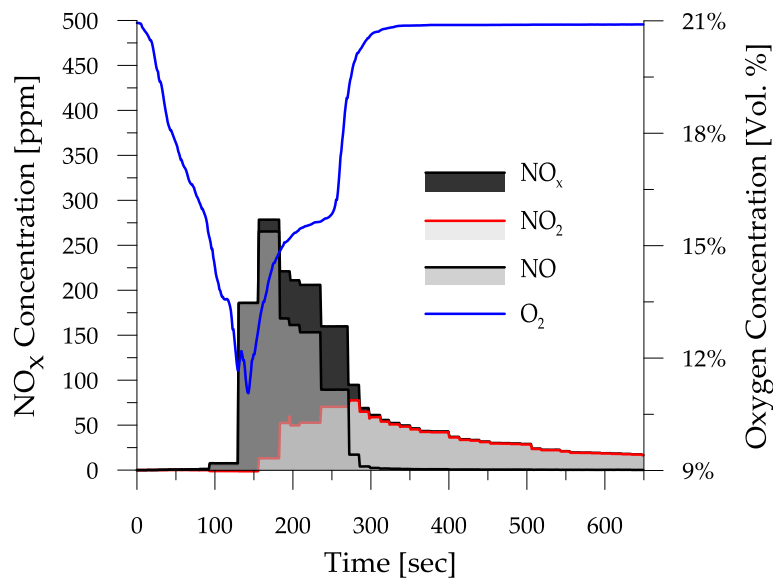
Figure 4-19: Measured NO_x concentrations during diesel bilge burn, StatX suppression

Subsequently, the same test for which data is shown in Figure 4-19 was repeated except the compartment door was closed for the 10 minute duration of the experiment. Due to the high concentration of gas seen in previous tests, the Novatech NO and NO_x detectors were modified and recalibrated to allow detection of concentrations as high as 1800 ppm. Results from one of several repeat tests of this scenario are plotted against time in Figure 4-20. As in the first stages of all previous tests with an obstructed fire, measured concentrations of NO and NO_2 before activation of the unit are consistent and exhibit similar trends to those shown in Figure 4-19. After activation of the aerosol unit at 160 seconds after ignition, the compartment door is closed and

concentration of NO_x increases gradually to a high value. Temperature-time data in the compartment (not shown here) and the rapid increase in O_2 concentration seen at around 170 seconds in Figure 4-20 confirm that the fire was suppressed very shortly after the aerosol was discharged into the bilge. Levels of NO appear to first increase after discharge of the unit, but then drop to values of around 5-15 ppm for the duration of the experiment. At the same time, peak NO_2 concentrations increase quickly and remain very high, ranging between 200 and 220 ppm for the duration of the experiment. It is interesting to note from the data plotted in Figure 4-19, that during the short period while the door was held closed, the concentration of NO_2 seems to be increasing in a similar fashion to that measured in this test and shown in Figure 4-20. The time evolution of nitrogen oxide concentrations in this test, clearly varies significantly from those measured during earlier tests, potentially as a result of cooling during activation, again suggesting that due to the specific compartment conditions encountered in this test, there may be a shift in the equilibrium between NO and NO_2 production during suppression of the fire and as the hot gases cool with the compartment door closed.
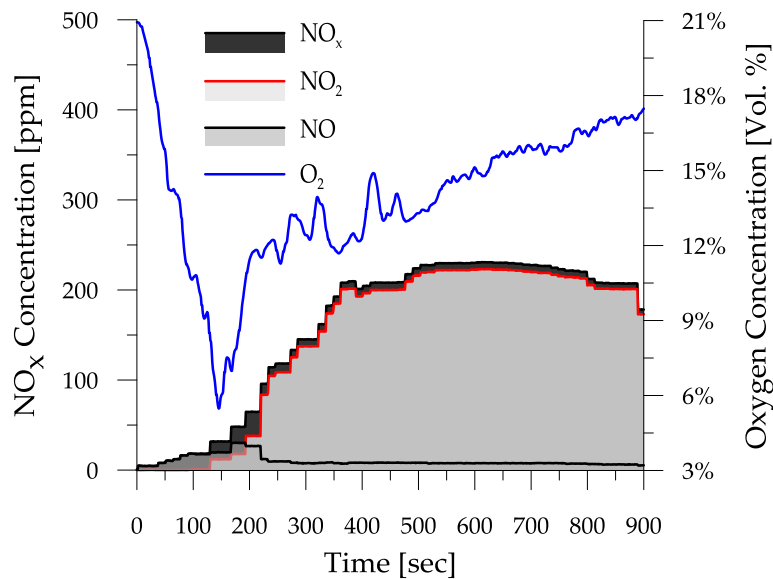
Figure 4-20: Measured NO_x concentrations during diesel bilge burn, StatX suppression, door closed

The shifts in concentrations of NO and NO_2 measured using the Novatech P-695 system were further confirmed via Gastec STR-800 samples taken at 840 seconds into the test. As presented in Figure 4-21 Gastec STR-800 samples indicated high concentrations of NO_2 of around 200 ppm (right edge of black tape in upper tube), while that for NO (lower) was much lower,

around 5 ppm. In both cases, the concentration values measured by the Gastec STR-800 system agree closely with those determined using the Novatech P-695 analyzers.

Figure 4-21: NO and NO$_2$ concentrations measured using Gastec STR-800 tubes during suppression of a diesel fire using a StatX aerosol (840 seconds)

In addition to the NO$_x$ measurements presented above, additional Gastec STR-800 samples were withdrawn at times of 480 seconds and 600 seconds respectively to determine whether any HCN or NH$_3$ is present in the hot layer gases after discharge of the aerosol unit. While no measurable concentrations of HCN are observed, NH$_3$ concentrations of approximately 300 ppm are recorded as indicated by the left hand side of the black tape in Figure 4-22.

Figure 4-22: NH$_3$ concentration measured using a Gastec STR-800 tube during suppression of a diesel fire using a StatX aerosol unit inside the UW burn room (600 seconds)

4.10 Results for Obstructed Bilge Fire with DSPA Agent Suppression

Concentrations of NO, NO$_2$ and NO$_x$ were measured during two different obstructed bilge diesel burns, suppressed using DSPA aerosol units. Measured concentrations of each gas (left axis) are plotted against time in Figure 4-23 for a case where the door was closed on suppression, then opened to a 0.3 m opening at 240 seconds into the test. Figure 4-25 shows data taken during the same scenario when the door was closed and sealed immediately after agent was discharged and held closed until the end of the test. Measured O$_2$ concentrations are plotted against the right hand axis of each plot. These scenarios are intended to generate a 'worst' case scenario in which any gases generated due to the combined interaction of the agent with the pre-existing hot fire gases are trapped in the upper hot gas layers. Measurements of NH$_3$ and HCN concentrations were also made using the Gastec sampling system during the scenario in Figure 4-25.

For the burn shown in Figure 4-23, NO and NO$_2$ concentration levels initially remain lower than values typically observed during any of the other tests. The reason for this has never

been determined. Upon activation of the aerosol unit (120 seconds), concentrations of NO and NO_x in the upper hot gases increase sharply to very high values, reaching levels near 490-500 ppm and capping out at the saturation limit of the detection system (i.e. peak concentrations exceeded the detection limit of 500 ppm). Upon suppression of the fire, as indicated by the sudden increase in O_2 concentration (Figure 4-23) and corresponding decrease in compartment temperatures (Figure 4-24), the concentrations of NO and NO_x begin to decrease. As they fall below the saturation limit of the detector, more representative concentrations of NO_2 are measured (210 seconds into the test), increasing to values of between 400-425 ppm supporting the existence of relatively high concentrations of NO and NO_2 in the upper layers of the compartment and suggesting again a possible shift in equilibrium between NO and NO_2 production as the fire is suppressed. After this point in the test, the compartment door was opened to 0.3 m, and concentrations of all three gases subsequently decreased back to ambient levels as they cooled, mixed with air and exited the compartment.
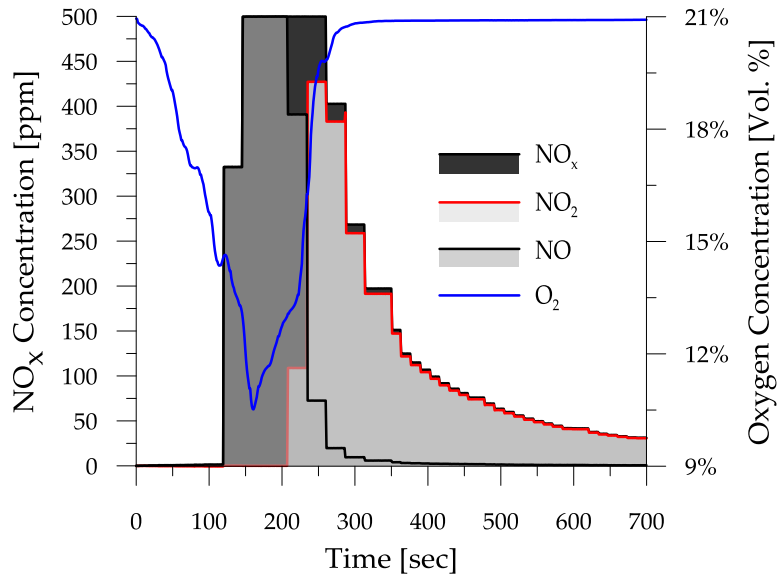
Figure 4-23: Measured NOx concentrations during diesel bilge burn, DSPA suppression, door closed
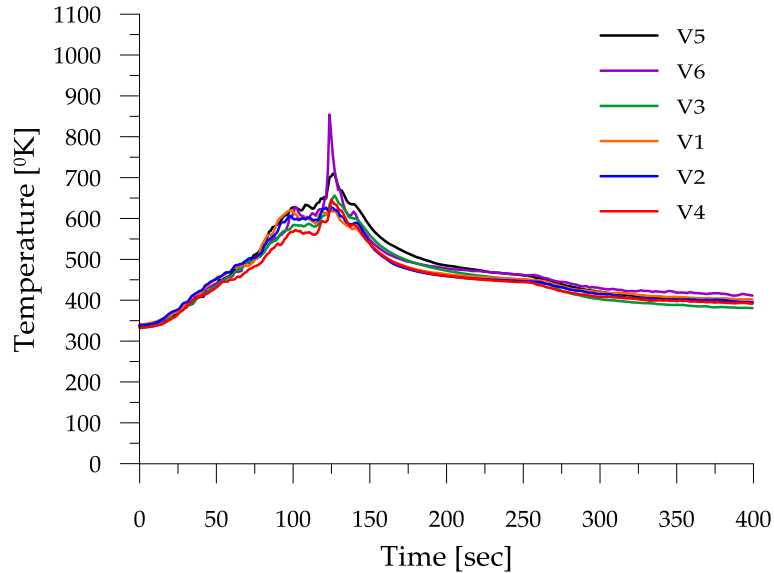
Figure 4-24: Measured temperature profiles during diesel bilge burn, DSPA suppression, door closed

The same test as Figure 4-23 was repeated, except here the compartment door was closed immediately after suppression and then held closed for the remainder of the test period (10 minutes). In anticipation of high levels of gas concentrations that would accumulate during the test, the Novatech P-695 NO and NO_x detectors were modified and recalibrated to allow detection of concentrations as high as 1800 ppm. Concentrations of NO, NO_2 and NO_x from a representative test are plotted on the left hand axis against time in Figure 4-25, with O_2 concentrations at the sampling location plotted against the right hand axis of the figure. Measured concentrations of NO and NO_2 before activation of the unit are consistent with those measured during the previous bilge test, as plotted in Figure 4-23. After activation of the aerosol unit at 118 seconds into the test, the compartment door is closed and the concentration of NOx increases quickly to high values as high as 500-600 ppm as the fire is suppressed. Levels of NO do not appear to increase to the high values seen in previous experiments, but instead reach values of around 200 ppm, somewhat lower than the values observed in the previous experiment and shown in Figure 4-23, and remain fairly constant for the duration of the experiment. At the same time, peak NO_2 concentrations are very high, ranging between 400 to 500 ppm for the duration of the experiment, which again is similar to the concentrations that were reported in the test data shown in Figure 4-23.

49
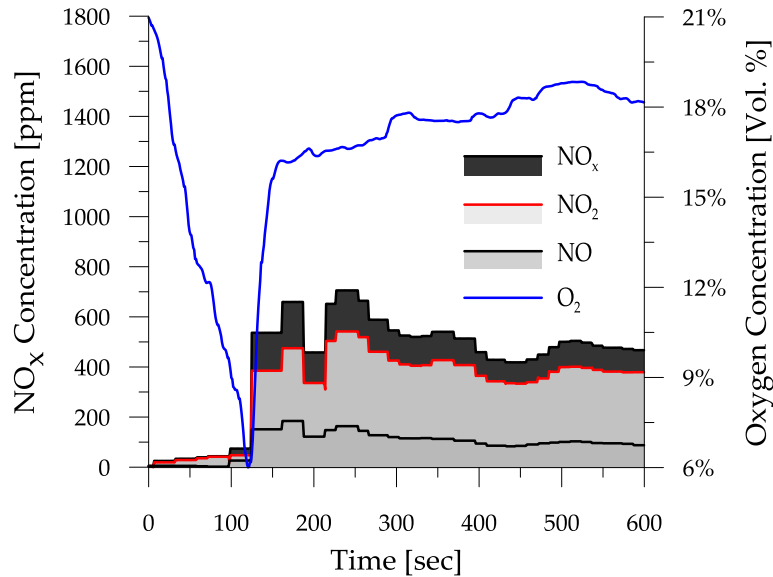
Figure 4-25: Measured NOₓ concentrations during diesel bilge burn, DSPA suppression, door closed

Again an attempt was made to confirm the concentrations of NO and NO_2 measured using the Novatech P-695 system via Gastec STR-800 samples taken at 500 seconds into the test. As presented in Figure 4-26, sampling tubes for NO (upper tube) and NO_2 (lower tube) indicated concentrations of around 200 ppm, respectively. While this would suggest that the Novatech P-695 data might be appropriate, the measured concentrations are at or above the saturation limits of the tubes so no direct conclusion could be drawn.

Figure 4-26: NO and NO₂ concentrations measured using Gastec STR-800 tubes during suppression of a diesel fire using a DSPA aerosol (500 seconds)

Additional Gastec STR-800 samples were again withdrawn at times of 650 seconds and 740 seconds into the test shown in Figure 4-25 to determine respectively whether any HCN or NH_3 was present in the hot layer gases after discharge of the aerosol unit. While no measurable concentrations of HCN were observed, NH_3 concentrations of approximately 260 ppm were recorded as marked by the left hand edge of the black tape shown in Figure 4-27.
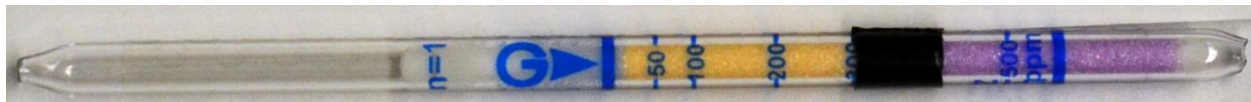
50

Figure 4-27: NH3 concentration measured using a Gastec STR-800 tube during suppression of a diesel fire using a DSPA aerosol unit inside the UW burn room (740 seconds)

4.11 Summary and Discussion of Obstructed Bilge Fire Test Results

Comparison of NO_x concentrations measured during StatX and DSPA activation and aerosol suppression of the bilge fire scenarios, Figure 4-19 and Figure 4-20, as well as Figure 4-23 and Figure 4-25, respectively, suggest that levels of nitrogen oxides are high in the hot fire gases of the burn compartment both during and immediately after activation for both variants of aerosol extinguisher. Depending upon how quickly the fire is suppressed, and therefore on the compartment environment that evolves after agent activation, concentrations of NO and NO_2 may shift relative to one another. The DSPA unit again appears to generate close to twice as much NO as the StatX unit with the exception of test in Figure 4-20 where NO reaches very low values. In most tests, peak concentrations of NO measured at the current sampling location surpass the IDHL limit for occupational exposure of 100 ppm set by OSHA [35]; noting again of course that these values are measured at a single location deep into the hot layer for a fire scenario in which the compartment door was held closed and the fire confined after discharge of the aerosol unit.

Trends in the time evolution of NO_2 during suppression of bilge fire with both the StatX and DSPA aerosol units appear to be similar for comparable test situations. NO_2 concentrations are observed to increase in all tests, and for the case in which the door is held closed after activation of the units they increase to extremely high levels and remain there until the compartment is ventilated. In all cases, NO_2 concentrations greatly exceed the 1-hour continuous exposure limit proposed by WHO [34], as well as both the OSHA IDHL and OSHA 15-minute exposure thresholds [35]. The results again point to the importance of appropriate operational procedures to minimize the likelihood that any personnel could be exposed to high levels of any of these gases during conduct of normal fire response activities.

4.12 Wood Crib Fire Characterization Test Results

To establish baseline concentration levels of NO, NO_2 and NO_x due to the wood crib fires that are used in the aerosol suppression tests, gas concentrations measurements were made during a wood crib characterization fire as it grew to a fully developed fire with the door open to 0.3 m. After it reached steady burning conditions and a marked hot layer had developed, the door was closed to mimic fire confinement on board a naval vessel. Representative values of measured concentrations of NO, NO_2 and NO_x are plotted on the left axis against time in Figure 4-28, with

corresponding hot layer O_2 concentrations on the right hand axis. The Gastec STR-800 sampling system was used to cross check measured values of NO and NO_2, as well as to probe for the presence of HCN and NH_3 in the hot layer during some of the wood crib fire tests.
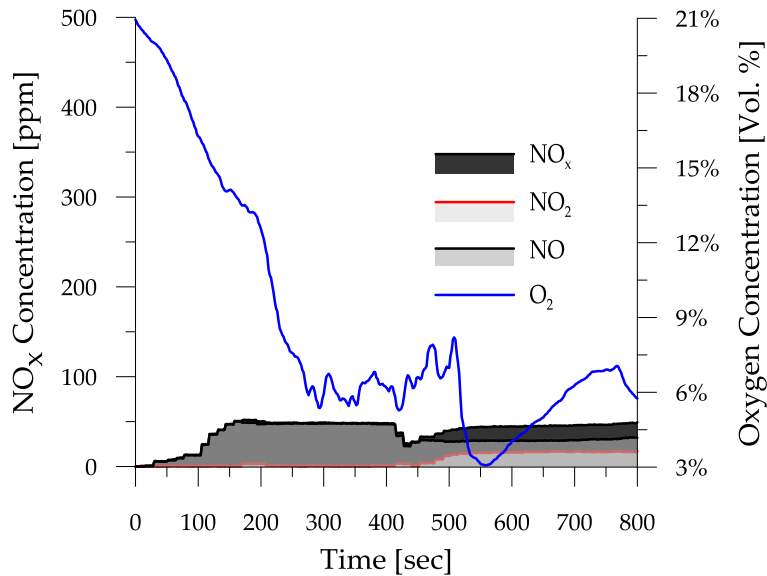
Figure 4-28-Measured NOx concentrations during a wood crib fire characterization burn with door initially open, then closed after development of hot layer (900⁰K)

It can be seen from Figure 4-28 that after ignition (0 seconds), the concentration of NO increases gradually to levels of approximately 50 ppm as the fire reaches steady burning. As peak concentrations of NO are reached, small concentrations of NO_2 are also measured (less than 5 ppm); however, combined concentrations of NO and NO_2 from the wood crib fire alone remain below 55 ppm throughout the test. The plots of O_2 concentration and temperature against time from the same test (temperature not shown here) confirm that the fire and thus the hot gas layer temperatures in the compartment grow steadily to around 900⁰K, after which the door is closed (515 seconds into the test). Following this, the O_2 concentration drops as the fire consumes any remaining oxygen in the compartment (Figure 4-28), then the temperature drops steeply, indicating suppression of the fire through O_2 starvation.

Gastec STR-800 samples withdrawn from the upper layer at 733 seconds into this test indicate concentrations of NO in Figure 4-29 of approximately 13-15 ppm, as demarcated by the left hand side of the black tape in the upper tube, and of NO_2 of below 15 ppm as indicated by the left hand side of the black tape on the lower tube. These values appear to confirm the concentration data obtained using the Novatech P-695 measurement system, particularly given the potential errors in each method discussed above.
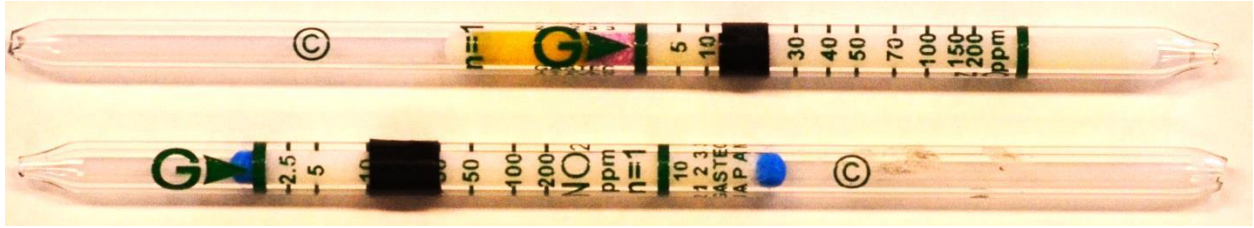
Figure 4-29: NO and NO₂ concentrations measured using Gastec STR-800 tubes during wood crib fire characterization (733 seconds)

In addition, concentrations of HCN and NH_3 are measured at 880 and 980 seconds into the test respectively using the Gastec STR-800 system. While no measurable concentrations of NH_3 were observed in these tests, HCN concentrations of approximately 10 ppm were recorded as marked by the left hand edge of the black tape seen in Figure 4-30.
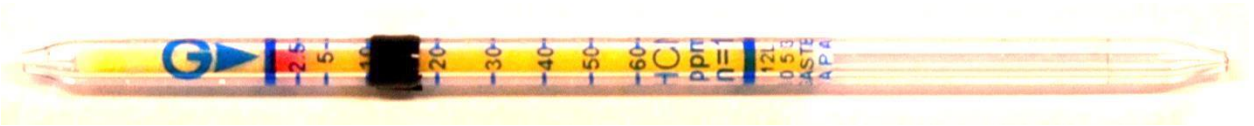
Figure 4-30: HCN concentration measured using a Gastec STR-800 tube during wood crib fire characterization (880 seconds)

4.13 Discussion of Wood Crib Fire Characterization Test Results

Both NO and NO_2 contribute to the total NO_x produced during the characterization fires. As expected based on literature relating to the combustion of wood cribs, measured concentrations of NO_x are around 50 ppm [61]. Measured concentrations of NO remain well below threshold values suggested in the OSHA guidelines [35]. The average NO_2 concentrations across the 10-15 minute period of the open wood crib fires are well below threshold levels established by OSHA [35] and barely exceed one hour average exposure levels proposed by WHO [34]. Additional NO or NO_2 generated as a result of the aerosol activation, however, might exacerbate this situation during aerosol suppression of compartment fires. Therefore, NO_x concentration data measured during the various aerosol suppression scenarios are presented and discussed in the following sections.

4.14 Results for Softwood Crib Fire with StatX Agent Suppression

Concentrations of NO, NO_2 and NO_x measured during two different wood crib fire test with StatX aerosol agent suppression are plotted on the left axis against time for the case with a 0.3 m open

door in Figure 4-31 and in Figure 4-33. On both plots, the corresponding O_2 concentrations are plotted on the right axis to provide an indication of fire development with time. Results in Figure 4-31 are for a representative case in which the door is initially open while the fire builds, then closed immediately after agent was discharged into the compartment (237 seconds), opened and closed again (362 and 482 seconds respectively) and finally opened (602 seconds) until the end of the test. In comparison, Figure 4-33 contains results for a test in which a fully developed fire was established within the compartment (hot layer temperatures of 900K), then an aerosol unit was discharged and the compartment door was immediately closed and kept sealed for 10-15 minutes. To supplement the information on NO_x evolution, additional measurements of NH_3 and HCN concentration were made using the Gastec sampling system in the test plotted in Figure 4-33.

For the StatX wood crib fire suppression test shown in Figure 4-31, concentrations of both NO and NO_2 increase after ignition (0 seconds), with NO concentrations reaching values of over 100 ppm and NO_2 concentrations over 150 ppm as the fire grows to steady state. These values are higher than those measured during the wood crib characterization fire discussed in Section 4.12. Prior to activation of the StatX aerosol unit both NO and NO_2 levels are already around 200-225 ppm. At activation of the StatX aerosol unit (237 seconds), as confirmed through the increase in upper layer O_2 concentration (Figure 4-31) and decrease in temperature (Figure 4-32), the NO and NO2 concentrations are 340 and 200 ppm respectively. In the early stages of fire suppression, the concentrations of these gases jump for a short period of time and then decrease gradually, likely since the compartment door is closed. When the door is opened again (360 seconds) and the fire begins to grow (see upper layer temperatures in Figure 4-32), concentrations of NO decrease sharply to values of around 40 ppm and then increase, while concentrations of NO_2 remain high for a period of time before decreasing to average values of around 150 ppm. Changes in concentrations of NO and NO_2 observed as the door is opened and closed during this test support the idea expressed in Section 4.4 that the equilibrium between the two gases may change significantly as the local conditions within the fire compartment change.
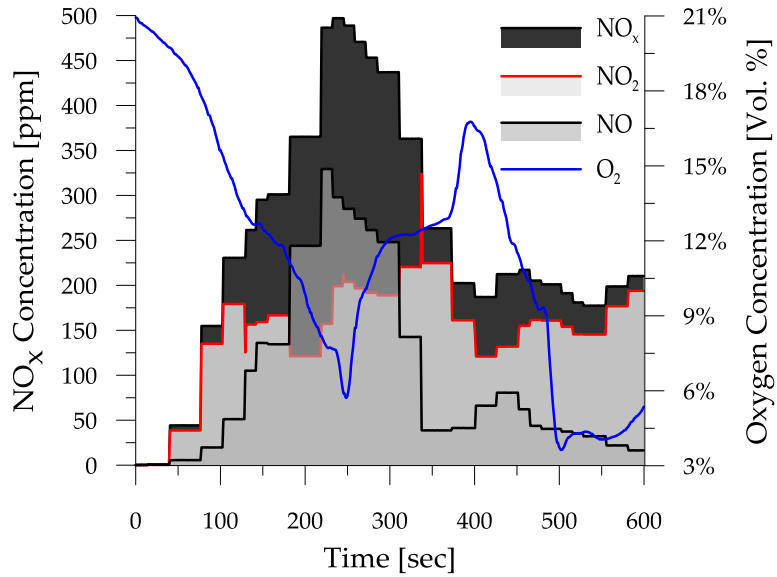
Figure 4-31: Measured NO$_x$ concentrations during a wood crib fire, StatX suppression
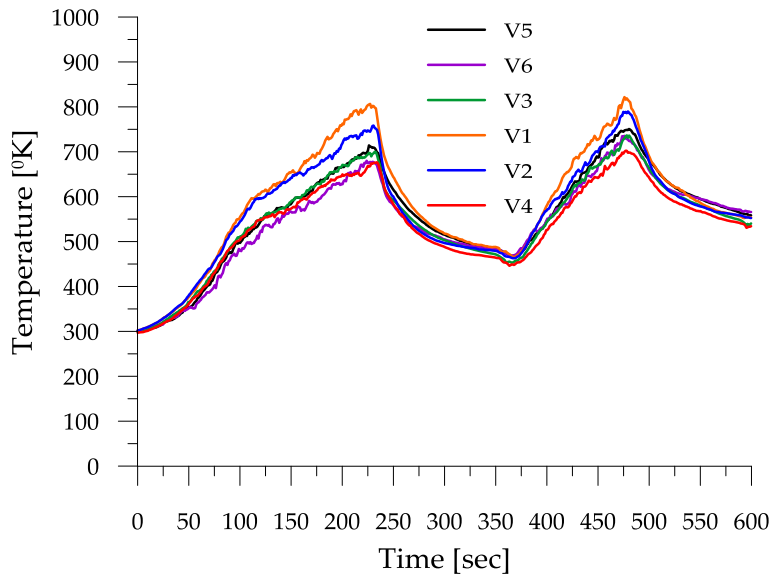
Figure 4-32: Measured temperature profiles during a wood crib fire, StatX suppression

Subsequent to the test in Figure 4-31, the same test was repeated except the compartment door was closed immediately after activation of the aerosol and held closed for the duration of the experiment. This scenario is intended to generate a 'worst' case scenario in which any gases generated due to interactions of the agent with the pre-existing hot fire gases would be trapped

in the upper hot gas layers. To better determine peak concentrations of gases which accrue from discharge of the extinguishing agent into a compartment in which a fully developed wood crib fire is burning, the Novatech P-695 NO and NO_x detectors were modified and recalibrated to allow detection of concentrations as high as 1800 ppm.

Plotted against time in Figure 4-33 are measured concentrations of NO, NO_2 and NO_x (left axis) and upper layer O_2 throughout the test. Values of the gas concentrations before activation of the unit are consistent with those measured during wood crib characterization fire discussed in Section 4.12. After activation of the aerosol unit at 349 seconds into the test, as confirmed through examination of the temperature time plots (not shown here), the compartment door is closed. Following this, measured concentrations of NO, NO_2 and NO_x do not increase as expected, but instead remain relatively constant at values below 50 ppm.

Figure 4-33: Measured NO_x concentrations during a wood crib fire, StatX suppression (door closed after agent discharge)

The low concentrations of NO and NO_2 measured using the Novatech P-695 system were further confirmed via Gastec STR-800 samples taken at 650 seconds into the test which indicated concentrations of NO (left side of black tape on the upper tube) and NO_2 (lower tube) of around 7 and 10 ppm respectively, as presented in Figure 4-34.

Figure 4-34: NO and NO₂ concentrations measured using Gastec STR-800 tubes during suppression of wood crib fire using a StatX aerosol (650 Seconds)

In addition to the NOₓ measurements presented above, additional Gastec STR-800 samples were withdrawn at times of 780 seconds and 900 seconds into the test shown in Figure 4-33 to determine, respectively, whether any HCN or NH₃ was present in the hot layer gases after discharge of the aerosol unit. While no measurable concentrations of NH₃ were observed, HCN concentrations of approximately 17-20 ppm were recorded as marked by the left hand side of the black tape in Figure 4-35.

Figure 4-35: HCN concentration measured using a Gastec STR-800 tube during suppression of a wood crib fire using a StatX aerosol unit (780 seconds)

4.15 Results for Wood Crib Fire with DSPA Agent Suppression

Concentrations of NO, NO₂ and NOₓ measured during two different wood crib fire tests with DSPA aerosol agent suppression are plotted on the left axis against time in Figure 4-36 and Figure 4-37, with corresponding O₂ concentrations on the right axis of each figure to indicate fire development with time. Figure 4-36 shows data for the case in which the fire is allowed to grow for a set period of time after ignition (approximately 245 seconds), then the DSPA unit is discharged and the door held closed for 155 seconds. The door is then opened and closed again several times to see if the aerosol has extinguished the fire resulting in some of the hot gases being vented. Figure 4-37 shows representative results for a comparable test in which a fully developed fire is established within the compartment (hot layer temperatures of 900K), an aerosol unit is discharged and then the compartment door is immediately closed and kept sealed for 10-15 minutes. To supplement the information on NOx evolution, additional measurements of NH₃ and HCN concentration are made using the Gastec STR-800 sampling system in the test plotted in Figure 4-37.

For the DSPA wood crib fire suppression test shown in Figure 4-36, the fire is allowed to grow with the door held open at 0.3m. During this time, NO levels increase, reaching values of over 500 ppm, higher than those measured during the wood crib characterization fire discussed in Section 4.12. After activation of the DSPA aerosol unit (248 seconds), measured concentrations of NO increase sharply and saturate the detector, as the fire is suppressed (this is verified by the increasing O_2 concentrations seen in Figure 4-36 as well). Following that, concentrations of NO drop back to values of around 25 ppm as the compartment door is opened and the gases are vented. Measured values of NO_2 are again suspect during the period over which the detector is saturated; however, accounting for the detection limits of the system, it is fair to say that for this fire and suppression scenario relatively high concentrations of both NO and NO_2 are present in the upper layers of the burn compartment for a period of time after discharge even with the opening and closing of the door.
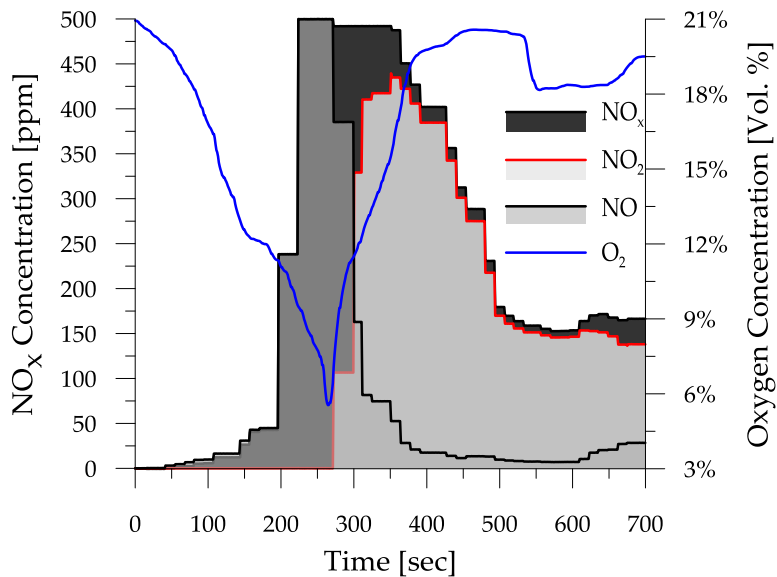
Figure 4-36: Measured NO_x concentrations during a wood crib burn, DSPA suppression

Subsequent to test in Figure 4-36, the same test is repeated except that after activation of the aerosol unit the compartment door is closed for the duration of the experiment. This scenario is again the intended 'worst' case scenario in which hot gases would be trapped in the upper layers of the compartment. As a result high values of concentration are expected and the Novatech P-695 NO and NO_x detectors are modified and recalibrated to allow detection of concentrations as high as 1800 ppm.

Plotted against time in Figure 4-37 are measured concentrations of NO, NO_2 and NO_x (left axis) and O_2 (right axis) from this repeat test. Measured concentrations of NO and NO_2 before

activation of the unit are consistent with those measured during wood crib characterization fires discussed in Section 4.12. After activation of the aerosol unit (444 seconds), the compartment door is closed and the fire is partially suppressed (as seen in both the plot of O_2 concentration (Figure 4-37) and the temperature-time plots for this test (not shown here)). Concentrations of NO decrease during this period, then remain at values of around 20 ppm for the remainder of the test. In contrast, and as has been seen in other tests in which the compartment door is held closed, NO_2 formation appears to be promoted after discharge of the aerosol and partial suppression of the fire, so that NO_2 concentrations increase, peaking at values of 590-600 ppm. Although there was moisture detected in the lines during this test, as there had been during the test plotted in Figure 4-33, these results appear to follow trends in data observed for other tests.
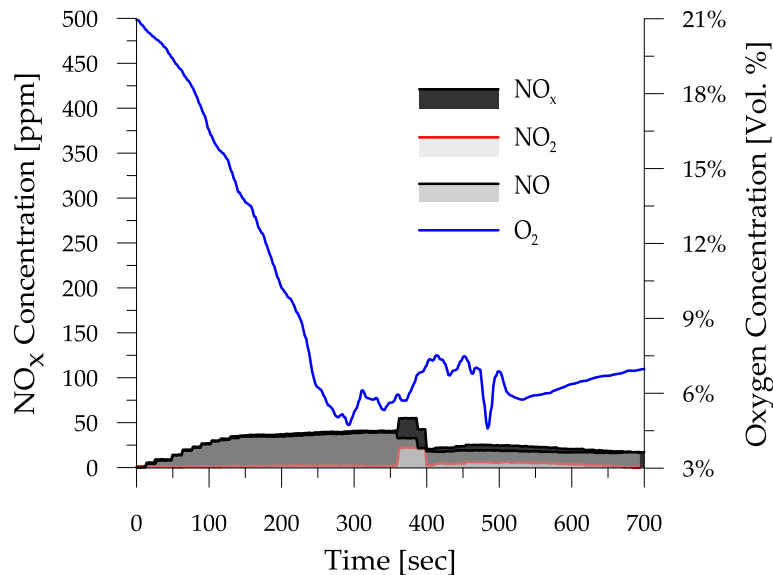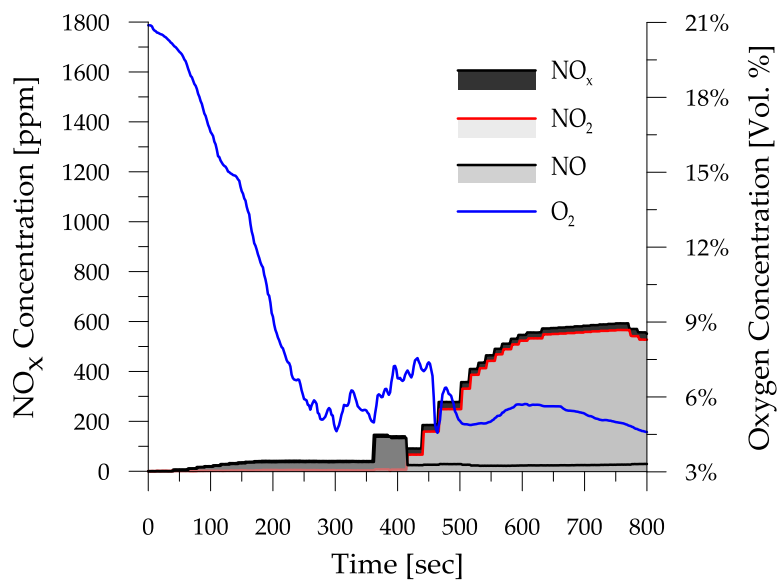

Figure 4-37: Measured NO_x Concentrations during a wood crib burn, DSPA suppression (door closed after agent discharge)

The concentrations of NO and NO_2 measured using the Novatech P-695 system are again confirmed by Gastec STR-800 samples taken at 710 seconds into the test. As shown in Figure 4-38, these samples indicate concentrations of NO (left hand side of black tape upper tube) of around 20 ppm and saturated the tube at 200 ppm for NO_2 (lower tube) consistent with data plotted in Figure 4-37 as well.

Figure 4-38: NO and NO₂ concentrations measured using Gastec STR-800 tubes during suppression of wood crib burn using a DSPA aerosol unit (710 seconds)

Additional Gastec STR-800 samples were withdrawn at times of 850 seconds and 960 seconds into the test shown in Figure 4-37 to determine respectively whether any HCN or NH₃ is present in the hot layer gases after discharge of the aerosol unit. While no measurable concentrations of HCN are observed, NH₃ concentrations of approximately 500 ppm are recorded as marked by the left hand side of the black tape in Figure 4-39.
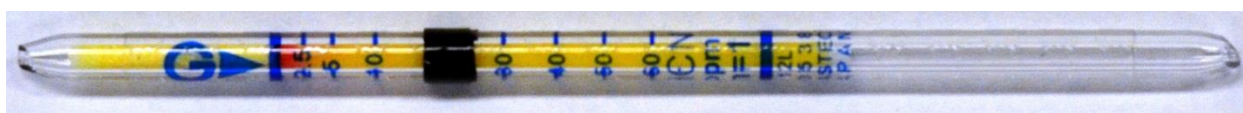

Figure 4-39: NH₃ concentration measured using a Gastec STR-800 tube during suppression of a Softwood using a DSPA aerosol unit (960 seconds)

4.16 Summary and Discussion of Softwood Crib Test Results

Comparison of NOₓ concentrations measured during StatX and DSPA activation and aerosol suppression of the softwood fires, Figure 4-31 and Figure 4-33 as well as Figure 4-36 and Figure 4-37 respectively, suggest that complex interactions between the crib fire and the aerosol, coupled with confinement of the compartment by closing the door, leads to varying concentrations of NO, NO₂, HCN and NH₃ across the tests. This is consistent with general expectation, since of all of these species are likely to be involved with NOₓ production during a fire [61]. Further, the concentrations of each would be anticipated to change as the compartment temperature and ventilation characteristics vary due to opening and closing of the door, since their relative generation is known to be very dependent on local factors such as temperature and oxygen concentration.

The evolution of NOₓ before agent discharge in both the Stat-X and DSPA aerosol suppression tests resembles the profile and concentration data from characterization test discussed in Section 4.12, as would be expected for the same fire situation. Measured concentrations of NO appear to be lower than in many of the tests conducted using the diesel fire scenarios. Here, measured concentrations do not surpass the IDLH limit for occupational

60

exposure of 100 ppm set by OSHA [11]; however, in one of the tests higher concentrations of NO are measured at the sampling position for a period of time suggesting that there is still the possibility for NO to collect in the hot upper layer gases.

Due to the combined aerosol activation and compartment confinement, measured NO_2 concentrations grow to high levels in many of the tests. These exceed the 1-hour continuous exposure limit proposed by WHO [34], and for all tests exceed both the OSHA IDHL and OSHA 15-minute exposure thresholds [35] for NO_2; however, it must again be noted that the high concentrations are measured at a single point deep within the hot upper layer gases and are sustained for only a very short periods of time.

Measurable concentrations of HCN and even relatively high concentrations of NH_3 are observed in some of the tests. Since concentrations of NO are quite low in the tests, this suggests that a series of additional chemical reactions may be occurring with NH_3 and promoting HCN formation. Even if measureable concentrations of these gases are sustained only locally around the measurement point, development of appropriate operational procedures for aerosol use coupled with compartment confinement are clearly necessary in order to minimize the likelihood that personnel could be exposed to levels of any of these gases above threshold values during conduct of normal fire response activities.

Results thus far focus on discussion of the combined interactions between the StatX and DSPA aerosol units as they are applied to suppress various diesel and softwood crib fires, with and without confinement of the compartment after activation of the extinguishing unit. Additional tests were conducted in order to assess the potential for generation of NO_x, HCN, NH_3 and other gases such as CO and CO2 should an aerosol unit discharge accidentally into a compartment where there is no fire. The results of these 'aerosol only' tests are presented in Section 4.17 for the StatX unit and Section 4.18 for the DSPA unit.

4.17 Results of Aerosol Agent Only Tests for StatX Unit

Concentrations of NO, NO_2 and NO_x were measured using the Novatech P-695 system during three tests conducted by discharging a StatX aerosol unit into the empty fire compartment, then immediately closing the door and keeping the compartment door sealed for 10 minutes. In Test A, gas concentrations are measured low in the compartment and near the outlet of the aerosol unit as per Figure 3-2, whereas for Test B and C, gas concentrations are measured in the upper ceiling level of the compartment as per Figure 3-1. To supplement the information on NO_x evolution, additional measurements of NH_3 and HCN concentration are made using the Gastec system in the latter two experiments. These tests are intended to benchmark the quantity of NO,

NO$_2$, NO$_x$ and CO that is created due to thermal decomposition of base aerosol compounds (such as KNO$_3$) and fuel binder during and immediately after activation of the aerosol unit. In addition, results are compared against 10 and 15 minute short term exposure limits for NO$_x$ [35, 62, 63] and CO [62] to better appreciate the potential impact of an accidental discharge of a unit into an occupied space.

Having measured sample concentrations of CO, it is desired that after several repeat tests, the results can be compared against published values for exposure limits and ceiling level concentrations of CO [62]. In addition, the tests are going to serve as a benchmark to identify the amount of CO created due to thermal decomposition of the fuel binder during and immediately after the aerosol discharge.

Upon activation of the StatX aerosol unit in Figure 4-40, concentrations of NO measured near the outlet of the unit (left axis) increase sharply to values of about 225 ppm, and then decrease back to 100 ppm where they remain for the duration of the experiment. Trends in the measured concentrations of CO and O$_2$ (right axis on both plots) at the same position, closely follow those of NO confirming that the NO is being formed through combustion reactions taking place during generation of the aerosol powder. Measured CO concentrations in Figure 4-41 sharply increase to peak values of 120 ppm and then decrease back to 60-70 ppm where they stagnate for the duration of the experiment. This decrease is likely a result of diffusion and mixing of the CO throughout the compartment with time after activation of the unit. In addition, as NO concentrations increase, NO$_2$ concentrations also increase, reaching peak values of around 40 ppm for a period of time and then decreasing to sustained levels of around 25 ppm for the duration of the 10 minute test. The observed decreasing concentrations of each gas is a result of buoyancy of the hot gases at the discharge of the unit, as well as diffusion and mixing of gases throughout the compartment with time. When the door is opened, the compartment ventilates (655 seconds) and concentrations of all gases return to ambient levels.

Figure 4-40: NO$_x$ concentrations for cold agent discharge (StatX-Test A)
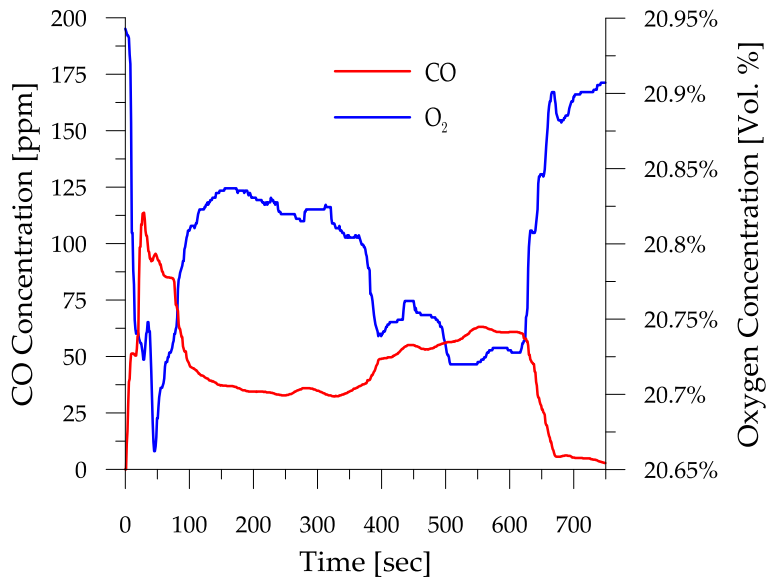
Figure 4-41: Measured CO concentrations for cold agent discharge (StatX-Test A)

Subsequent to the previous test in Figure 4-40, the gases in test B (Figure 4-42) are measured in the upper ceiling pre- and post-activation of the aerosol unit. Recorded concentrations indicate a spike in NO concentration to a peak value of 350 ppm, higher than the peak measured in the previous test A in Figure 4-40. Concentrations of O$_2$ follow the inverse trend suggesting that this is a result of the heated aerosol discharge gases rising and collecting near the

measurement location at the ceiling, while CO concentrations closely follow NO formation confirming NO creation through combustion. CO emissions recorded in Figure 4-43 show a sharp increase to values of 290 ppm, potentially as a result of heated aerosol exhaust gases collecting near the ceiling of the test compartment, doubling the value of the previous test in Figure 4-41. However, NO and CO concentrations decay after a short period of time, to much lower sustained values of 20-50 ppm for the remainder of the 10 minute test. As NO concentrations decrease, NO_2 concentrations increase to correspondingly higher peak values of around 100-110 ppm, then also decrease to levels of around 25 ppm for the duration of the test. The steep decrease to lower concentrations can likely be attributed to mixing in the upper regions of the compartment in this scenario, as well as leakage of agent and gases observed around the compartment door. Once the door is opened and the compartment ventilated, all gas concentrations return to ambient levels.

Additional NO_x concentrations are recorded using Gastec STR-800 probe for test presented in Figure 4-42 to affirm the magnitude of concentration recorded by the Novatech P-695 system. These samples, taken at approximately 100 seconds into the test, suggest concentrations of NO and NO_2 of 70 and 200 ppm, respectively, both higher than the values obtained with the Novatech P-695 system (Figure 4-42). These differences in concentration may potentially be explained by the fact that the Gastec STR-800 Probe which is located directly above the discharging aerosol unit, while the Novatech P-695 probe is positioned further downstream from the aerosol discharge. Local pockets of NO_2 could also have attributed for the saturation of the Gastec STR-800 sample, and an equilibrium shift between NO and NO_2 concentrations may have taken place with distance from the discharge port of the unit as well.
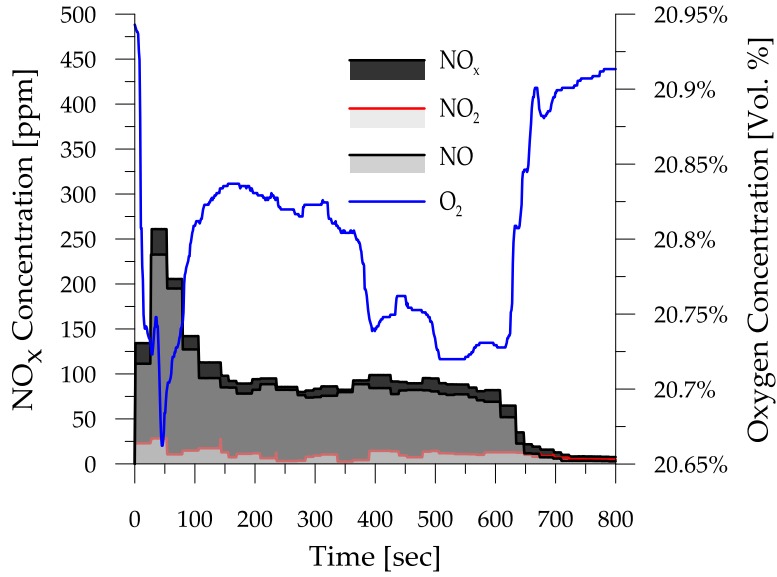
Figure 4-42: NO$_x$ concentrations for cold agent discharge (StatX-Test B)

Figure 4-43: Measured CO concentrations for cold agent discharge (StatX-Test B)

Figure 4-44: Measured NO$_x$ concentrations for cold agent discharge (StatX-Test B, 100 seconds)

In addition to the NO$_x$ measurements above, additional Gastec STR-800 samples were withdrawn at times of 229 and 339 seconds into the test, to ascertain whether any HCN or NH$_3$, respectively, was present in the hot layer for test in Figure 4-42. While no measurable concentration of HCN was observed, NH$_3$ concentrations of 25-30 ppm were recorded as indicated by the left edge of the black tape in Figure 4-45.

Figure 4-45: Measured NH$_3$ concentrations for cold agent discharge (StatX-Test B, 339 seconds)

A repeat of test B (Figure 4-42) was performed on a separate day with tighter compartment door sealing in test C (Figure 4-46). Gases in the test are withdrawn from the upper layer of the compartment, during activation of the StatX aerosol agent. Concentrations of NO in test C increase to peak values of 400 ppm immediately on activation of the aerosol with a corresponding decrease in O$_2$ and increase in CO concentration as seen in the other tests. Measured concentrations of CO immediately peak at values of 115 ppm, which is more than two times less than the values recorded in the previous test in Figure 4-43. However, values in test C stagnate around 100 ppm for the duration of the experiment whereas in the previous test B, they gradually drop due to larger unattended compartment leakage. The higher gas concentrations at the beginning of the previous test B can be a result of heated aerosol exhaust gases rising and collecting near the inlet of the sampling probe, while the lower values in test C can be attributed to lower compartment temperatures and mixing of CO in the upper regions. Throughout the remainder of the test, NO concentrations slowly decay as a function of time, leveling out at values around 100 ppm until the compartment door is opened and ventilated (not shown in this plot). The higher peak values of NO could have potentially accrued due to hot exhaust gases rising and collecting near the ceiling of the compartment, followed by gradual decrease to lower NO concentrations due to mixing and diffusion in the upper ceiling regions as well as unattended compartment leakage of the agent. Similar to the trend in CO, concentrations of NO$_2$ rise to lower peak values of around

25-30 ppm and remain constant through the remainder of the time as seen in Figure 4-46. After the test time is completed, the compartment is opened and ventilated (not shown on plot).

Additional NO$_x$ concentrations were measured using the Gastec STR-800 probe for the test presented in Figure 4-48 to compare to those obtained using the Novatech. The samples, taken at approximately 170 seconds into the test, suggest concentrations of NO and NO$_2$ of 150 and 20 ppm, respectively, which confirm the values measured using the Novatech P-695 as well (Figure 4-46).

Figure 4-46: NO$_x$ concentrations for cold agent discharge (StatX-Test C)

Figure 4-47: Measured CO concentrations for cold agent discharge (StatX-Test C)

Figure 4-48: Measured NO$_x$ concentrations for cold agent discharge (StatX-Test C, 170 seconds)

Additional Gastec STR-800 samples were withdrawn at times of 330 seconds and 450 seconds into the test, respectively, to determine whether any HCN or NH$_3$ was present in the hot layer gases after discharge of the aerosol unit. While no measurable concentrations of HCN are observed, an NH$_3$ concentration of 50 ppm is recorded, as indicated by the left side of the black tape on the tube in Figure 4-49. This would again be consistent with the processes expected during aerosol agent discharge.

Figure 4-49: Measured NH$_3$ concentrations for cold agent discharge (StatX-Test C, 450 seconds)

4.18 Results of Aerosol Agent Only Tests for DSPA Unit

Concentrations of NO, NO_2 and NO_x are measured using the Novatech P-695 system during three tests conducted by discharging a StatX aerosol unit into the empty fire compartment, then immediately closing the door and keeping the compartment door sealed for 10 minutes. In Test D, gas concentrations are measured low in the compartment and near the outlet of the aerosol unit as per Figure 3-2, whereas for Test E and F, gas concentrations are measured in the upper ceiling level of the compartment as per Figure 3-1. To supplement the information on NO_x evolution, additional measurements of NH_3 and HCN concentration are made using the Gastec system in the latter two experiments. These tests are intended to benchmark the quantity of NO, NO_2, NO_x and CO that was created due to thermal decomposition of base aerosol compounds (such as KNO_3) and fuel binder during and immediately after activation of the aerosol unit. In addition, results are compared against 10 and 15 minute short term exposure limits for NO_x [35, 62, 63] and CO [62] to better appreciate the potential impact of an accidental discharge of a unit into an occupied space.

Having measured sample concentrations of CO, it is desired that after several repeat tests, the results can be compared against published values for exposure limits and ceiling level concentrations of CO [62]. In addition, the tests are going to serve as a benchmark to identify the amount of CO created due to thermal decomposition of the fuel binder during and immediately after the aerosol discharge.

Upon activation of the DSPA aerosol unit for Test D, Figure 4-50, concentrations of NO measured near the outlet of the unit (left axis) increase sharply to values of 500 ppm, and then slowly decrease back to 100 ppm where they remain for the duration of the experiment. Trends in the measured concentrations of CO (Figure 4-52) and O_2 (right axis on both plots) at the same position closely follow those of NO confirming that the NO is being formed through combustion reactions taking place during generation of the aerosol powder. CO concentrations sharply increase to peak values of 2700 ppm and then decrease back to more steady levels of 750 ppm. As NO concentrations decrease, NO_2 concentrations increase, jumping to a constant value of around 150 ppm. They subsequently decrease back to ambient levels with the door opening; however, measured values are suspect in this test since NO_2 levels are determined by the Novatech P-695 system as the difference between the NO and the NO_x values, therefore cannot be accurately determined when the detector is saturated for either NO or NO_x. Once the NO and NO_x values decrease well below saturation, more representative values of NO_2 are likely measured as seen by the step increase in NO_2 concentration almost 85 seconds into the test.
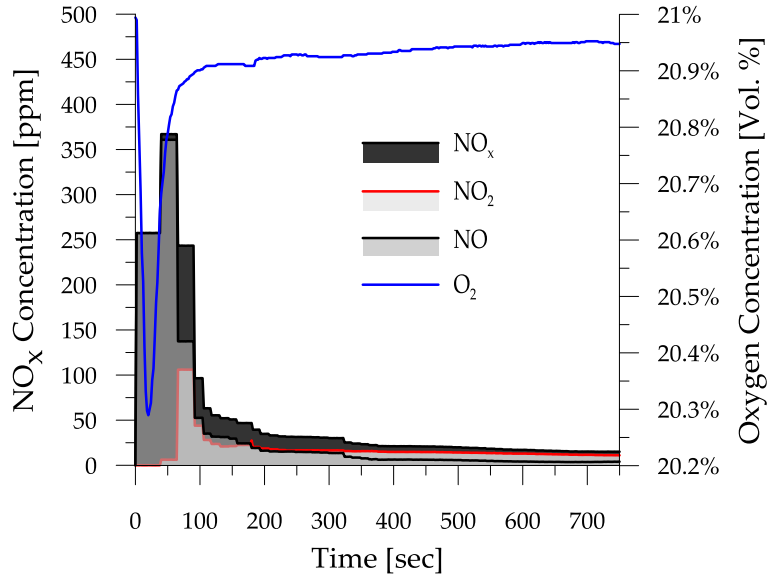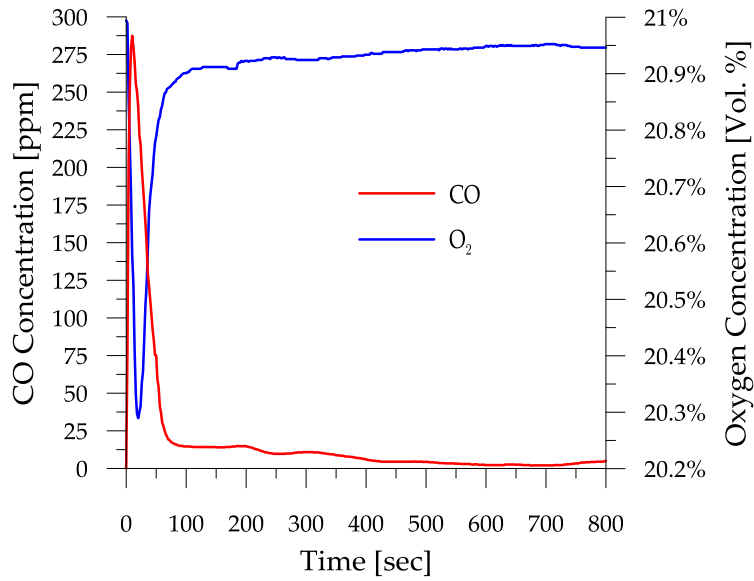
Figure 4-50: NOₓ concentrations for cold agent discharge (DSPA-Test D)
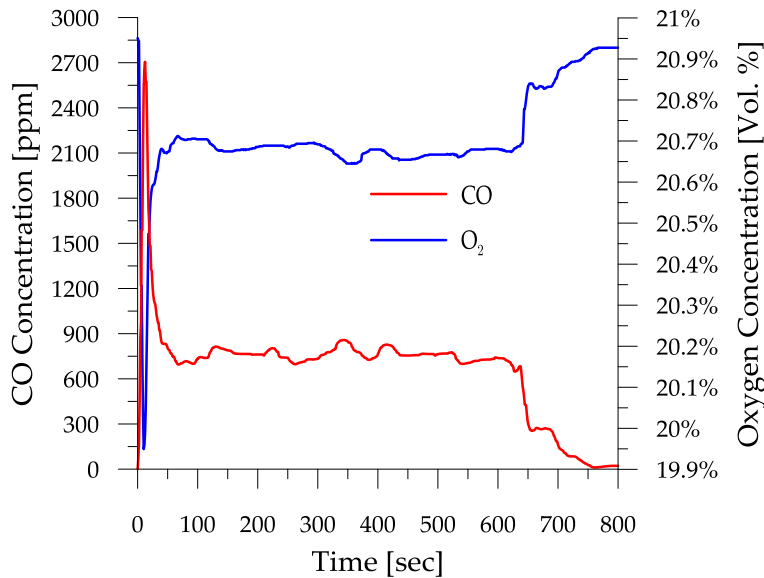
Figure 4-51: Measured CO concentrations for cold agent discharge (DSPA-Test D)

In a subsequent test, Test E, the gases are measured in the upper ceiling layer pre- and post-activation of the aerosol unit, as plotted in Figure 4-52. Recorded concentrations indicate an immediate spike in NO concentration to a peak value of 500 ppm, and CO value of 3190 ppm. Both of the values are higher than in the previous test, Test D above, suggesting that the heated aerosol discharge gases rise and collect near the measurement location at the ceiling. Trends in CO concentrations are similar to those for NO formation, again confirming NO creation through combustion reactions during generation of the aerosol. Due to saturation of the Novatech P-695 detector, NO_2 levels do not likely register any representative values until 140 seconds into the

test. After this, they peak at values of 350 ppm, then shortly after reaching that value they decay again due to unattended compartment leakage and mixing in the upper regions of the compartment.

Additional NO$_x$ concentrations were recorded using Gastec STR-800 probe for test presented in Figure 4-54. The samples, taken at approximately 210 seconds into the test, suggest concentrations of NO and NO$_2$ of 200 and 50 ppm, respectively. The NO concentration saturates the tube but confirms that high concentrations of NO can exist within upper regions of the compartment after discharge of the aerosol. Apparent differences in the measured NO$_2$ concentrations can most probably again be explained through the different sampling locations for the Gastec STR-800 and Novatech P-695 sampling systems.
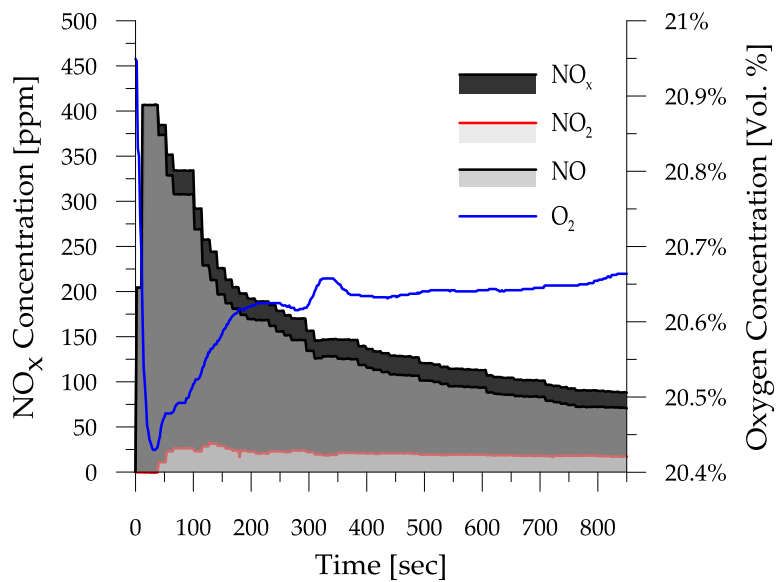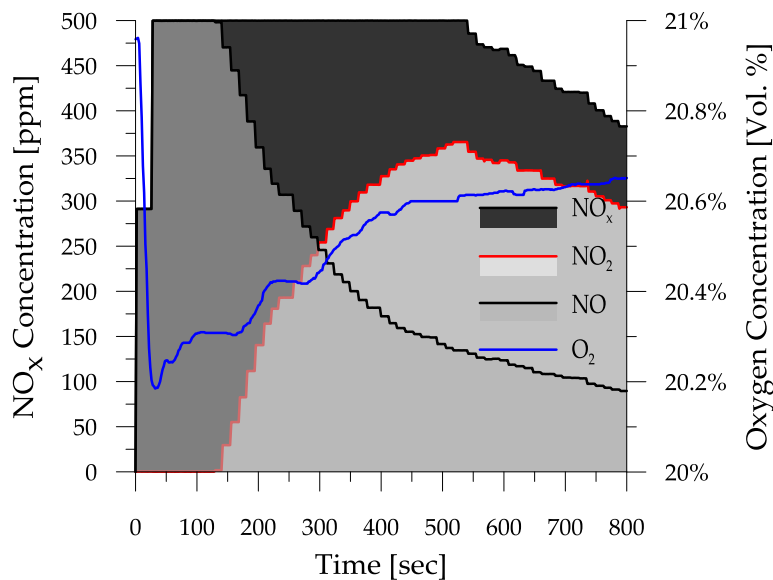

Figure 4-52: NO$_x$ concentrations for cold agent discharge (DSPA-Test E)
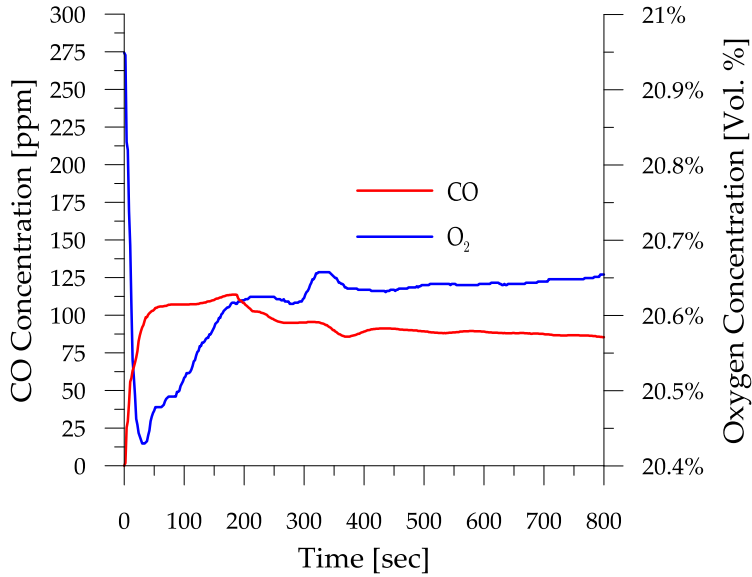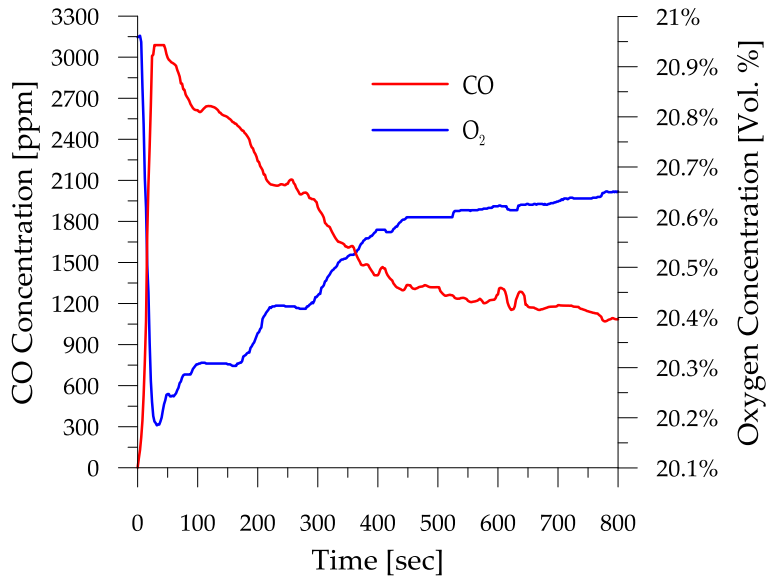
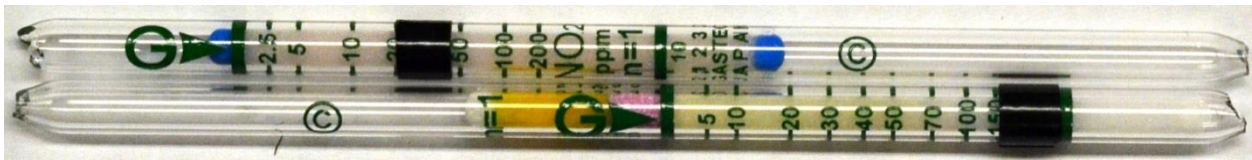**Figure 4-53: Measured CO Concentrations for Cold Agent Discharge (DSPA-Test E)**

Figure 4-54: Measured NO$_x$ concentrations for cold agent discharge (DSPA-Test E, 210 seconds)

In addition to the NO$_x$ measurements, additional Gastec STR-800 samples were withdrawn at times of 325 seconds and 445 seconds into the test to determine whether any HCN or NH$_3$, respectively, is present in the hot layer gases after discharge of the aerosol unit. While no measurable concentrations of HCN are observed, NH$_3$ concentrations of 300 ppm are recorded as indicated by the left edge of the black tape in Figure 4-35.

Figure 4-55: Measured NH$_3$ concentrations for cold agent discharge (DSPA-Test E, 445 seconds)

A repeat Test E (Figure 4-52) was performed on a separate day with tighter compartment door sealing, designated here as Test F (Figure 4-56). Gases in the test are withdrawn from the upper layer of the compartment, during and after activation of the DSPA aerosol agent. Concentrations of NO in Test F increase to peak values of 500 ppm immediately on activation of the aerosol unit with a corresponding decrease in O_2 and increase in CO concentration as seen in the other tests. Measured concentrations of CO immediately peak at values of 1400 ppm, which is more than two times less than the values recorded in the previous Test E (Figure 4-53). However, the values in test F gradually decrease to concentrations of around 1000 ppm for the duration of the experiment whereas in Test E they are seen to decrease to much lower values due to larger unattended compartment leakage. The higher gas concentrations at the beginning of the previous Test E can be a result of heated aerosol exhaust gases rising and collecting near the inlet of the sampling probe, while the lower values in Test F can be attributed to variations in mixing of the gases in the upper compartment region. Throughout the remainder of the test, NO concentrations slowly decayed as a function of time, leveling out at 100 ppm until the compartment door is opened and ventilated (not shown in this plot). Similar in trend to CO, concentrations of NO_2 increased to high peak values of 220 ppm and remained constant through the remainder of the time as seen by Figure 4-56.

The concentrations of NO and NO_2 measured using the Novatech P-695 system (Figure 4-56) were further confirmed via Gastec STR-800 samples taken at 265 seconds into the test which indicated concentrations of NO (upper tube) and NO_2 (lower tube) of around 200 ppm respectively for both, as marked by the right hand edge of the black tape around the two tubes shown in Figure 4-58.
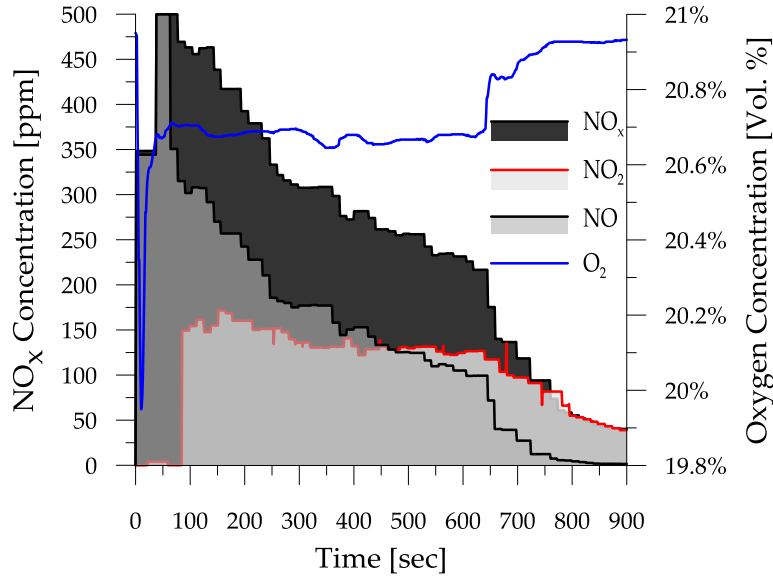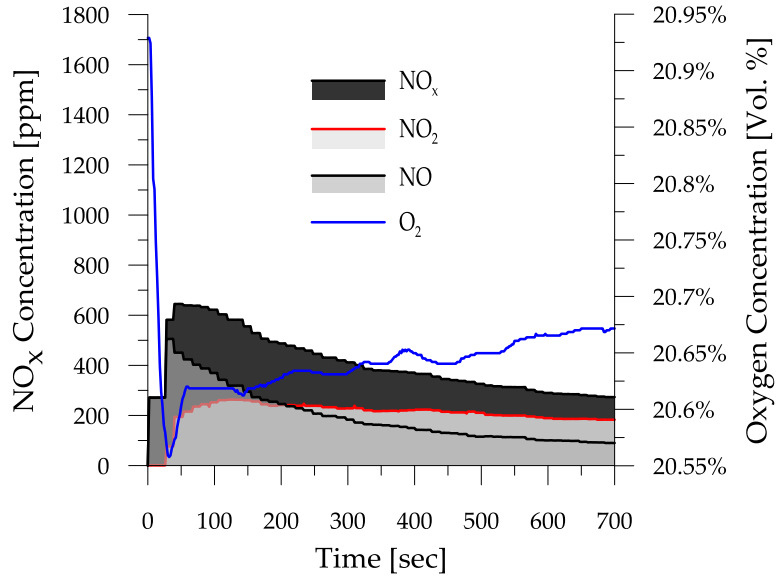
Figure 4-56: NOx concentrations for cold agent discharge (DSPA-Test F)
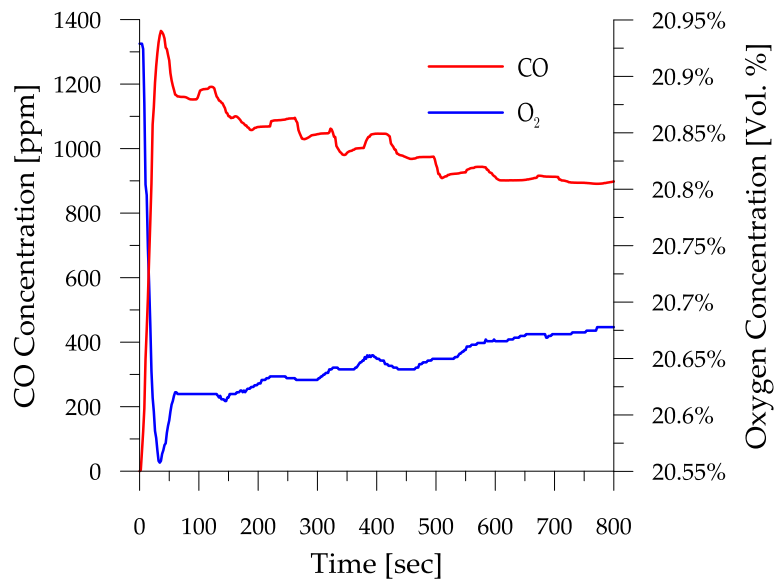
Figure 4-57: Measured CO concentrations for cold agent discharge (DSPA-Test F)

Figure 4-58: NOx concentrations for cold agent discharge (DSPA-Test F, 265 seconds)

74

Additional Gastec STR-800 samples were withdrawn at times of 400 seconds and 520 seconds into the test, respectively, to determine whether any HCN or NH_3 was present in the hot layer gases after discharge of the aerosol unit. Measurable concentrations of HCN and NH_3 are recorded at 40 and 60 ppm respectively, as indicated by the left side of the black tape on the sampling tubes shown in Figure 4-59 and Figure 4-60. This would again be consistent with the oxidation pathways expected due to aerosol agent generation and discharge.

Figure 4-59: Measured HCN concentrations for cold agent discharge (DSPA-Test F, 400 seconds)

Figure 4-60: Measured NH_3 concentrations for cold agent discharge (DSPA-Test F, 520 seconds)

4.19 Summary and Discussion of Aerosol Agent Only Test Results

Comparison of NO_x concentrations measured during StatX and DSPA activation and aerosol suppression of the agent only tests Figure 4-40, Figure 4-42, Figure 4-46 and Figure 4-50, Figure 4-52, Figure 4-56, respectively, indicate different temporal distributions of NO and NO_2 in different regions of the compartment during activation and aerosol generation from the two units. NO is produced during and immediately after activation for both variants of aerosol extinguisher, both in the regions immediately adjacent to the unit and in the upper layers of the compartment. In both cases, measured concentrations of NO surpass the IDHL limit for occupational exposure of 100 ppm set by OSHA [35]; however, it would be expected that such concentrations would normally be seen for a fairly short period of time after activation of the aerosol units and would dilute through mixing and ventilation over time. The results, however, do again point to the importance of appropriate operational procedures to minimize the likelihood that any personnel could be exposed to levels above either OSHA threshold during conduct of normal fire response activities.

Measured concentrations of NO_2 are also higher for the DSPA over the StatX units. For both units and measurement locations, NO_2 concentrations exceed the 1-hour continuous exposure limit proposed by WHO [34], as well as both the OSHA IDHL and OSHA 15-minute exposure thresholds [35], suggesting that care should be taken regarding potential exposure of personnel should an aerosol unit release even into a cold, relatively well sealed compartment. Trends in the time evolution of NO_2 for the StatX and DSPA aerosol units in agent only tests when the door was closed throughout the experiment seem to compare well, showcasing similar trends in NO_2 production within in their respective brand category.

Measured CO concentrations during all aerosol generation in the sealed fire compartment, indicate slightly different temporal distributions of CO. Carbon monoxide is produced during and immediately after activation for both variants of aerosol extinguisher. With respect to StatX, the second aerosol test produced upwards of two times higher concentrations than those produced during activation of the first and third StatX variant. In the second StatX case, peak measured concentrations of CO significantly surpass the ceiling limit of 200 ppm set by NIOSH for occupational exposure [63]. In contrast, concentrations of CO measured during the first and third StatX agent test are below the NIOSH but slightly above the OSHA ceiling limit. High CO concentrations are seen for very short periods of time after activation of the aerosol units and when allowed enough time for adequate mixing are well below NIOSH and OSHA ceiling levels. Personnel would most likely be exposed to lower levels of CO concentration during accidental aerosol discharge or during the conduct of normal fire response activities due to ventilation and consequent mixing of the gas throughout the compartment. Since the measured values of concentration in these tests do appear to have exceeded the ceiling limits, StatX units should be further tested to understand the potential for generation and dispersal of high concentrations of CO within different sizes of compartment, as well as any implications in terms of procurement and safe storage of these aerosol extinguishing units.

With respect to the DSPA-4 discharge tests, Figure 4-51, Figure 4-53 and Figure 4-57, respectively, indicate high levels of CO generated in the sealed fire compartment. In all cases, peak measured concentrations of CO significantly surpass the ceiling limit of 200 ppm set by NIOSH for occupational exposure [63]. In all tests, high CO concentrations are seen for short periods of time after activation of the aerosol units but even after mixing appear to still be well above NIOSH and OSHA ceiling levels. Personnel may be exposed to high levels of CO concentration during accidental aerosol discharge or during the conduct of normal fire response activities. Since the measured values of concentration in these tests do exceed the ceiling limits, DSPA units should be further tested to understand the potential for generation and dispersal of high concentrations of CO within the compartment, as well as any implications in terms of procurement and safe storage of these aerosol extinguishing units.

Key results of the full set of gas tests described in this Chapter are summarized in Tables 4-1 through 4-7 for ease of reference. The associated discussion is contained in the individual sections above.

Table 4-1: Diesel characterization fire with the corresponding concentrations of the peak prime gases sampled with Novatech P-695 and Gastec STR-800 pump

Test No.	Fire Suppression Test Scenarios			
	Novatech P-695		Gastec STR-800	
	Sampled Gas	Concentration (ppm)	Sampled Gas	Concentration (ppm)
Diesel Char. Fire	NO (ppm)	25	NO (ppm)	22.5
	NO2 (ppm)	<5	NO2 (ppm)	5
			NH3 (ppm)	0
			HCN (ppm)	0

Table 4-2: Softwood characterization fire with the corresponding concentrations of the peak prime gases sampled with Novatech P-695 and Gastec STR-800 pump

Test No.	Fire Suppression Test Scenarios			
	Novatech P-695		Gastec STR-800	
	Sampled Gas	Concentration (ppm)	Sampled Gas	Concentration (ppm)
Softwood Char. Fire	NO (ppm)	50	NO (ppm)	10-13
	NO$_2$ (ppm)	<5	NO$_2$ (ppm)	15
			NH$_3$ (ppm)	0
			HCN (ppm)	10

Table 4-3: Unobstructed diesel fire suppression test with the corresponding concentrations of the peak prime gases sampled with Novatech P-695 and Gastec STR-800 pump

Test No.	Fire Suppression Test Scenarios							
	Novatech P-695					Gastec STR-800		
	Sampled Gas	Concentration (ppm)				Sampled Gas	Concentration (ppm)	
		Stat-X Test 1	Stat-X Test 2	DPSA 5-4 Test 1	DSPA 5-4 Test 2		Stat X Test 2	DPSA 5-4 Test 2
1	NO (ppm)	250	300	Inconclusive	800	NO (ppm)	200	200
	NO2 (ppm)	50	75	Inconclusive	1600	NO2 (ppm)	200	200
						HCN (ppm)	0	0
						NH3 (ppm)	105	500

Table 4-4: Obstructed diesel fire suppression test with the corresponding concentrations of the peak prime gases sampled with Novatech P-695 and Gastec STR-800 pump

Test No.	Fire Suppression Test Scenarios		
	Novatech P-695		
	Sampled Gas	Concentration (ppm)	
		Stat-X Test 1	DPSA 5-4 Test 1
2	NO (ppm)	150	375
	NO2 (ppm)	140	50

Table 4-5: Bilge diesel fire suppression test with the corresponding concentrations of the peak prime gases sampled with Novatech P-695 and Gastec STR-800 pump

Test No.	Fire Suppression Test Scenarios							
	Novatech P-695					Gastec STR-800		
	Sampled Gas	Concentration (ppm)				Sampled Gas	Concentration (ppm)	
		Stat-X Test 1	Stat-X Test 2	DPSA 5-4 Test 1	DSPA 5-4 Test 2		Stat X Test 2	DPSA 5-4 Test 2
3	NO (ppm)	275	25	Inconclusive	200	NO (ppm)	5	200
	NO2 (ppm)	75	220	Inconclusive	600	NO2 (ppm)	200	200
						HCN (ppm)	0	0
						NH3 (ppm)	300	260

Table 4-6: Softwood crib fire suppression test with the corresponding concentrations of the peak prime gases sampled with Novatech P-695 and Gastec STR-800 pump

Test No.	Fire Suppression Test Scenarios							
	Novatech P-695					Gastec STR-800		
	Sampled Gas	Concentration (ppm)				Sampled Gas	Concentration (ppm)	
		Stat-X Test 1	Stat-X Test 2	DPSA 5-4 Test 1	DSPA 5-4 Test 2		Stat X Test 2	DPSA 5-4 Test 2
4	NO (ppm)	340	30	500	20	NO (ppm)	5	20
	NO2 (ppm)	200	25	450	600	NO2 (ppm)	7	200
						HCN (ppm)	20	0
						NH3 (ppm)	0	500

Table 4-7: Cold agent discharge test with the corresponding concentrations of the peak prime gases sampled with Novatech P-695 and Gastec STR-800 pump

Test No.	Fire Suppression Test Scenarios						
	Novatech P-695						
	Sampled Gas	Concentration (ppm)					
		Stat-X Test A	Stat-X Test B	DPSA 5-4 Test C	DSPA 5-4 Test D	DSPA 5-4 Test E	DSPA 5-4 Test F
	NO (ppm)	225	350	400	500	500	500
	NO2 (ppm)	40	110	30	150	350	220
	CO (ppm)	120	290	115	2700	3190	1400
5	**Gastec STR-800**						
	Sampled Gas	Concentration (ppm)					
			Stat-X Test B	DPSA 5-4 Test C		DSPA 5-4 Test E	DSPA 5-4 Test F
	NO (ppm)	N/A	70	150	N/A	200	200
	NO2 (ppm)	N/A	200	20	N/A	50	200
	HCN(ppm)	N/A	0	0	N/A	0	40
	NH3 (ppm)	N/A	30	50	N/A	300	60

5 Powder Characterization Using X-Ray Diffraction (XRD)

To better understand the chemistry of the aerosols used and aid in further research , the raw solid tablet, as the well as the powder aerosol generated during discharge of each handheld unit was assessed using visual observation, as well as more detailed analysis using the X-ray diffraction system described in Section 3.5. By visual observation, the solid by products of the chemical fire suppression are mostly small white crystalline structures, so any different compounds cannot be distinguished based on colour or size of particulate. From an examination of the product information and other literature it was found that the expected composition might include: potassium bicarbonate ($KHCO_3$), potassium nitrate (KNO_3), ammonium bicarbonate (NH_4HCO_3) as well as a small percentage of other compounds that are undisclosed [8]. Further, it was suggested that during aerosol formation, potassium hydroxide (KOH) can recombine with hydrogen cyanide (HCN) to form potassium cyanide (KCN). As such, it is felt important to identify any potential dangers that may arise from handling or post discharge clean-up of the suppression agents.

5.1 Powder Characterization of StatX and DSPA Raw Tablets

Diffraction patterns obtained via X-ray diffraction of the raw StatX and DSPA tablets are contained in Figure 5-1 and Figure 5-2 below, respectively. Comparison with patterns in existing X-ray diffraction libraries [39], identified the main component in the raw tablet for each unit as a mineral form of potassium nitrate, niter. However, the presence of other compounds listed above, such as potassium carbonate (K_2CO_3) or ammonium bicarbonate (NH_4HCO_3) could not be confirmed through XRD analysis.
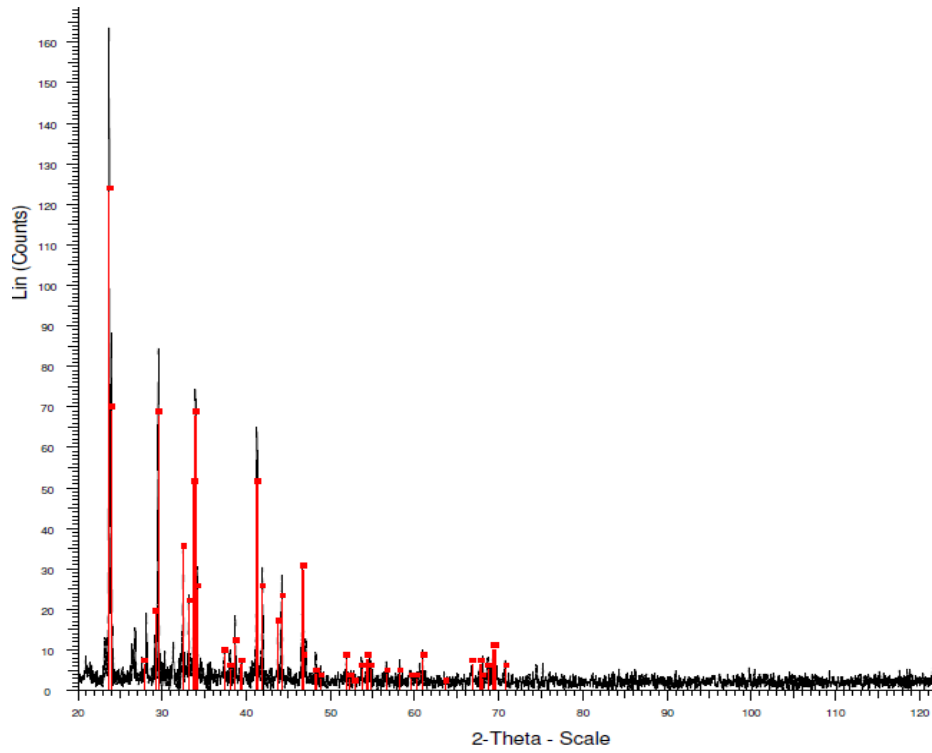
Figure 5-1: Diffractogram of the raw StatX aerosol tablet
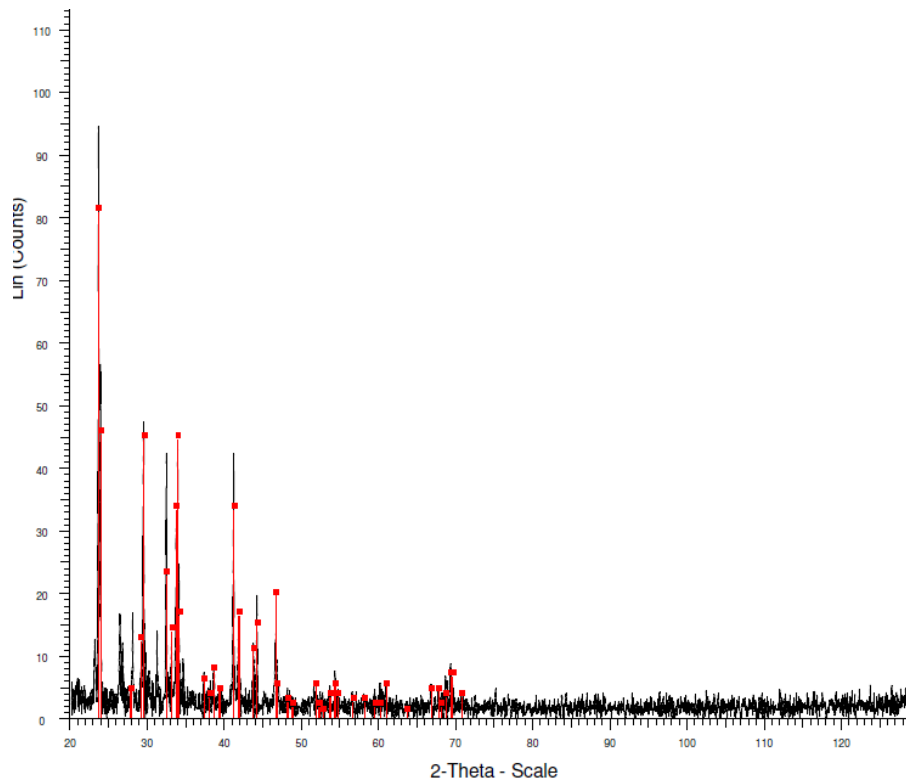
Figure 5-2: Diffractogram of the raw DSPA aerosol tablet

Niter is a strong oxidizing agent known to be used in aerosol powder generation [64]. While it is known to have relatively low acute toxicity, it is listed as a carcinogen and can be harmful if swallowed, particularly for vulnerable populations [65].   It forms an acid (pH 5.5 – pH 8) in the presence of water. Under thermal decomposition, niter is known to produce nitrogen and potassium oxides, some of which may be toxic, and it may also partake in further reactions to produce various other chemical compounds.

5.2 Characterization of the StatX and DSPA Aerosol Powder

The aerosol extinguishing powder generated during and after discharge of each unit was collected and analyzed using the same X-ray diffraction unit as was used for analysis of the raw aerosol tablets discussed above. Figure 5-3 and Figure 5-4 contain the patterns obtained from the StatX and DSPA aerosols, respectively.
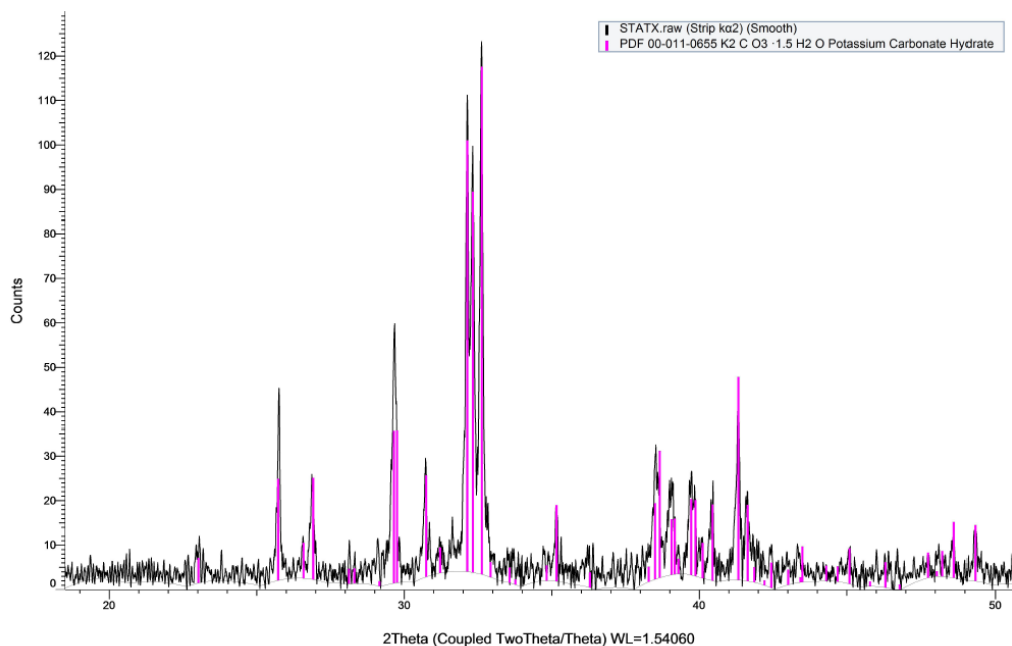
Figure 5-3: Diffractogram of the post discharged StatX aerosol agent
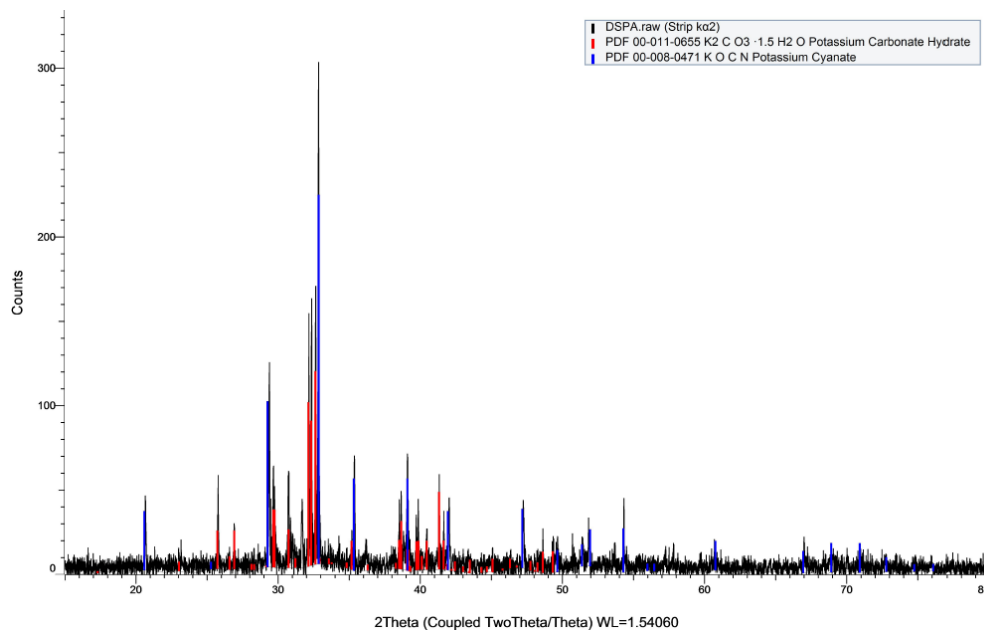
Figure 5-4: Diffractogram of the post discharged DSPA aerosol agent

The diffraction patterns from both the StatX and DSPA aerosol powders indicated that a major component of the powder is potassium carbonate (K_2CO_3), which is also a decomposition product of potassium bicarbonate ($KHCO_3$), one of the main components in the aerosol tablets, when temperatures are in the excess of 500^0C [20]. In the case of the DSPA aerosol, another potassium salt - potassium cyanate (KCNO) was also seen. Since potassium cyanate may be a by-product of reactions with ammonia (NH_3) based compounds, this is consistent with the production of NH_3 and HCN seen in the DSPA agent only tests (Section 4.18). No other compounds were identified in the aerosol powders for either variant of extinguisher.

Potassium carbonate exhibits mild toxic properties when ingested through the mouth or nose, or when brought into contact with the eyes. Ingestion of large quantities of potassium carbonate are known to cause severe abdominal pain, breathing difficulties and fainting [50]. Potassium cyanate (KOCN) is not considered a harmful by-product in itself; however, based on the present work no information could be obtained on which intermediate reactions might have been involved in the production of potassium cyanate (KOCN). Since this reaction may have proceeded through intermediate reactions that involve ammonia (NH_3) and highly toxic gases such as phosgene ($COCl_2$) [53], the presence of materials such as KOCN in the aerosol powder point to the importance of appropriate operational procedures, but might also suggest that a more thorough investigation be conducted into the chemical mechanisms of the aerosol generation to determine the potential for generation of compounds that were not directly studied in this research.

6 Assessment of Corrosion Effects due to Aerosol Deposition on Materials

One key component in the solid, aerosol forming agent in both the StatX and DSPA handheld extinguishing units is potassium nitrate, KNO_3, which is an ionic salt, a strong oxidizing agent and a natural solid source of nitrogen [66]. After activation of the extinguisher, the KNO_3 as well as any organic oxidizers and binding agents in the solid tablet react to generate fluid aerosols in the proximity of the extinguishing units. The aerosols can be comprised of particulates such as potassium carbonate (K_2CO_3) and potassium bicarbonate ($KHCO_3$), as well as ammonium bicarbonate (NH_4HCO_3), potassium cyanate ($KCNO$) and other materials depending on the nature of the reacting compounds and details of the reaction and decomposition processes. The particles are expelled into the fire environment and, when exposed to high temperatures, the potassium carbonate particulate, K_2CO_3, can dissociate into potassium radicals which interact with the hydroxyl, OH, oxygen, O, and hydrogen, H radicals that normally drive the hydrocarbon combustion process. This interaction interrupts the combustion chemistry to suppress the fire, and also leads to production of more stable molecules such as potassium hydroxide (KOH) [7], as well as gases such as H_2O, CO_2, and NO_x [67].

Both potassium hydroxide (KOH) and potassium carbonate can dissociate to the potassium ion (K+) and either hydroxide (OH^-) or carbonate (CO_3^{-2}) ions in water. The resulting solutions are strongly basic with pH levels on the order of 12-14. As a result potassium hydroxide is classified as a class 8 (corrosive) chemical [68]. In terms of potential impact of the powders generated during aerosol suppression, if basic solutions are generated, they can have adverse effects on humans and on many materials that might be in the surrounding area. According to OSHA, direct contact with KOH has the potential to cause skin burns and eye damage, as well as damage to the lungs through inhalation [69]. In addition, such strong bases can damage materials, leading to erosion, corrosion and even potential failure of a component.

In this latter respect, it is of interest to evaluate the effects of the aerosol powders on sensitive electrical equipment and other materials that might be found on board a naval vessel. For this, a number of common marine components and materials including:

- Computer and electronic boards
- High tensile and mild steel
- CD discs
- Copper-beryllium alloy and
- NOMEX fabric

are placed in the UW burn compartment during the series of agent only tests, and diesel fire tests with agent suppression that were described in Chapter 3.3 above. Mild and high tensile steels are very common onboard navy vessels but generally exhibit relatively poor corrosion resistance so those samples were painted with an anti-corrosion paint as would be typically found on board the vessel. Copper beryllium alloys are similar to copper, but generally exhibit improved corrosion characteristics over many steels, particularly against alkalis and some organic acids [52, 53], so tests to determine impact of aerosols on those alloys are considered as complementary to the results above. The other samples are representative of the protective equipment worn by the attack teams (Nomex) and of the wide range of materials typically found in an electronics room, CD's, computer cabinets and circuit boards.

After exposure, each sample is visually inspected for deposition and other signs of immediate impact, then sealed in a bag. Thereafter, the condition of the sample is monitored every month, documenting any change in the characteristics of the exposed surface.

The following discussion outlines the results obtained from the corrosion tests.

6.1 Post Agent Release: Visual Observation of Damage

Based on potentially high alkalinity of the aerosol powder that is produced during agent discharge and suppression, a first step in the impact analysis involves visual inspection of each material coupon immediately after exposure to see whether there is any immediate damage to the surfaces.

In scenarios with both StatX and DSPA units, there is clear evidence of deposition of aerosol powder and for the case of fire suppression tests, both powder and soot on the surface. In most cases, this is accompanied by some discolouration of the surface suggesting some short term impact due to the aerosol exposure. To follow longer term changes, the surface of each material is examined using optical microscopy at regular intervals after exposure. Results of these analyses are contained in the sections below. Examinations of the computer and electronic boards are outlined in detail in Section 6.2, while results for all other materials are summarized into Tables indicating the overall results in Section 6.3. Specific microscope images from, and other details of, the latter results are compiled in [70].

6.2 Computer Boards

6.2.1 Computer Board Exposed to StatX agent

In the first test, a functioning computer board was mounted to a computer tower and left inside the testing compartment during an agent only test and a diesel suppression test using the StatX FR extinguishing unit. The computer was then placed in a conditioning chamber and left for six

months. Prior to disassembling the computer for examination of the internal components via optical microscopy, the computer was turned on to check if the system would still boot. The computer cards exposed during the agent only test failed to boot up properly, but the computer actually ran for half an hour with no status change. Even when the computer was restarted manually, no change was observed. Using a different board exposed during a diesel fire suppression test, on the other hand, the computer did boot up properly and continued to run through the half hour test period. To further assess the impact of aerosol exposure on the electrical boards, the cards were pulled out and examined using the optical microscope. Figure 6-1 below shows one of the computer cards at the time of system disassembly after exposure to the aerosol. Damage to the board is clearly evident in the Figure.
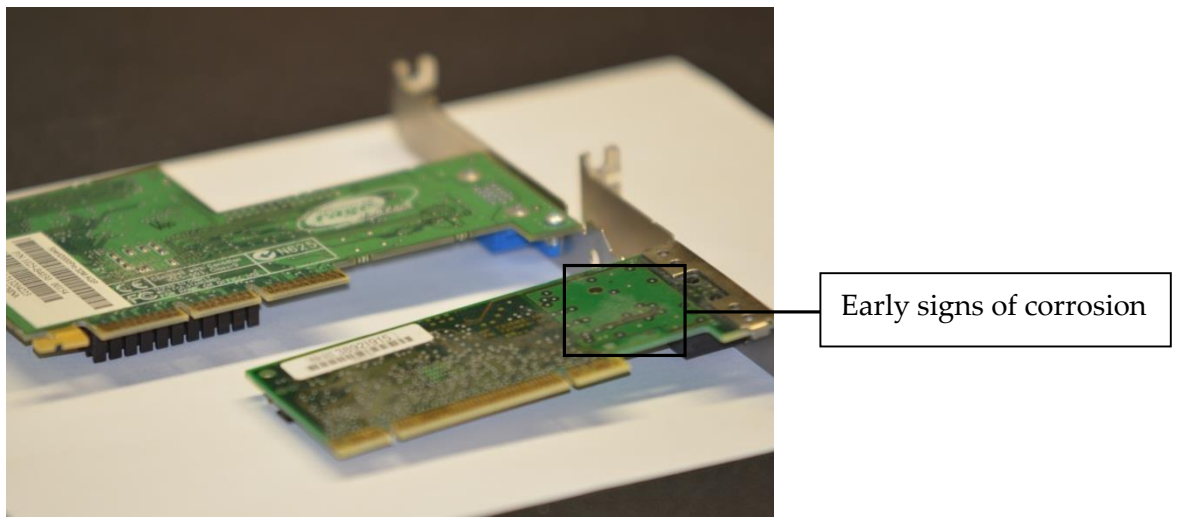
Figure 6-1: Computer card after six months of exposure to StatX aerosol agent

Images of conductive pathways and electrical connectors on the computer cards were take pre- and post-exposure to better ascertain the potential severity of corrosion resulting from aerosol powder deposition during fire suppression. Representative images are recorded in Figure 6-2 before exposure, and Figure 6-3 and Figure 6-4 after exposure respectively.
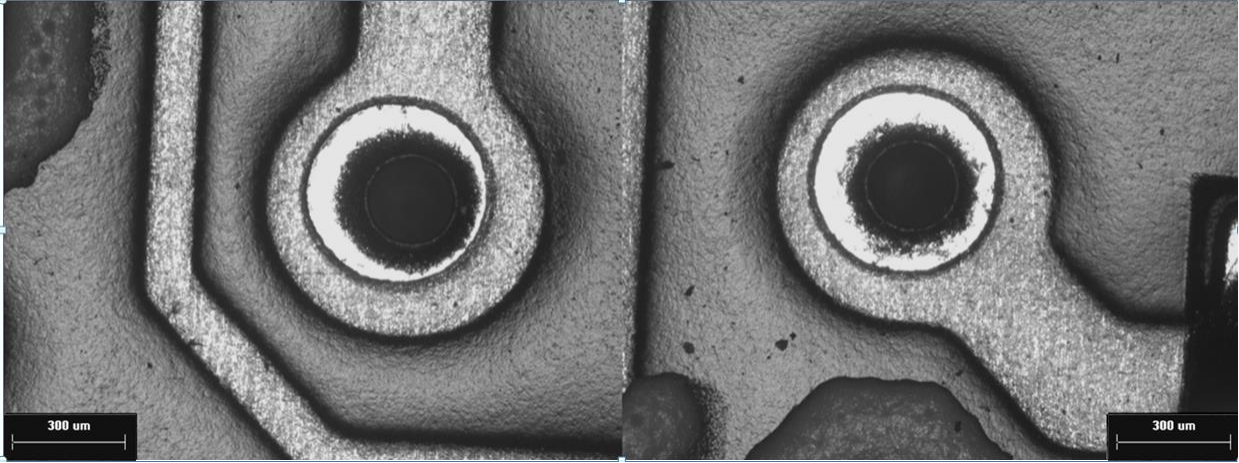
a) Conductive pathway in the PCB   b) Electrical connector in the PCB

Figure 6-2: Computer card before exposure to StatX aerosol agent
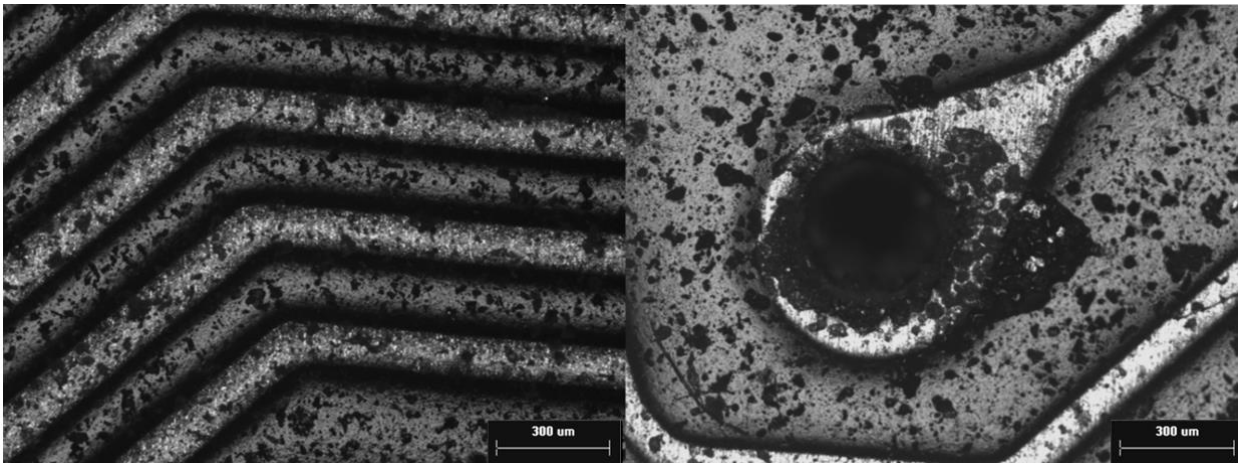
a) Conductive pathways in the PCB   b) Electrical connector in the PCB

Figure 6-3: Computer card six months after exposure to StatX aerosol agent in room environment
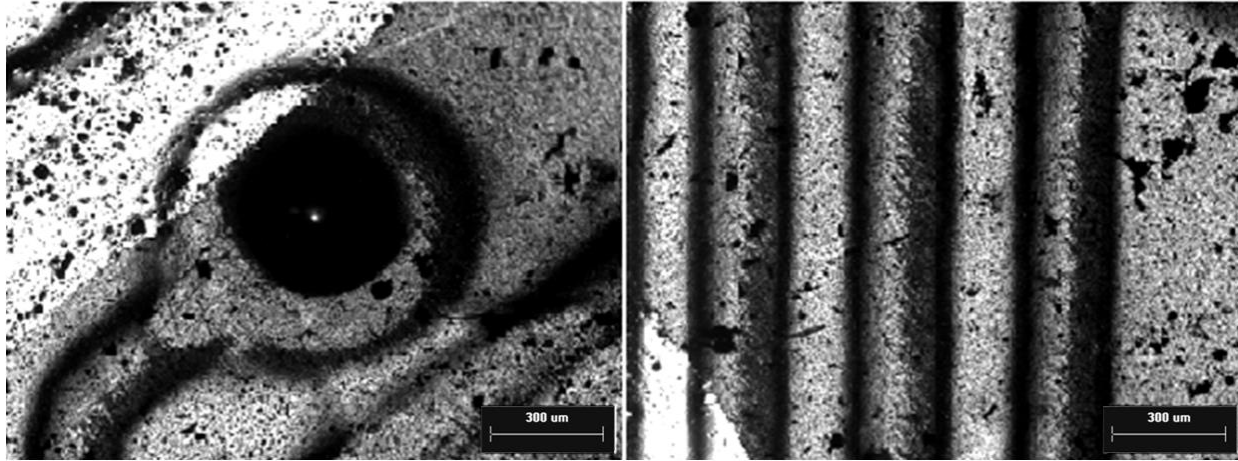
a) **Electrical connector in the PCB**   b) **Conductive pathway in the PCB**

Figure 6-4: Computer card six months after exposure to StatX aerosol agent and diesel effluents in room environment

During and after aerosol only or aerosol suppression tests with the StatX handheld aerosol extinguisher, powder residue is visible on the electronic circuit boards and any other material coupons within the compartment. As evidenced through Figure 6-3 and Figure 6-4 above, varying levels of pitting corrosion took place on the surfaces of both the conductive pathways and the electrical connectors over the period of six months after exposure. Similar impacts are seen for exposure of other materials as well. In general, a higher degree of pitting corrosion is observed in the case of cold agent discharge compared to the mixture of agent and diesel effluents deposited after suppression of a fire.

6.2.2 Computer Board Exposed to DSPA agent

The same tests as outlined above for the StatX aerosol unit were repeated with a functioning computer exposed during an agent only test and diesel suppression test using the DSPA extinguishing unit. The computer was again placed in a conditioning chamber and left for six months. Prior to disassembling the computer for examination of the internal components via optical microscopy, the computer was turned on to check if the system would still boot. In this test, both computer cards, that exposed to agent only and that exposed in a diesel fire suppression test, booted up properly, and ran normally for half an hour. The mouse and keyboard were also fully operational.

Following this, the system was turned off and the computer boards were pulled out and examined using the optical microscope. Figure 6-5 below shows one of the computer cards after exposure to the aerosol at the time of system disassembly with an area that showed early signs of corrosion marked by the black square.
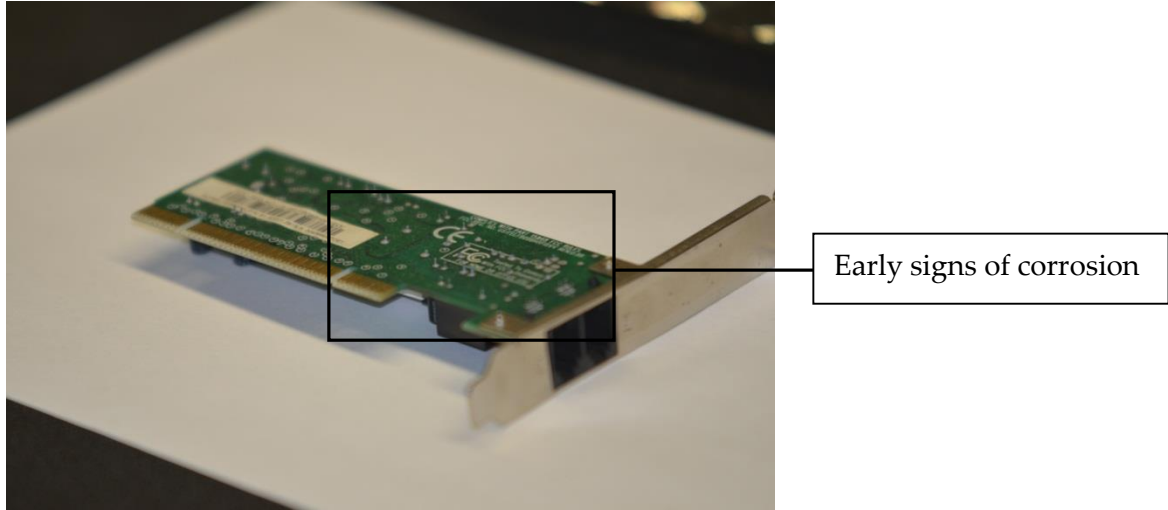
Figure 6-5: Computer card after six months of exposure to DSPA aerosol agent

To ascertain the severity of corrosion, the computer cards were placed under an optical microscope and images of pre and post exposure are recorded in Figure 6-6, and Figure 6-7 and Figure 6-8 respectively. Through comparison of Figure 6-6 to both Figure 6-7 and Figure 6-8, the residue deposition and corrosion of various components on the board exposed to the aerosol are notable but in this case did not lead to immediate malfunction of the computer system.
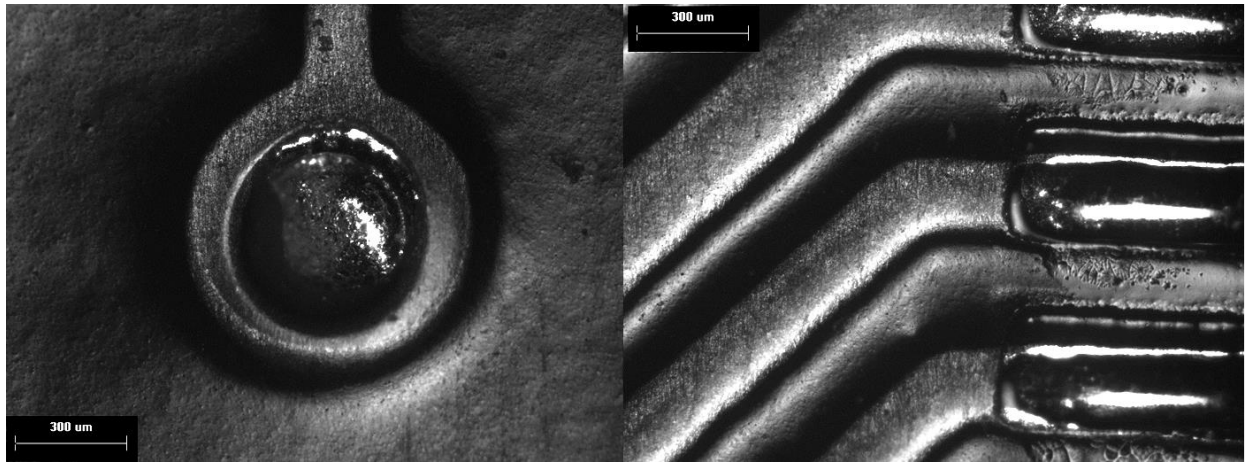
a) **Electrical connector in the PCB**　　　　　b) **Conductive pathways in the PCB**

Figure 6-6: Computer card before exposure to DSPA aerosol agent
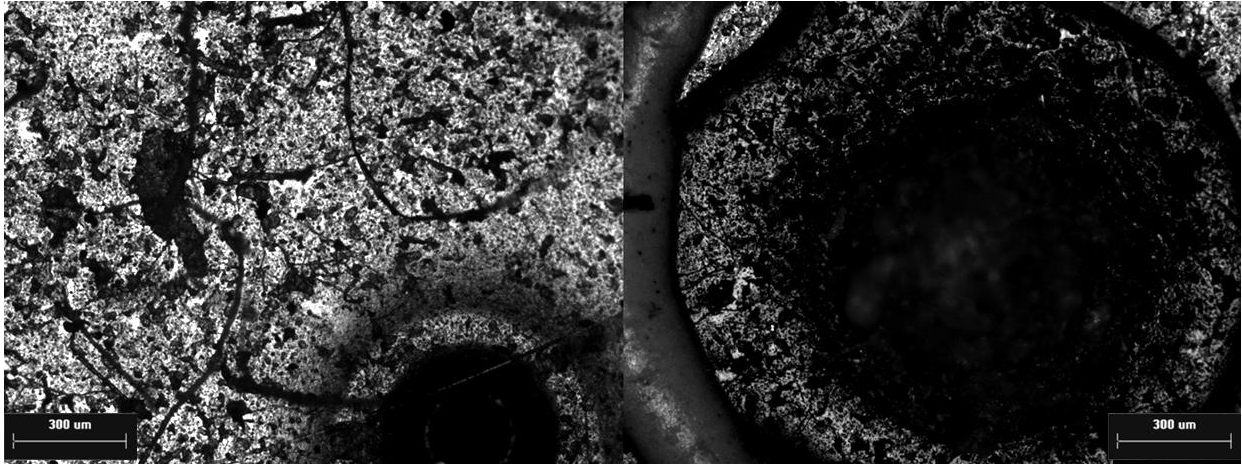
a)   **Resin impregnated Board with Conductor**   b)   **Electrical conductor in the PCB**

Figure 6-7: Computer card six months after exposure to DSPA aerosol agent in room enviroment
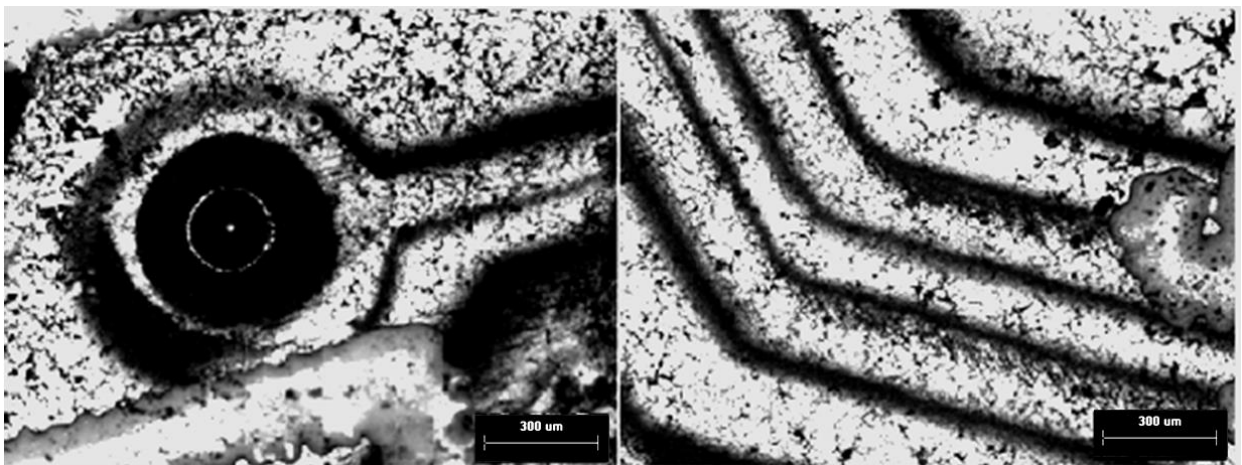
a)   **Electrical connector in the PCB**   b)   **Conductive pathway in the PCB**

Figure 6-8: Computer card six months after exposure to DSPA aerosol agent and diesel effluents in room environment

Referring to the figures, it appears that the damage to the board and connectors consists of deep pitting and possible intergranular corrosion leading to the large visible cracks depicted in Figure 6-7-a. With the level of damage seen, it appears quite possible that computers or other electrical equipment could malfunction during or after exposure to the aerosol agent generated by this unit as well.

6.2.3 Computer Board Summary

Analysis of computer boards exposed to ambient air, exposed to only aerosol agent and exposed to aerosol agent and diesel fire gases have allowed for qualitative assessment of the potential for corrosion during the test scenarios. Although much of the residue could be wiped away with a cloth, it is purposely left on the surfaces in this evaluation to simulate a real life scenario where computer equipment could not be attended to immediately. Evidence concludes that sensitive computer cards that are in a room during aerosol activation and suppression will experience some deposition of the particulate on their exposed surfaces. The exposure to the gases and particulate generated and discharged during aerosol activation has a potential to lead to significant corrosion on all sample surfaces. Impacts can include oxidation of the exposed surface, as well as deep pitting/crevice corrosion of the exposed electronic board. In both sets of tests above, exposure of the boards during cold agent discharge appeared to result in more severe corrosion than during fire suppression. This may be a result of the amount of particulate that deposited on the material surface, since as that amount increases, it might be expected that the corrosion rate also increases. Unfortunately, in the present tests there was no adequate way to measure differences in particles during deposition for different test situations [71]. Nonetheless, the tests do demonstrate that if computer boards are left unattended for long periods of time after exposure, corrosion of the board, connectors and conductive pathways can be sufficiently severe to lead to complete malfunction of a computer system. As a result, more investigation is required to develop a better understanding of the corrosion mechanisms at play and thereby to better assess potential methods for mitigation of corrosion to materials and systems that might be exposed during aerosol discharge or suppression in marine enclosures.

6.3 Additional Material Coupons and Corrosion Results

Additional assessment of the potential for post-agent corrosion of materials was focussed towards evaluation the impact of aerosol suppression agent generation and deposition on other materials that might be found on board naval vessels. These included AISI 1018 mild steel and AISI 4140 high tensile steel (MS and HTS), computer discs (CDs), copper beryllium alloy and NOMEX fabric found in personal protective equipment. As noted in Section 6.1, discolouration of the surfaces of all material coupons exposed to aerosol powders is observed. This led to a sequence of repeated examinations of surface changes in these samples over an extended period of time using optical microscopy as described above for the computer cards. The key results of these examinations are summarized, respectively, in Table 6-1 and Table 6-2 for exposure of the coupons during cold agent discharge of the StatX and DSPA units and in Table 6-3 and Table 6-4 for exposure during StatX and DSPA suppression of the diesel fire. For each material tested, the

respective Table contains a brief outline of the level and type of corrosion, as well as a potential mechanism for the damage observed. For completeness, a more detailed presentation and description of the entire set of microscopic images from these tests is contained in Appendix B of the thesis.

Table 6-1, below, contains a summary of the observed impact on the material coupons after being exposed to aerosol particulate (StatX agent only test) for a time span of a year.

Table 6-1: Corrosion results based on StatX cold agent discharge

Group	Aerosol Variant	Material	Corrosion (Y/N)	Type of Corrosion	Mechanism
Cold Agent Discharge	StatX	MTS	No	Mild discolouration	Chemical reaction between agent and protective paint
		HTS	No	Mild discolouration Particulate deposition	Chemical reaction between agent and protective paint
		Computer Disc Treated	Yes	Small pitting	Surface irregularities Temperature Chemical composition Presence of K_2CO_3
		Computer Disc Untreated	Yes Marked damage	Small and severe pitting Other residue	Surface irregularities Temperature Chemical composition Presence of K_2CO_3
		Copper Beryllium	No	Discolouration Small marks	Possible minor oxidation of copper substrate
		NOMEX	No	General discolouration from powder deposition	N/A

Continued examination of the samples using optical microscopy has revealed that the most predominant forms of interactions are chemical discolouration of the material surface with little evidence of further damage or more severe pitting of the surfaces such as is also seen for the computer components above. Materials such as mild and tensile steel usually do not respond well to corrosive agents, but in these tests the steel was covered with an anti-corrosion paint, as would be found in seagoing vessels. As a result, though the surfaces of these samples are discoloured, with some evidence of shallow pits, there is no evidence of damage to the metal substrate under long term exposure to aerosol powder residue. The computer discs showed the

most severe damage, manifest as surface pitting, even where the aerosol particulate was wiped away with a microfiber cloth immediately after exposure. As expected, the material coupons that are known to have strong inherent resistance to corrosion, such as the copper beryllium alloys (and some of the copper shielding on the computer boards discussed above), showed little to no evidence of damage. The fire resistant NOMEX cloth sample similarly showed no signs of deterioration under long term exposure to the aerosol powder.

Table 6-2: Corrosion results based on DSPA cold agent discharge

Group	Aerosol Variant	Material	Corrosion (Y/N)	Type of Corrosion	Driving Force
Cold Agent Discharge	DSPA	MTS	No	Discolouration Soot and particulate deposition Very shallow pits	Chemical reaction between agent and protective paint
		HTS	No	Discolouration Soot and particulate deposition Shallow pitting	Chemical reaction between agent and protective paint
		Computer Disc Treated	Yes	Small pitting	Surface irregularities Temperature Chemical composition Presence of K_2CO_3
		Computer Disc Untreated	Yes	Small and severe pitting Other residue	Surface irregularities Temperature Chemical composition Presence of K_2CO_3
		Copper Beryllium	No	Discolouration Soot and particulate deposition	Possible minor oxidation of copper substrate
		NOMEX	No	Discolouration Particulate deposition	N/A

Results of exposure of the same materials during agent only tests using the DSPA unit are summarized in Table 6-2. The most predominant form of damage amongst material coupons is again discolouration of the samples, with many samples also subject to varying levels of pitting corrosion. Results are very similar to those shown in Table 6-1, for which materials that have no inherent corrosion resistance show the most severe pitting damage, compared to the other

materials. Therefore, the CDs are most severely affected, even when the aerosol particulate is wiped away with a microfiber cloth. Materials with inherent corrosion resistance, such as the painted steels and copper beryllium, are discoloured but show little to no other changes in their surfaces after prolonged exposure. The NOMEX sample again collects the aerosol particulate but otherwise appears relatively unaffected by exposure to the aerosol particulate generated during the DSPA aerosol agent only test.

Table 6-3: Corrosion results based on combined exposure to StatX particulate and diesel fire

Group	Aerosol Variant	Material	Corrosion (Y/N)	Type of Corrosion	Driving Force
Cold Agent Discharge + Diesel Burn	StatX	MTS	Yes	Noticeable discolouration Soot and particulate deposition Some pitting	Chemical reaction between agent and protective paint
		HTS	Yes	Noticeable discolouration Soot and particulate deposition Shallow surface pitting	Chemical reaction between agent and protective paint
		Computer Disc Untreated	Yes	Small and severe pitting Soot and particulates	Surface irregularities Temperature Chemical Composition Presence of KOH Molecules
		Copper Beryllium	No	Discolouration Small marks and larger particulate	Possible minor oxidation of copper substrate

Results summarized in Table 6-3 are for tests in which each material is exposed to both the StatX aerosol agent and the environment developed during the diesel fire in the compartment. Microscopic examination was again conducted on a regular basis from a short time after exposure until a full year had elapsed. Consistent with observations summarized for the agent only test results shown in Table 6-1, the most predominant form of corrosion amongst material coupons was pitting, often accompanied by surface discolouration as well as soot and aerosol particulate deposition. In general, the severity of damage was higher in these tests, when compared against agent only tests.

From Table 6-3, the only material that does not appear to be affected by exposure to the combination of aerosol particulate and diesel fire environment is the copper beryllium alloy. This is likely due to that material's strong inherent corrosion resistance. The CD is again most severely affected, though both mild and high tensile steel do show some effects of the combined exposure, even though a layer of corrosion resistant paint has been applied to the material surface.

Table 6-4: Corrosion results based on combined exposure to DSPA particulate and diesel fire

Group	Aerosol Variant	Material	Corrosion (Y/N)	Type of Corrosion	Driving Force
Cold Agent Discharge + Diesel Burn	DSPA	MTS	Yes	Noticeable discolouration Soot and particulate deposition Some pitting	Chemical reaction between agent and protective paint
		HTS	Yes	Noticeable discolouration Soot and particulate deposition Some pitting	Chemical reaction between agent and protective paint
		Computer Disc Untreated	Yes	Small and severe pitting Soot and other particulate residue	Surface irregularities Temperature Chemical Composition Presence of KOH Molecules
		Copper Beryllium	No	Discolouration Few marks Soot and larger particulate deposition	Possible minor oxidation of copper substrate

Table 6-4 contains the results of interactions between each material sample, DSPA aerosol agent and the diesel fire environment. Material coupons were again left exposed and examined at regular intervals for a period of a year after the test. Results are very much the same as those already observed for exposure to the StatX aerosol powder and diesel fire environment as summarized in Table 6-3.

6.4 Summary of Corrosion Test Results

The main goal of performing corrosion analysis is to assess the damage, if any, which might occur due to interaction of the aerosol particulate with various materials during accidental cold agent discharge or during fire scenarios.

During and after aerosol only or aerosol suppression tests with StatX and DSPA handheld aerosol extinguishers, a film of soot and aerosol powder was visible on the material coupons and other surfaces within the test compartment. Although much of the residue could be wiped away with a cloth, it is evident that objects that are in a room during aerosol activation and suppression will experience some deposition of the particulate on their exposed surfaces requiring appropriate steps be taken during post exposure cleanup operations.

Comparison of the four tests summarized in Table 6-1, Table 6-2, Table 6-3 and Table 6-4 show that discolouration of many surfaces does occur during these tests. If the residue is not cleaned from the surfaces, low to moderate levels of surface pitting occurs as well, depending on the material under test. Material coupons exposed to agent in conjunction with the hot fire and combustion environment, experience greater levels of corrosion than do those exposed only to the aerosol particulate alone. This is undoubtedly due in part to the higher temperatures, as well as the inherent water and other gaseous species contained in the hot gases to which the samples are initially exposed in a fire situation, but also may be due to the formation of different end products during agent generation versus agent suppression of a fire. For example, in the tests summarized in Table 6-1 and Table 6-2, the aerosol particulate arises directly through the thermal decomposition of the base aerosol powder, rather than including additional products that might be formed during chemical interactions with the free flame radicals or hot combustion gases present in the diesel fire suppression tests (Table 6-3 and Table 6-4).

Key results of the full set of preliminary corrosion tests described in this Chapter are summarized in Table 6-5 below. From the Table, it can be seen that after exposure, pitting and corrosion of circuit boards, CD discs and other sensitive electronic components could occur, and if these are poorly cleaned or not cleaned for a period after exposure, the damage could potentially be sufficiently severe as to lead to complete malfunction of a system. Other materials suffer minor discolouration and/or surface damage in the form of pitting after extended periods of time. It must be noted, however, that these results are only a preliminary investigation into possible interactions between aerosol agents and materials during fire suppression. As such, it is recommended that specific corrosion testing would need to be carried out to more completely ascertain the potential for damage to a full suite of materials and environments representative of any particular suppression application of interest.

Table 6-5: Corrosion table summary

Material Coupon	Corrosion (Cold Agent StatX)	Corrosion (Cold Agent DSPA)	Corrosion (Agent +Diesel StatX)	Corrosion (Agent +Diesel DSPA)
Circuit Board Conductor	Yes	Yes	Yes	Yes
Circuit Board Electrical Pathway	Yes	Yes	Yes	Yes
Mild Tensile Steel (1018)	No	No	Yes	Yes
High Tensile Steel (4140)	No	No	Yes	Yes
Computer Disc	Yes	Yes	Yes	Yes
Copper Beryllium	No	No	No	No
NOMEX Fire Resistant Clothing	No	No	N/A	N/A

7   Conclusions

Despite any potential advantages to the development and use of aerosol agents for fire suppression, it was determined that there is limited understanding of the prime gases evolved during aerosol generation and suppression, as well as of potential impacts of the use of aerosol suppression systems in terms of particulate deposition and damage to affected surfaces. These limitations make it difficult to weigh the advantages versus potential disadvantages of the use of aerosols in various suppression situations. The current research was therefore focussed on characterization of the gases and particulate matter formed during discharge of, and suppression with, handheld aerosol suppression units.

To meet the research objectives, as series of full-scale tests were conducted in a custom designed single compartment test chamber in which key factors such as fire heat release rate and thermal conditions in the compartment, as well as time and location of agent release could be monitored and controlled. Two different variants of handheld aerosol extinguishers were tested against five different fire environments, including

Diesel fire with agent suppression (Test 1)

Obstructed diesel fire with agent suppression (Test 2)

Diesel bilge fire with agent suppression (Test 3)

Wood crib fire with agent suppression (Test 4), and

Cold agent discharge (Test 5).

Concentrations of various gases were measured during aerosol discharge and suppression to explore the potential creation of harmful by-products due to thermal decomposition and subsequent aerosol powder generation from the solid state agent contained in the handheld units. Aerosol powder deposition was observed after each test, and post suppression corrosion or other damage was monitored on a range of materials and electronic components.

7.1 Aerosol Suppression of Class B Fires

In the diesel fire and obstructed diesel fire tests, Tests 1 and 2, increases in levels of NO_x and NH_3 effluents were observed when the aerosol agents are used to suppress the fire. Results suggest that, independent of suppression agent employed, peak measured concentrations of NO in the hot gases of the upper layer of the compartment surpass the IDHL limit for occupational exposure of 100 ppm set by OSHA [35]. Although there were potential issues with saturation of the Novatech P-695 NO_x detector during some tests, measured NO_2 concentrations quickly rose

to values that far exceed the 1-hour continuous exposure limit proposed by WHO [34], as well as both the OSHA IDHL and OSHA 15-minute exposure thresholds [35] at the chosen measurement locations. In addition, local measured concentrations of NH$_3$ reach values well above the published exposure threshold values for both types of aerosol unit All the results support the importance of appropriate operational procedures to minimize the likelihood that any personnel could be exposed to potentially high levels of NO or NO$_2$ during conduct of normal fire response activities.

In contrast to Test 1 and Test 2, results from the bilge fire test, Test 3, reveal a slightly different temporal distribution of NO$_x$ inside the compartment. In these, the aerosol units were submerged in water as they activated. Potentially as a result of cooling during activation, lower levels of NO, but much higher concentrations of NO$_2$ are measured in the upper hot layer. In all cases, NO$_2$ concentrations greatly exceed the 1-hour continuous exposure limit proposed by WHO [34], as well as both the OSHA IDHL and OSHA 15-minute exposure thresholds [35]. Despite the changes in distribution of NO$_x$, these results confirm the need for appropriate operational procedures when aerosol suppression units are deployed.

7.2 Aerosol Suppression of Class A Fires

The results of aerosol suppression of softwood crib fires in Test 4, led to varying concentrations of NO, NO$_2$, HCN and NH$_3$ across the tests. Results are consistent with general expectation, since all of these species are likely to be involved with NOx production during a wood fire. Measured concentrations of NO appear to be lower than in the tests involving the diesel fire and often did not surpass the IDLH limit for occupational exposure of 100 ppm set by OSHA [11]; however, in one of the tests higher concentrations of NO were measured suggesting that there is still the possibility for NO to collect in the hot upper layer gases. Measured NO$_2$ concentrations grew to very high levels in many of the tests, exceeding the 1-hour continuous exposure limit proposed by WHO [34], as well as both the OSHA IDHL and OSHA 15-minute exposure thresholds [35] for NO$_2$. Furthermore, measurable concentrations of HCN and even relatively high concentrations of NH$_3$ are observed in some tests suggesting a series of additional chemical reactions are likely taking place. Similar to the other fire situations, then, these results indicate the importance of operational procedures for deployment and use of even handheld aerosol extinguishing units

7.3 Cold Agent Discharge

A final set of tests (Test 5) were conducted to evaluate the gases evolved during generation and discharge of an aerosol unit into a cold compartment environment (no fire). For both units tested, measured concentrations of NO surpass the IDHL limit for occupational exposure of 100 ppm set

by OSHA. Trends in NO_2 concentration are similar across units and values exceed the 1-hour continuous exposure limit proposed by WHO, as well as both the OSHA IDHL and OSHA 15-minute exposure thresholds. Although it would be expected that such concentrations would normally be seen only for a fairly short period of time after activation of the aerosol units and would dilute quite quickly throughout the environment due to mixing and ventilation, it does suggest that care should be taken regarding potential exposure of personnel should an aerosol unit release into a cold, relatively well sealed compartment.

CO was produced during generation and discharge of aerosol into the cold compartment in all the above tests. Peak measured concentrations of CO were found to be near or above the ceiling limit of 200 ppm set by NIOSH for occupational exposure [63]. The high CO concentrations are seen locally and only for very short periods of time after activation suggesting that, due to ventilation and consequent mixing of the gas throughout the compartment, personnel would most likely only be exposed to lower levels of CO concentration should an aerosol unit accidentally discharge into a space.

7.4 Aerosol Corrosion Tests

A number of common marine materials and electronic components were placed in the burn compartment during the agent only tests and the diesel fire tests with agent suppression to evaluate the effects of aerosol powder deposition on different surfaces. Exposed samples were then examined at regular intervals for up to a year after the test.

Exposure of most materials to the gases and particulate generated and discharged by both of the present aerosol units led to low to moderate corrosion on some of the material surfaces. Depending on the material that was exposed, impacts can include discolouration of the exposed surface, as well as deep pitting of the exposed materials. Due in part to the higher temperatures, as well as the inherent water and other gaseous species contained in the hot gases to which the samples are exposed during fire suppression situations, and potentially due also to the formation of different end products during agent generation versus agent suppression of a fire, more severe corrosion was evident on samples that had been exposed during suppression of a fire. In either case, the level of damage seen suggests that post-exposure surface interactions pose a legitimate threat to the material substrate and the structural integrity of some materials. For the most part, the naval materials tested in this research exhibited fairly high resistance to such corrosion; however, damage to CDs indicates the potential for loss of data after exposure and similarly, the impact on the board, connectors and conductive pathways of the computers tested are shown to be sufficient to lead to malfunction of circuit boards.

8 Recommendations

Based on the experience gained during the research outlined in this thesis, several recommendations can be made towards possible future investigations. These are outlined in the following sections.

8.1 Experimental Setup

- In a fully developed fire environment, the flow field is highly turbulent, leading to both spatial and temporal variations in the concentrations of all gaseous species. Therefore, sampling the concentrations of gases at multiple locations over time would give a better representation of the average species concentrations inside the compartment.
- In future tests, and the compartment should be better sealed to minimize the level of leakage that can occur during testing.
- In future testing, the Novatech P-695 gas analysis sampling stream should be re-calibrated in its entirety between every test to determine any differences in lag due to sampling configuration. The chemiluminescence analyzers should always be carefully set and calibrated to a range larger than that anticipated for the experiments at hand to minimize the potential for saturation of the detectors and resultant loss of NO_2 concentration data.

8.2 Characterization of Aerosol Units

- The raw agent composition, as well as the powder residue, from both StatX and DSPA units should be analyzed in more depth to better understand the species produced during agent discharge, as well as the potential impacts of powder deposition on various surfaces after exposure to an aerosol.

8.3 Recommendations Arising from Aerosol Suppression of Class A Fires

Regardless of introducing the aerosol agents for Class A fire suppression, the deep seated embers always produce the threat for an onset of rapid fire growth after opening of fire compartment. Some combination of aerosol activation with complementary methods of fire suppression, such as oxygen starvation or water might be most appropriate for a suppression strategy involving aerosol units in the case of a deep seated class A fire.

8.4 Recommendations arising from Agent Discharge Tests

- Aerosols should not be activated in the close vicinity of personnel due to the high temperatures and localized high concentrations of CO and NO_2 that are generated as a

result of thermal decomposition of solid agent tablet. Therefore, the importance of staying far away from aerosol canisters as they are activated cannot be overstated.

8.5 Corrosion Test Recommendations

- Due to chemical nature of the aerosol powders, surfaces should be cleaned immediately after an accidental discharge or suppression of a fire with an aerosol unit. This will help to mitigate the chances of corrosion taking place. Use of agents near sensitive electronics should be avoided, since particulate can make its way into the casings through small openings and if left unattended could lead to detrimental damage to a unit. Further studies should also be conducted into the impact and damage that might accrue to a wider array of material coupons than those that were studied here.
- It is recommended that aerosols should not be stored in high risk areas due to the chance of, and consequence from, accidental activation of a unit.
- Finally, based on the results seen in the present research, it is recommended that SOPs be written to address both the proper operational procedures for, and the requirements for cleanup after, use of handheld aerosol suppression units.

9   Works Cited

[1]   R. Carboy, "Aerosol Offers Effective Fire Suppression for Your Server Room," Peripheral Manufacturing Inc., Denver, United States of America.

[2]   S. Yechiel, "New Products Using Particulate Aerosol Technology," National Institute of Standards and Technology, Sderot, Israel, 1994.

[3]   D. Spring and D. Ball, "Alkali Metal Salt Aerosols as Fire Extinguishants," Fire and Safety International and Kidde Graviner Ltd., Colnbrook, United Kingdom, 1995.

[4]   C. Kibert and D. Dierdorf, "Encapsulated Micron Aerosol Agents (EMAA)," University of Florida, New Mexico, United States of America.

[5]   A. Chattaway, R. Dunster, R. Gall and D. Spring, "The Evaluation of Non-Pyrotechnically Generated Aerosols as Fire Suppressants," Fire and Safety International and Kidde Graviner Ltd., Colnbrook, United Kingdom, 1995.

[6]   N. Kopylov, B. P. V.S. Ilitchkine and I. Novikov, "Toxic Hazard Assciated with Fire Extinguishing Aerosols: The Current State of the Art and a Method for Assessment," in *Halon Options Technical Working Conference*, Albuquerque, United States of America, 2001.

[7]   E. Jacobson, "Enhancement of Fire Survivability by Employing Pyrotechnically Generated of Propelled Agents," National Institute of Standards and Technology (NIST), Washington, United States of America, 2005.

[8]   AFG Flame Guard Ltd, "Dry Sprinkler Powder Aerosol, Type 5: Technical White Paper," AFG Flame Guard Ltd, 2005.

[9]   Fireway LLC, "StatX Aerosol Generator Technical White Paper," Fireway LLC, [Online]. Available: http://www.statx.com/pdf/860StatX_WhiteP_Cor.pdf. [Accessed 22 02 2013].

[10] Fireway LLC, "Equipment Exposure Issues for StatX Aerosol Generators," Fireway LLC, [Online]. Available: http://www.statx.com/Whitepaper_Equipment_Exposure.asp. [Accessed 08 03 2013].

[11] B. Craig and D. Anderson, "Potassium Carbonate," in *Handbook of Corrosion Data: 2nd Edition*, Ohio, United States of America, ASM International, 2002, pp. 639-641.

[12] International Program on Chemical Safety, "Potassium Carbonate Material Safety Data Sheet - ICSC 1588," IPCS, 21 April, 2005. [Online]. Available: http://www.inchem.org/documents/icsc/icsc/eics1588.htm. [Accessed 15 March, 2013].

[13] C. J. Voelkert, "Fire and Fire Extinguishment," Voelkert, Craig J., 2009.

[14] A. K. Kim, "Overview of Recent Progress in Fire Suppression Technology," National Research Council (NRC), Ottawa, Canada, 2002.

[15] S. R. Sheinson and D. Barylski, "Shipboard Total Flooding Fire Protection Systems for Halon 1301 Replacement," The Navy Technology Center for Safety and Survivability, Washington, United States of America.

[16] D. Dougal, An Introduction to Fire Dynamics 3rd Ed., West Sussex, United Kingdom: John Wiley & Sond Ltd., 2011.

[17] C. J. Kibert and D. Dierdorf, "Encapsulated Micron Aerosol Agents (EMAA)," Air Base Fire Protection and Crash Rescue Section, New Mexico, United States of America.

[18] A. N. Baratov, N. A. Baratova, Y. A. Myshak and D. Y. Myshak, "Practice of Use of Aerosol Extinguishing Agents Obtained by Combustion of Propellants," International Association for Fire Safety Science, Moscow, Russia.

[19] T. D. Sheehan, "Royal Canadian Navy Evaluation of Handheld Aerosol Extinguishers," University of Waterloo, Waterloo, Canada, 2013.

[20] I. C. Hisatsune and T. Adl, "Thermal Decomposition of Potassium Bicarbonate," *The Journal of Physical Chemistry*, vol. 74, no. 15, pp. 2875-2877, 1970.

[21] T. O. Hosotsubo, K. Itoh, T. Maeda and Y. Yamazaki, "R&D on High-Performance Electrode Materials using Petroleum Pitch-based Carbon Fiber," Petroleum Energy Center, 2001.

[22] L. L. Simmons, L. F. Lowden and T. C. Ehlert, "A Mass Spectrometric Study of K2CO3 and K2O," *The Journal of Physical Chemistry*, vol. 81, no. 8, pp. 706-709, 1977.

[23] L. V. Gurvich, G. A. Bergman, L. N. Gorokhov, V. S. Iorish, V. Y. Leonidov and V. S. Yungman, "Thermodynamic Properties of Alkali Metal Hydroxides. Part II. Potassium, Rubidium, and Cesium Hydroxides," *Journal of Physical Chemistry*, vol. 26, no. 4, pp. 1031-1110, 1997.

[24] K. H. Stern, "Individual Nitrites and Nitrates," in *High Temperature Properties and Thermal Decomposition of Inorganic Salts with Oxyanions*, Boca Raton, United States of America, CRC Press LCC, 2000, pp. 147-148.

[25] T. Takagi, T. Tatsumi and M. Ogasawara, "Nitric Oxide Formation from Fuel Nitrogen in Staged Combustion: Roles of HCN and NHi," *Combustion and Flame* , vol. 35, no. 1, pp. 17-25, 1979.

[26] H. S. Luftman, "Neutralization of Formaldehyde Gas by Ammonium Bicarbonate and Ammounium Carbonate," *Applied Biosafety*, vol. 10, no. 2, pp. 101-106, 2005.

[27] C. K. Law, "Oxides of Nitrogen," in *Combustion Physics*, New York, United States of America, Cambridge University Press, 2006, pp. 116-119.

[28] C. E. Baukal Jr., "NOx," in *Oxygen-Enhanced Combustion*, Boca Raton, United States of America, CRC Press LLC., 1998, pp. 47-49.

[29] J. M. Samaniego, F. N. Egolfopoulos and C. T. Bowman, "Effect of Chemistry and Turbulence on NO formation in Oxygen-Natural gas Flames," Center for Turbulence Research , Stanford, United States of America, 1996.

[30] F. J. Barnes, J. H. Bromly, T. J. Edwards and R. Madngezewsky, "NOx Emissions from Radiant Gas Burners," *Journal of the Institute of Energy*, vol. 155, pp. 184-188, 1988.

[31] M. R. Beychok, "NOx Emission From Fuel Combustion Controlled," *The Oil and Gas Journal*, pp. 53-56, 1973.

[32] A. L. Shihadeh, M. A. Toqan, J. M. Beer, P. F. Lewis, J. D. Teare, J. L. Jimenez and L. Barta, "Low NOx Emission From Aerodynamically Staged Oil-Air Turbulent Diffusion Flames," The Combustion Research Facility, Institute of Technology, Cambridge, United States of America, 1994.

[33] F. G. Favorite, L. M. Roslinski and R. C. Wands, "Guides for Short Term Exposures of the Public to Air Pollutants," AMRL-TR-71-120 Paper No.16, Aerospace Medical Research Laboratory, Wright Patterson Air Force Base, Washington, United States of America, 1971.

[34] World Health Organization, "Nitrogen Dioxide," World Health Organization, Copenhagen, Denmark, 2000.

[35] Occupational Safety and Health Administration (OSHA), "Nitrogen Dioxide (NO2)," 1, January 2014. [Online]. Available: https://www.osha.gov/dts/chemicalsampling/data/CH_257400.html. [Accessed 07 January, 2012].

[36] USA Environmental Protection Agency, "Nitrogen Dioxide (NO2) Standards-Table of Historical NO2 NAAQS," 6 June, 2011. [Online]. Available: http://www.epa.gov/ttn/naaqs/standards/nox/s_nox_history.html. [Accessed 7 January, 2012].

[37] U.S. Department of Labour, "Occupational Health Guideline for Hydrogen Cyanide," U.S. Department of Health and Human Services, Washington, United States of America, 1978.

[38] The National Institute for Occupational Health and Safety (NIOSH), "Occupational Safety and Health Guideline for Ammonia (NH3)," U.S. Department of Health and Human Services, Atlanta, United States of America, 1992.

[39] The National Institute for Occupational Health and Safety (NIOSH), "Documentation for Immediately Dangerous To Life or Health Concentrations (IDLHs)," Center for Diesease Control and Prevention, 1, May 1994. [Online]. Available: http://www.cdc.gov/niosh/idlh/7664417.html. [Accessed 14, January 2014].

[40] World Health Organization, "Air Quality Guidelines for Europe, 2nd edition," World Health Organization (WHO) Regional Publications, European Series, No. 91, Copenhagen, Denmark, 2000.

[41] United States Department of Labour, "Occupational Safety and Health Guideline for Carbon Monoxide," Occupational Safety and Health Administration (OSHA), Washington, United States of America , 1996.

[42] National Research Council, "Carbon Monoxide," in *Emergency and Continuous Exposure Guidance Levels for Selected Airborne Contaminants*, Washington, United States of America, National Research Council (NRC), 1987, pp. 67-105.

[43] M. Connell and a. D. J. Glocking, "Large-Scale Tests of Pyrotechnically Generated Aerosol Fire Extinguishing Systems for the Protection of Machinery Spaces and Gas Turbine Enclosures in Royal Navy Waships," Ministry of Defence Abbey Wood, Bristol, United Kingdom, 2004.

[44] International Maritime Organization (IMO), "IMO FP44 MSC Circ. 1007: Guidelines for the Approval of Fixed Aerosol Fire Extinguishing Systems as Referred to in SOLAS/FSS Code for Machinery Spaces," International Maritime Organization (IMO), London, United Kingdom, 2008.

[45] T. Sheehan, "Royal Canadian Navy Evaluation of Handheld Aerosol Extinguishers," University of Waterloo, Waterloo, Canada, 2013.

[46] T. Sheehan, A. Topic, W. Elizabeth, G. Hitchman and A. Strong, "Marine Evaluation of the Aerosol Knockdown Tools," Waterloo University, Waterloo, Canada, 2012.

[47] International Organization for Standardization (ISO), "ISO 9705: Fire Tests - Full Scale Room Test for Surface Products," International Organization for Standardization (ISO), Geneva, Switzerland, 1993.

[48] M. Obach, "Effects of Initial Fire Attack Suppression Tactics on the Firefighter and Compartment Environment," University of Waterloo, Waterloo, Canada, 2011.

[49] American Standards for Testing and Materials, "Standard Guide for Measurement of Gases Present or Generated During Fires (ASTM E800-5)," ASTM International, Chicago, United States of America, 2005.

[50] Novatech Inc., "Novatech Gas Analysis Manual," University of Waterloo Live Fire Research Facility, Waterloo, Canada, 2007.

[51] R. J. Jernigan, "Chemilumibescence NOx and GFC NDIR CO Analyzers for Low Level Source Monitoring," Thermo Environmental Instruments, Massachusetts, United States of America.

[52] Teledyne Monitor Labs, "TML 41M/H Nitrogen Oxides Analyzer," Teledyne Monitor Labs Inc., Engelwood, United States of America, 2009.

[53] R. H. Munch, "Instrumentation: Paramagentic Analyzers Operate Without Chemicals and will Rapidly Detect as Little as 0 to 5% Oxygen," *Industrial Engineering Chemistry*, vol. 41, no. 3, pp. 97A-98A, 1949.

[54] Servomex Group Limited, "Servomex Emissions Analyzers, ServoPRO 4900," Servomex Group Limited, East Sussex, England, 2014.

[55] Rousemount Analytical , "Non-Dispersive Infrared Analyzer Module," Rousemount Analytical , Anaheim, United States of America, 1999.

[56] GASTEC, *Instructions for Nitrogen Oxide and Nitrogen Dioxide Detector Tube (No. 10)*, Fukayanaka, Japan: Gastec Corporation.

[57] Zefon International, "Gastec Hydrogen Cyanide Detector Tubes," Zefon International Inc., Stratford, Canada, 2014.

[58] Scintag Inc., "Chapter 7:Basics of X-ray Diffraction," Cupertino, United States of America, Scintag Inc., 1999, pp. 7.1-7.25.

[59] J. R. Connolly , "Introduction Quantitative X-Ray Diffraction Methods," 18 April, 2012. [Online]. Available: http://epswww.unm.edu/xrd/xrdclass/09-Quant-intro.pdf. [Accessed 4 August, 2013].

[60] DHHS (NIOSH) Publication Number 88-116, "Current Intelligence Bulletin 50: Carcinogenic Effects of Exposure to Diesel Exhaust," 31, August 1988. [Online]. Available: http://www.cdc.gov/niosh/docs/88-116/. [Accessed 7, January 2012].

[61] O. Abdulaziz, "Combustion Products from Ventilation Controlled Fires: Toxicity Assesment and Modelling," University of Leeds, Leeds, United Kingdom, 2012.

[62] Work Safe Alberta, "Carbon Monoxide at Work Site," Work Safe BC, Edmonton, Canada, 2009.

[63] National Institute for Occupational Safety and Health (NIOSH), "Recommendations for occupational safety and health: Compendium of policy documents and statements," U.S. Department of Health and Human Services, Public Health Service, Centers for Disease Control, National Institute for Occupational Safety and Health, Cincinnati, United States of America, 1992.

[64] Sigma-Aldrich, "Potassium Nitrate (KNO3)," Sigma-Aldrich, 2015. [Online]. Available: http://www.sigmaaldrich.com/catalog/product/sial/p8394?lang=fr&region=CA. [Accessed 21 January 2015].

[65] Toxnet, "Potassium Nitrate, Human Health Effects," Toxicology Data Network (Toxnet), 05 December 2014. [Online]. Available: http://toxnet.nlm.nih.gov/cgi-bin/sis/search/a?dbs+hsdb:@term+@DOCNO+1227. [Accessed 21 January 2015].

[66] B. J. Kosanke, B. Sturman, K. Kosanke, I. v. Maltitz, T. Shimizu, M. A. Wilson, N. Kubota, C. Jennings-White and D. Chapman, "Pyrotechnic Chemistry," Whitewater, United States of America, Journal of Pyrotechnics Inc, 1st Edition, 2004, pp. 5-6.

[67] V. Vladimir, S. Kopylov, A. Sychev, V. Ugolv and D. Zhyganov, "The Mechanism of Fire Suppression by Condensed Aerosols," in *Halon Options Technical Working Conference*, Albuquerque, United States of America, 2005.

[68] Cameo Chemicals, "Potassium Hydroxide, [CONTAINING CORROSIVE LIQUID]," 2012. [Online]. Available: http://cameochemicals.noaa.gov/chemical/17497. [Accessed 26 January, 2013].

[69] Occupational Safety and Health Administration (OSHA), "Potassium Hydroxide," United States Department of Labour, Washington, United States of America, 2004.

[70] E. Weckman, A. Topic, T. Sheehan and G. Hitchman, "Maritime Evaluation of Aerosol Fire Knock Down Tools, Part 2: Toxicity and Corrosion Potential," DRDC DOCUMENT NUMBER: DRDC-RDDC-2014-C32, Halifax, 2014.

[71] C. Trepanier and R. A. Pelton, "Effects of Temperature and pH on the Corrosion Resistance of Passivated Nitinol and Stainless Steel," Nitinol Devices and Components , Fremont, United States of America, 2004.

[72] World Health Organization, "Hydrogen Cyanide and Cyanides: Human Health Aspects," World Health Organization (WHO) Regional Publications, European Series, No. 61, Geneva, Switzerland, 2004.

[73] National Institute for Occupational Safety and Health (NIOSH), "Nitric Oxide and Nitrogen Dioxide," National Institute for Occupational Safety and Health (NIOSH), Atlanta, United States of America, 1994.